



**YAYASAN BRATA BHAKTI DAERAH JAWA TIMUR
UNIVERSITAS BHAYANGKARA SURABAYA
LEMBAGA PENELITIAN DAN PENGABDIAN PADA MASYARAKAT
(LPPM)**

Kampus : Jl. A. Yani 114 Surabaya Telp. 031 - 8285602, 8291055, Fax. 031 - 8285601

SURAT KETERANGAN

Nomor: Sket/ 41 /I/2023/LPPM/UBHARA

Kepala Lembaga Penelitian dan Pengabdian kepada Masyarakat (LPPM) Universitas Bhayangkara Surabaya menerangkan bahwa:

Nama : Dr. Amirullah, ST, MT.
NIP : 197705202005011001
NIDN : 0020057701
Unit Kerja : Universitas Bhayangkara Surabaya

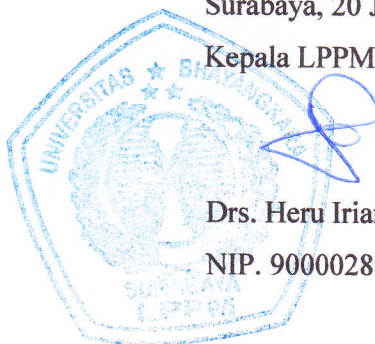
Benar telah melakukan kegiatan:

1. Mereview makalah jurnal internasional bereputasi berjudul CURRENT HARMONICS QUALITY MITIGATION TECHNIQUE FOR THREE-PHASE POWER SYSTEM BASED ON EXTENDED FRYZE ADAPTIVE NOTCH FILTER dari Journal of Engineering Science and Technology (JESTEC), Publisher: Taylor's University Malaysia Tahun 2022, Terindeks Scopus Q3.
2. Telah melakukan korespondensi email dengan editor/pengelola jurnal dalam rangka mereview substansi materi makalah jurnal dalam selang waktu yang telah ditentukan sebelumnya. Bukti korespondensi email dan bukti pendukung adalah benar sudah dilakukan oleh yang bersangkutan serta sudah dilampirkan bersama surat ini.

Demikian surat keterangan ini dibuat untuk kepentingan kelengkapan pengusulan Guru Besar.

Surabaya, 20 Januari 2023

Kepala LPPM



Drs. Heru Irianto, M.Si.

NIP. 9000028

Lampiran 1

**Bukti Korespondensi Email
dengan Editor/Pengelola
Jurnal**

Paper ID ee2246 /Requesting paper review for JESTEC, First round of Review Process/

8 pesan

Jestec <Jestec@taylors.edu.my>

7 November 2022 pukul 11.24

Dear Dr.

Greetings from the Editorial Board of JESTEC.

The following attached manuscript titled

CURRENT HARMONICS QUALITY MITIGATION TECHNIQUE FOR THREE-PHASE POWER SYSTEM BASED ON EXTENDED FRYZE ADAPTIVE NOTCH FILTER

has been submitted to JESTEC for consideration for publication.

As an expert in its topic area, I am writing to request that you review it and make a recommendation regarding its acceptability..

I hope that you will agree to review this manuscript. I would appreciate, if possible, receiving your review by **November 25, 2022**.

If you would like to have more time to complete the review, could you please indicate the time frame you expect to return the review report?

I appreciate your contribution in maintaining the quality and value of JESTEC and look forward to your response.

Best regards

Some quick guidelines to our respected reviewers

Whenever appropriate, we would appreciate if you evaluate the paper based on the following seven criteria. Please try not to focus on the editorial issues/mistakes as too many of them may lead to the author's frustration. When we revise their paper, we want the authors to focus on our comments/concern related to these seven criteria.

1. **Research question**: why the authors do this research and what is its importance and application.
2. **Novelty**: a paper gives new ideas, derivations, applications that have been not studied before or little- or not in depth-studied.
3. **Literature review**: identify the research gap with recent references from 2016 onwards.
4. **Research methodology**: analytical, numerical or experimental or mixed. What is the authors' contribution, assumptions and/or approximations used, description of apparatus and its limitations, steps of experiments, etc.?
5. **Quality of results**: ensure the quality, the depth, and the logic of the discussion.
6. **Insight**: conveyed and recommendations that others might use for future work.
7. **English**: used effectively to communicate the ideas that easy to understand with no grammatical errors or typos.

Assoc. Prof. Dr. Abdulkareem Sh. Mahdi Al-Obaidi, CEng MIMechE

Executive Editor, Journal of Engineering Science & Technology

<http://jestec.taylors.edu.my>

2 lampiran



Review Report - 2017.docx

62K



ee2246.docx

3680K

Amirullah Ubhara Surabaya <amirullah@ubhara.ac.id>
Kepada: Jestec <Jestec@taylors.edu.my>
Cc: Amirullah Ubhara Surabaya <amirullah@ubhara.ac.id>
Bcc: Amirullah Amirullah <amirullah.ubhara.surabaya@gmail.com>

8 November 2022 pukul 07.54

Dear Prof,

Thanks a lot for sending me this entitled paper.

I will review it before the deadline.

Dr Amirullah
Power Quality, Power Distribution, Power Electronics, and Renewable Energy base Artificial Intelligent Research
Universitas Bhayangkara Surabaya Indonesia

[Kutipan teks disembunyikan]

Jestec <Jestec@taylors.edu.my>
Kepada: Amirullah Ubhara Surabaya <amirullah@ubhara.ac.id>

8 November 2022 pukul 08.17

Dear Dr Amirullah.

Thank you in advance for the support and accepting the review invitation.

Best regards

Abdulkareem

[Kutipan teks disembunyikan]

Amirullah Ubhara Surabaya <amirullah@ubhara.ac.id>
Kepada: Jestec <Jestec@taylors.edu.my>
Cc: Jestec <Jestec@taylors.edu.my>
Bcc: Amirullah Ubhara Surabaya <amirullah@ubhara.ac.id>

17 November 2022 pukul 20.23

Dear Dr Abdulkareem

Here I send you the reviewed paper entitled **CURRENT HARMONICS QUALITY MITIGATION TECHNIQUE FOR THREE-PHASE POWER SYSTEM BASED ON EXTENDED FRYZE ADAPTIVE NOTCH FILTER.**

The second paper will be reviewed tomorrow (paper ID: ee2250)

Dr Amirullah
Power Quality, Power Electronics, dan Renewable Energy Research
Universitas Bhayangkara Surabaya Indonesia

[Kutipan teks disembunyikan]

2 lampiran



Review Report - 2017_ee2246_Reviewed Dr. Amirullah.docx
41K



ee2246_Reviewed Dr. Amirullah.docx
3689K

Jestec <Jestec@taylors.edu.my>
Kepada: Amirullah Ubhara Surabaya <amirullah@ubhara.ac.id>

17 November 2022 pukul 21.35

Dear Dr.

Thank you for your kind email.

We confirm that we received your review report.

We will reply you later with some details.

Best regards

JESTEC Editor

<https://jestec.taylors.edu.my>

[Kutipan teks disembunyikan]

Jestec <Jestec@taylors.edu.my>
Kepada: Amirullah Ubhara Surabaya <amirullah@ubhara.ac.id>

30 Desember 2022 pukul 21.02

Dear Dr.

On behalf of the Journal Review Panel, I want to express our sincere thanks for your effort shown in reviewing this paper. We highly appreciate this effort and support and hope to call upon you again to review future manuscripts.

Kindly accept the attached appreciation letter.

Best regards

Assoc. Prof. Dr. Abdulkareem Sh. Mahdi Al-Obaidi, CEng MIMechE

Editor-in-Chief, Journal of Engineering Science & Technology

<http://jestec.taylors.edu.my>

From: Amirullah Ubhara Surabaya <amirullah@ubhara.ac.id>

Sent: Thursday, November 17, 2022 9:23 PM

To: Jestec <Jestec@taylors.edu.my>

[Kutipan teks disembunyikan]

[Kutipan teks disembunyikan]



Amirullah Ubhara Surabaya_3.pdf

199K

Amirullah Ubhara Surabaya <amirullah@ubhara.ac.id>

31 Desember 2022 pukul 10.05

Kepada: Jestec <Jestec@taylors.edu.my>

Cc: Amirullah Ubhara Surabaya <amirullah@ubhara.ac.id>

Bcc: Amirullah Amirullah <amirullah.ubhara.surabaya@gmail.com>

Dear Prof. Abdulkareem.

Since 2021, I have reviewed three papers in Jectec. In the previous email, you told me that my name and affiliation will be listed at <https://jestec.taylors.edu.my/reviewers.html> if I have reviewed three papers.

This is my request and I will be happy if you fulfil it.

Dr Amirullah, ST, MT.
Department of Electrical Engineering
Faculty of Engineering
Universitas Bhayangkara Surabaya
Jl. Ahmad Yani Frontage Road Ahmad Yani No.114, Surabaya
East-Java, Indonesia 60231

[Kutipan teks disembunyikan]

Jestec <Jestec@taylors.edu.my>

2 Januari 2023 pukul 09.54

Kepada: Amirullah Ubhara Surabaya <amirullah@ubhara.ac.id>

Yes, Dr.

Sure, give us some time.

Best regards

JESTEC Editor

[Kutipan teks disembunyikan]

RE: Paper ID ee2246 /Requesting paper review for JESTEC, 2nd round of Review Process/

3 pesan

Jestec <Jestec@taylor.s.edu.my>
Kepada: Amirullah Ubhara Surabaya <amirullah@ubhara.ac.id>

30 Desember 2022 pukul 21.12

Dear Dr

Your Reviewer number is: 3

The paper you earlier reviewed has been revised according to your comments/concern.

Could you kindly have a look at the revised paper and check whether the author(s) addressed all your comments/concern.

We appreciate receiving your feedback before or latest by **12/1/2023**

Attached for your reference, please find

- the original paper
- your review report
- the revised paper and
- the outlining how the author(s) addressed your and other reviewers' comments.

Thank you

Assoc. Prof. Dr. Abdulkareem Sh. Mahdi Al-Obaidi, CEng MIMechE

Editor-in-Chief, Journal of Engineering Science & Technology

<https://jestec.taylor.s.edu.my>

From: Amirullah Ubhara Surabaya <amirullah@ubhara.ac.id>

Sent: Thursday, November 17, 2022 9:23 PM

To: Jestec <Jestec@taylor.s.edu.my>

Subject: Re: Paper ID ee2246 /Requesting paper review for JESTEC, First round of Review Process/

Dear Dr Abdulkareem

Here I send you the reviewed paper entitled **CURRENT HARMONICS QUALITY MITIGATION TECHNIQUE FOR THREE-PHASE POWER SYSTEM BASED ON EXTENDED FRYE ADAPTIVE NOTCH FILTER.**

The second paper will be reviewed tomorrow (paper ID: ee2250)

Dr Amirullah

Power Quality, Power Electronics, dan Renewable Energy Research

Universitas Bhayangkara Surabaya Indonesia

Pada tanggal Sel, 8 Nov 2022 pukul 08.17 Jestec <Jestec@taylor.edu.my> menulis:

Dear Dr Amirullah.

Thank you in advance for the support and accepting the review invitation.

Best regards

Abdulkareem

From: Amirullah Ubhara Surabaya <amirullah@ubhara.ac.id>

Sent: Tuesday, November 08, 2022 8:54 AM

To: Jestec <Jestec@taylor.edu.my>

Cc: Amirullah Ubhara Surabaya <amirullah@ubhara.ac.id>

Subject: Re: Paper ID ee2246 /Requesting paper review for JESTEC, First round of Review Process/

Dear Prof,

Thanks a lot for sending me this entitled paper.

I will review it before the deadline.

Dr Amirullah

Power Quality, Power Distribution, Power Electronics, and Renewable Energy base Artificial Intelligent Research

Universitas Bhayangkara Surabaya Indonesia

Pada tanggal Sen, 7 Nov 2022 pukul 11.24 Jestec <Jestec@taylor.edu.my> menulis:

Dear Dr.

Greetings from the Editorial Board of JESTEC.

The following attached manuscript titled

**CURRENT HARMONICS QUALITY MITIGATION TECHNIQUE FOR THREE-PHASE POWER SYSTEM BASED ON EXTENDED
FRYZE ADAPTIVE NOTCH FILTER**

has been submitted to JESTEC for consideration for publication.

As an expert in its topic area, I am writing to request that you review it and make a recommendation regarding its acceptability..

I hope that you will agree to review this manuscript. I would appreciate, if possible, receiving your review by **November 25, 2022**.

If you would like to have more time to complete the review, could you please indicate the time frame you expect to return the review report?

I appreciate your contribution in maintaining the quality and value of JESTEC and look forward to your response.

Best regards

Some quick guidelines to our respected reviewers

Whenever appropriate, we would appreciate if you evaluate the paper based on the following seven criteria. Please try not to focus on the editorial issues/mistakes as too many of them may lead to the author's frustration. When we revise their paper, we want the authors to focus on our comments/concern related to these seven criteria.

1. **Research question**: why the authors do this research and what is its importance and application.
2. **Novelty**: a paper gives new ideas, derivations, applications that have been not studied before or little- or not in depth-studied.
3. **Literature review**: identify the research gap with recent references from 2016 onwards.
4. **Research methodology**: analytical, numerical or experimental or mixed. What is the authors' contribution, assumptions and/or approximations used, description of apparatus and its limitations, steps of experiments, etc.?
5. **Quality of results**: ensure the quality, the depth, and the logic of the discussion.
6. **Insight**: conveyed and recommendations that others might use for future work.
7. **English**: used effectively to communicate the ideas that easy to understand with no grammatical errors or typos.

Assoc. Prof. Dr. Abdulkareem Sh. Mahdi Al-Obaidi, CEng MIMechE

Executive Editor, Journal of Engineering Science & Technology

<http://jestec.taylors.edu.my>

4 lampiran

 **outlining of Review Report_v3.docx**
55K

 **Review Report - 3 Reviewed.docx**
3689K

 **Review Report - 3.docx**
41K

 **ee2246 R1.pdf**
2280K

Amirullah Ubhara Surabaya <amirullah@ubhara.ac.id>
Kepada: Jestec <Jestec@taylors.edu.my>
Cc: Amirullah Ubhara Surabaya <amirullah@ubhara.ac.id>
Bcc: Amirullah Amirullah <amirullah.ubhara.surabaya@gmail.com>

31 Desember 2022 pukul 09.47

Dear Prof. Abdulkareem

I as reviewer #3 have looked at the revised paper from the author entitled **CURRENT HARMONICS QUALITY MITIGATION TECHNIQUE FOR THREE-PHASE POWER SYSTEM BASED ON EXTENDED FRYZE ADAPTIVE NOTCH FILTER.**

My decision is **accepted without modification** (file attached).

Dr. Amirullah
Department of Electrical Engineering
Faculty of Engineering Universitas Bhayangkara Surabaya

[Kutipan teks disembunyikan]

 **outlining of Review Report_v3_acc without modif_Amirullah_31 Dec 2022.docx**
53K

Jestec <Jestec@taylors.edu.my>
Kepada: Amirullah Ubhara Surabaya <amirullah@ubhara.ac.id>

2 Januari 2023 pukul 09.47

Dear Dr.

Thank you for your time in reviewing the said paper.

We highly appreciate your support and commitment.

Best regards

JESTEC Editor

<http://jestec.taylors.edu.my>

[Kutipan teks disembunyikan]

Lampiran 2

Bukti Pendukung

CURRENT HARMONICS QUALITY MITIGATION TECHNIQUE FOR THREE-PHASE POWER SYSTEM BASED ON EXTENDED FRYZE ADAPTIVE NOTCH FILTER

Abstract

The power quality problem, especially regarding harmonics contamination, has dramatically affected the overall power system stability. In response to this, using an Active Power Filter (APF) is considered one of the compelling methods to overcome harmonics issues. This paper presents the implementation of Shunt APF with an improved adaptive notch filter known as Extended Fryze Adaptive Notch Filter (EFANF) for fundamental signal extraction. The adaptive notch filter has improved the utilization from a single-phase to three-phase application for direct fundamental signal extraction and is designed to cater DC link voltage regulation controllers based on the power loss equation. This extraction algorithm inherits simple design construction and frequency tracking, eliminating PLL reliance on synchronization. The algorithm's effectiveness in operation for the Shunt APF is validated through simulation using MATLAB/Simulink and experiment work by integrating the algorithm with DSPACE RS1104. Based on both evaluations, the results obtained show a satisfactory and reasonable agreement in mitigating the harmonics for multi-load conditions. Simulation and experimentally proven harmonics mitigation managed to reduce under 5% following the IEE standard, and the algorithm function within expectation for both steady and transient state conditions. Furthermore, the DC link also tended to be maintained by the algorithm.

Keywords: Adaptive notch filter, Fryze, shunt active power filter, Harmonics.

1. Introduction

The development of power systems has shaped multiple power generation, transmission, distribution, and application segments. All the advancements are often polluting and distorting the power system by increasing the utilization of non-linear loads, mainly contributed by power-electronics devices [1–3]. The need for power electronics devices can exponentially increase within the industrial and consumer sectors. Based on the extensive use of sensitive loads, such as computers and microprocessor-based industrial controllers, and now with the emergence of renewable energy such as solar and wind and the growth of electric vehicles, there is a growing need for effective harmonic measurement and compensation systems. Although conventional solutions have been used to mitigate power quality, such as passive filters in terms of harmonics, the solution is deemed ineffective, especially when involving load changes. As implementation of standard regulation in power flow is becoming more rigid such as IEEE519 and IEC 61000-3-2, active power compensation is seen as a better choice in realizing power quality (PQ) control.

Active power compensation offers better PQ compensation, especially harmonics, power factor, and active-reactive power control. Furthermore, the protection, management, performance, and efficiency of active power compensation are realized through continuous development in developing signal processing, detection, and extraction within mathematical algorithms and hardware throughout the past years. One of the apparatuses demonstrating a solid ability to eliminate harmonics is the Active Power Filter (APF) system. Such filters are an excellent way to reduce harmonic disturbances of voltage and current, sudden voltage fluctuations, transient disturbances, and current and voltage faults. Currently, there are multiple topologies of active power compensation available for additional compensation, such as series active power filter [4], shunt active power filter (SAPF), hybrid active power filter, and Unified Power Quality Conditioner (UPQC). Effective and efficient compensations are compulsory when dealing with harmonics' power quality. Hence, a precise algorithm is essential for extracting harmonics elements in controlling the power system's active power filter (APF). Over the years, various identification and extraction techniques have been developed; the methods can be divided into time and frequency domains.

The methods used in the frequency-based domain vary from commonly used fast Fourier and discrete Fourier algorithms, Kalman Filtering algorithm to wavelet transformation algorithm [5–7]. When using the mentioned techniques, most of the algorithms designed in the frequency domain require transformation, which is a little tedious to be applied in the time domain and usually incongruous with changing load in the power system. Another drawback of the frequency domain method is that it requires numerous cycles for better current estimation. In applying APF, the commonly used extraction method is usually within the time domain to cater to the changing waveform of loads in real-time situations, especially when involved with data acquisition. The time-domain techniques are divided into a few categories: classical methods derived from instantaneous power theory [8–10] and synchronous power theory [11–13], such as PQ, PQR, etc. DQ method. However, these methods usually involve multi-conversion planes and require additional filters to extract the information.

Another emerging method is the intelligent algorithms, which vary from the neural network, adaptive neural network, and adaptive linear neuron, where all these algorithms require training within the process [14–17]. Besides these three methods, another method used in the APF is the notch filter method, which is simple in design and can accommodate changes in loads [18]. The work introduced adaptive notch filters as harmonics, interharmonics processing methods, and time-domain signal analysis [19]. However, the method is limited to only processing information due to the algorithm's lack of a controlling method for DC link control. Yazdani et al. also proposed the ANF for three-phase application [20], which performed harmonic reactive current extraction and harmonic decomposition. However, the work was limited to monitoring and extraction only. In some other works, the ANF replaces the lowpass filter function in the PQ algorithm for shunt APF [21–23] with a three-phase four-wire system.

Although the strategy takes advantage of the transformation of the frame for instantaneous power flow, the application of ANF has increased the algorithm's complexity as the method includes the transformation process and integration of the ANF for filtering purposes. This strategy undermines the ANF's capability to directly filter the system's fundamental signal.

To utilize the potential of the ANF in shunt APF application. This paper presents an extended ANF application for harmonics extraction, DC link control, and current control. Within this method, three elements are focused on as the APF control system: the computational algorithm of reference current, the voltage regulation for the DC link control, and the generation of the firing pulse of the voltage source inverter (VSI). The main section of the paper is the proposed Extended Fryze Adaptive Notch Filter (EFANF) as the main algorithm component. The algorithm implements the Adaptive Notch Filter (ANF) extraction algorithm and the Fryze algorithm as system power control. Adjacent to the adaptive capability of the ANF, the algorithm also provides self-synchronization for the EFANF. This section also discusses the implementation of DC link voltage regulation, where the PI method is introduced as stability control within the EFANF, all highlighted in sections 2 and 3. The simulation and experimental works results are explained in section 4 of the paper. Finally, section 5 concludes the research contribution and highlights the overall significance of the impact of the work.

2. Principle operation of shunt APF

Shunt APF is implemented using a current control-voltage source inverter (CC-VSI), as shown in figure 1. The CC-VSI are connected in parallel with the non-linear loads through filter inductance. The CC-VSI performs the main task within the power quality system: inject (opposite magnitude) any unwanted harmonics current components produced due to the load current in the supply system at the point of common coupling (PCC).

The instantaneous current source of the overall system is given in equation 1 where $i_s(t)$ is the source current, $i_L(t)$ is the load current and $i_c(t)$ is the compensation current.

$$i_s(t) = i_L(t) - i_c(t) \quad (1)$$

Meanwhile, the instantaneous voltage source $v_s(t)$ is given in equation 2, and the non-linear load current can be considered as the embodiment of fundamental current component and harmonics current components, as shown in equation 3

$$v_s(t) = V_m \sin \omega t \quad (2)$$

$$\begin{aligned} i_L(t) &= \sum_{n=1}^{\infty} I_n \sin(n\omega t + \phi_n) \\ &= I_1 \sin(\omega t + \phi_1) + \sum_{n=2}^{\infty} I_n \sin(n\omega t + \phi_n) \end{aligned} \quad (3)$$

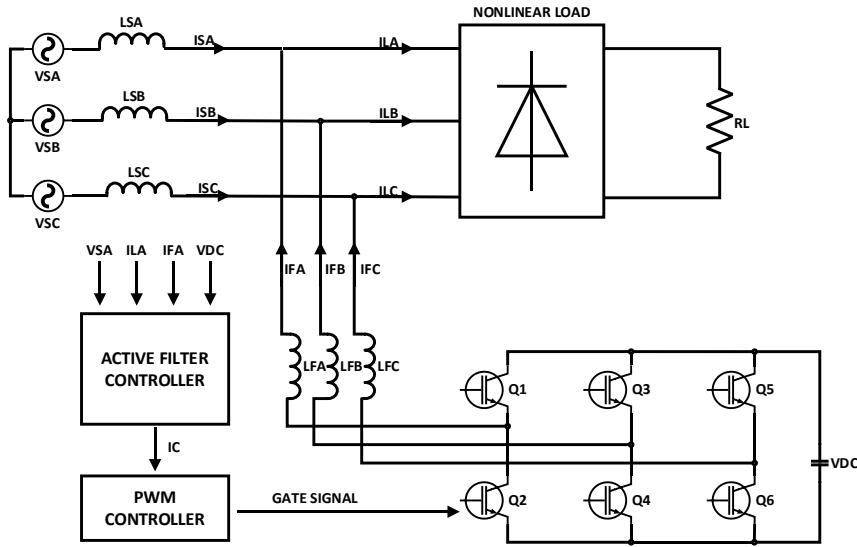


Fig. 1. Shunt APF System

The instantaneous power of the load $p_L(t)$ can be figured out based on equation 4 given as

$$\begin{aligned} p_L(t) &= i_s(t) \times v_s(t) \\ &= V_m \sin^2 \omega t \times \cos \phi_1 + V_m I_1 \sin \omega t \times \cos \omega t \times \sin \phi_1 \\ &\quad + V_m \sin \omega t \left(\sum_{n=2}^{\infty} I_n \sin(n\omega t + \phi_n) \right) \\ &= p_f(t) + p_r(t) + p_h(t) \end{aligned} \quad (4)$$

The equation consists of active power $p_f(t)$, reactive power $p_r(t)$, and harmonics-induced power $p_h(t)$. Based on this, the real power drawn from the load is given in equation 5.

$$p_f(t) = V_m I_1 \sin^2 \omega t \times \cos \phi_1 \quad (5)$$

3. Principle Of Current Control System

The structure of the current control system is shown in figure 1. The system can be divided into three major components. The first part is the computation of the reference current using an extended fryze adaptive notch filter (EFANF), the second part is the self-synchronization of the EFANF, and the third component is the DC link voltage regulation and the firing pulses for the APF.

3.1. Adaptive Notch Filter

Ideally, an adaptive notch filter (ANF) works in the concept of a linear gain applied for all the frequencies except a specified frequency where the frequency gain is zero. Based on this characteristic, the filter can withdraw an implicit signal of the sinusoidal waveform from the specified frequency's measured component of an electrical power system. ANF has well been researched in removing noises within the sinusoidal waveform[24]. Originally, ANF is based on an IIR filter[25]; however, with improvement in the notch frequency, the filter can adapt to notch frequency change with time by tracking the input signal frequency variation. This tracking capability eliminates the need for the signal frequency to be consistent, as is usually required for the typical notch filter to work efficiently. The ANF's dynamic operation can refer to the following set of differential equations.

$$\ddot{x} + \theta^2 x = 2\varepsilon\theta e(t) \quad (6)$$

$$\dot{\theta} = -\gamma x \theta e(t) \quad (7)$$

$$e(t) = u(t) - \dot{x} \quad (8)$$

The ANF can be composed of the following elements based on the differential equations. The input signal of the ANF is given by $u(t)$. The estimation frequency of the ANF system is given by θ . The accuracy and convergence speed are determined by two coefficients within the ANF known as γ and ε . The two coefficients, however, must compensate each other for the ANF to work effectively and most efficiently, $\dot{\theta}$ represents the updated law for the frequency estimation [26].

In a functional single sinusoidal input $u(t) = A_1 \sin(\omega_0 t + \varphi_1)$, the used ANF has an explicit characteristic where it has a unique periodic orbit located at O as shown in equation 9. For a single ANF system, three functional outputs will be produced by the ANF, which are the filtered cos signal noted by \bar{x} but in negative magnitude, filtered sin signal noted as $\dot{\bar{x}}$ which is identified as the input signal and finally $\bar{\theta}$ as the frequency of the signal.

$$O = \begin{pmatrix} \bar{x} \\ \dot{\bar{x}} \\ \bar{\theta} \end{pmatrix} = \begin{pmatrix} -A_1 \cos(\omega_0 t + \varphi_1) / \omega_0 \\ A_1 \sin \omega_0 (\omega_0 t + \varphi_1) \\ \omega_0 \end{pmatrix} \quad (9)$$

When involving a three-phase power system, for a shunt active power filter, the measurement of the waveform will apply three-phase waveforms of voltage and

current for supply and load. Any three-phase sinusoidal voltage or current can be represented based on equation 10.

$$u(t) = \begin{pmatrix} u_a(t) \\ u_b(t) \\ u_c(t) \end{pmatrix} = \begin{pmatrix} A_a \sin(\omega t + \phi_a) \\ A_b \sin(\omega t + \phi_b) \\ A_c \sin(\omega t + \phi_c) \end{pmatrix} \quad (10)$$

For the three-phase application, improvement can be applied to the ANF in terms of frequency tracking as the filter shares the common frequency ω_0 in the same electrical power system. Based on this, the frequency law of triple ANF can be shared, thus reducing the complexity of the ANF from the 9th order to the 7th order integration function. The ANF will work in parallel order in extracting the fundamental components by sharing the standard frequency over time. The fundamental equation of the ANF for a three-phase system can be nominated in equations 11,12, and 13, where the phase is represented as n for phases a, b, and c. Meanwhile, the updated law of frequency is based on the summation of the error signal of all three phases.

$$\ddot{x}_n + \theta^2 x_n = 2\varepsilon \theta e_n(t) \quad (11)$$

$$\dot{\theta} = -y\theta \sum x_n e_n(t) \quad (12)$$

$$e_n(t) = u_n(t) - \dot{x}_n \quad (13)$$

When the equation is expanded to the respective phase, the ANF phase error equation is given as equation 14, the error for each phase is inserted into equation 12, where the ANF phase update law is given as equation 15.

$$e_n(t) = \begin{pmatrix} e_a(t) \\ e_b(t) \\ e_c(t) \end{pmatrix} = \begin{pmatrix} u_a(t) - \dot{x}_a \\ u_b(t) - \dot{x}_b \\ u_c(t) - \dot{x}_c \end{pmatrix} \quad (14)$$

$$\begin{aligned} \dot{\theta} &= -y\theta \sum x_n e_n(t) = -y\theta (x_a e_a(t) + x_b e_b(t) + x_c e_c(t)) \\ &= -y\theta (x_a (u_a(t) - \dot{x}_a) + x_b (u_b(t) - \dot{x}_b) + x_c (u_c(t) - \dot{x}_c)) \\ &= -y(\theta x_a (u_a(t) - \dot{x}_a) + \theta x_b (u_b(t) - \dot{x}_b) + \theta x_c (u_c(t) - \dot{x}_c)) \end{aligned} \quad (15)$$

The ANF for each phase is given as equation 16, where θ is obtained from the integration of $\dot{\theta}$ and x obtained from the double integration of \ddot{x} .

$$\begin{pmatrix} ANF_a \\ ANF_b \\ ANF_c \end{pmatrix} = \begin{pmatrix} \ddot{x}_a + \theta^2 x_a = 2\varepsilon \theta e_a(t) \\ \ddot{x}_b + \theta^2 x_b = 2\varepsilon \theta e_b(t) \\ \ddot{x}_c + \theta^2 x_c = 2\varepsilon \theta e_c(t) \end{pmatrix} \quad (16)$$

3.2. Reference current estimation

In a three-phase power system, based on equation 4, the power flow within the system usually consists of absolute power, reactive power, and harmonics power. Therefore, the power term containing all efficient and non-efficient powers terms in the three-phase system is defined as eq 17.

$$S_e^2 = (3V_{e1}I_{e1})^2 + (3V_{e1}I_{eH})^2 + (3V_{eH}I_{e1})^2 + (3V_{eH}I_{eH})^2 \quad (17)$$

Where $(3V_{e1}I_{e1})^2$ refers to the fundamental effective apparent power and $(3V_{e1}I_{eH})^2 + (3V_{eH}I_{e1})^2 + (3V_{eH}I_{eH})^2$ refers to nonfundamental effective apparent power. By applying ANF for the measured voltage and current, their fundamental components can be extracted, and the fundamental power for the system can be obtained based on the extracted components. Based on this, the estimation of the reference supply current will be produced. However, to ensure the successful task of SAPF, the DC link voltage needs to be controlled to ensure that it is maintained at the reference value. As the DC link of a SAPF acquires its power from the line and is accustomed to losses due to switches and active power transfer, the DC link voltage is exposed to various disturbances, leading to instability of the voltage. To be overwhelmed with this condition, a DC link control is essential to the SAPF. The DC-link reference is determined and compared with this system's measured DC link voltage. The error between the reference and measured DC link voltage is passed into the proportional-integral controller (PI). Loss is integrated into the instantaneous power equation, as in equation 18.

$$\bar{p}_{3\phi} = v_a i_a + v_b i_b + v_c i_c + P_{dc} \quad (18)$$

The error or difference obtained from DC link voltage measurement is shown in equation 19, and the PI controller is applied towards the error to get the value as power losses of DC-link shown in equation 20 below.

$$e_{vdc}(t) = v_{dcref} - v_{dcsense} \quad (19)$$

$$P_{dc} = P_{dc}(t-1) + K_p(e_{vdc}(t) - e_{vdc}(n-1)) + K_i e_{vdc}(t) \quad (20)$$

Meanwhile, the three-phase reference supply is obtained through the fryze equation [27–30], where this method determines the reference current based on the average value of three-phase instantaneous power. The equivalent conductivity calculates the average current, and the average admittance is determined based on the concept of aggregate voltage as follows,

$$G_e = \frac{\bar{p}_{3\phi}}{V_2^2}, \quad \text{where } V_2^2 = \sqrt{v_a^2 + v_b^2 + v_c^2} \quad (22)$$

When the equation is expanded, the reference current can be given as,

$$i_{refk} = G_e v_k, \quad k = (a, b, c) \quad (23)$$

$$\vec{i}_{refk} = \begin{bmatrix} \vec{i}_{refa} \\ \vec{i}_{refb} \\ \vec{i}_{refc} \end{bmatrix} = \begin{bmatrix} \frac{(v_a i_a + v_b i_b + v_c i_c + P_{dc}) \times v_a}{\sqrt{v_a^2 + v_b^2 + v_c^2}} \\ \frac{(v_a i_a + v_b i_b + v_c i_c + P_{dc}) \times v_b}{\sqrt{v_a^2 + v_b^2 + v_c^2}} \\ \frac{(v_a i_a + v_b i_b + v_c i_c + P_{dc}) \times v_c}{\sqrt{v_a^2 + v_b^2 + v_c^2}} \end{bmatrix} \quad (24)$$

The individual reference current for each phase sequence can be obtained from equation 24.

4.Result and Analysis

The performance of the proposed EFANF is verified by simulation and experimental works. Table 1 describes the parameters of design that are being applied in the simulation.

Table 1. Simulation Parameters

Parameter	Value
Source Voltage	415 V (RMS), 50 Hz
Source Impedance	1Ω, 1mH
DC Link Capacitance	3300 μF
DC Link Reference Voltage	700 V
Filtering Inductor	5 mH
ANF Gains	$\varepsilon = 0.16$, $\gamma = 180$
Non-linear load (3 Phase rectifier with 3 load conditions)	Resistive Load
	R1 = 80 Ω, R2= 50 Ω and R3 = 36 Ω
	Resistive with Inductive Load
	R1L1 = 77Ω 30H, R2L2 = 69Ω 36H
	R3L3= 41Ω 41H
	Resistive with Capacitive Load
	R1C1 = 65Ω 12uF, R2C2 = 65Ω 19uF and R3C3 = 65Ω 36uF

4.1. Simulation Results

The performance, reliability, and efficiency of the EFANF for a balanced three-phase SAPF are initially simulated and evaluated using MATLAB-Simulink. According to the circuit shown in figure 1, inputs for the EFANF algorithm are based on the measured $i_{sa}, i_{sb}, i_{sc}, i_{la}, i_{lb}, i_{lc}$ and the three-phase source voltage v_{sa}, v_{sb}, v_{sc} to come out with currents references $\vec{i}_{refa}, \vec{i}_{refb}, \vec{i}_{refc}$ for the APF. Evaluation is based on resistive load for three load conditions and tested for sudden changes of load for increasing and decreasing current and the keenness of the EFANF to succumb to the changes. The operation is tested to activate the APF after reaching a simulation time of 0.1s.

The system will be subjected to a non-linear rectifier with three different resistivity values for the output. Figure 2 shows the output waveform of the power system connected with SAPF at the point of PCC. The measurement is taken before the PCC for source voltage (V_s) and sources current (I_s) and after the PCC for load voltage (V_l) and load current (I_l). As shown in Figure 2, the system's voltage is a pure sinusoidal waveform, and the load is a distorted waveform due to the rectifier. Figure 5 focuses on phase-A waveforms for source voltage, source current, load voltage, and load current. Based on the Fast Fourier Transform (FFT) analysis, it can be shown that the harmonics due to non-linear load are given in figure 7, where the THD value is 28.29 percent.

Based on figure 3, the current source waveform is being mitigated from the distortion by the SAPF. From point 0.1s, the load waveform has become sinusoidal, and at the same time, no distortion occurred within the source voltage and load voltage, and there is not also change that happened towards the load current. The APF is successfully mitigating the harmonics at the PCC. To evaluate the APF currents, details of the reference current, compensation current, and filter current are given in figure 4. It is shown that the EFANF managed to extract the fundamental current after three cycles of the waveform, and the compensation current is provided in the equation below.

$$i_{comp} = i_{source} - i_{ref} \quad (22)$$

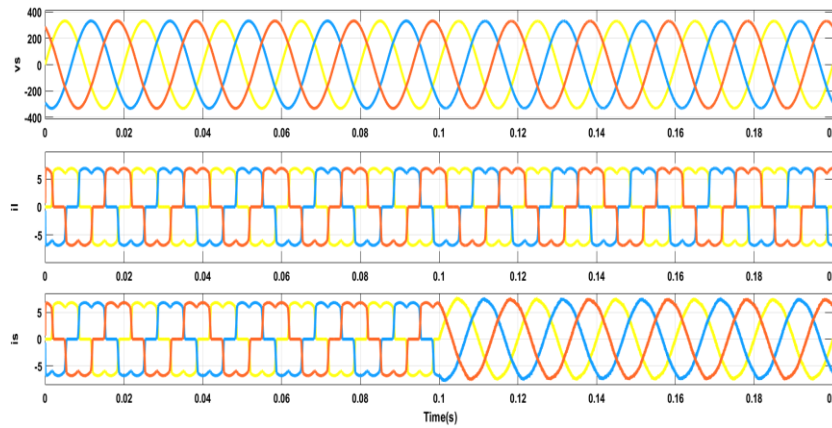


Figure 2. Simulation results of 80 Ω load for source voltage, load current, and source current before and after activation of APF.

Figure 4 shows the waveform for the reference current, compensation current, and filter current for phase a. The ANF produces the reference current and inputs it into the APF current control. The difference between the reference and source current will have the required compensation current for the APF to mitigate the harmonics. At simulation time 0.1s, the APF is activated, and the filtering current follows the required harmonics mitigation value for the load. The total harmonics distortion value of the source current after connecting APF is seen to reduce to 3.20 % due to the compensation current, as shown in Figure 5.

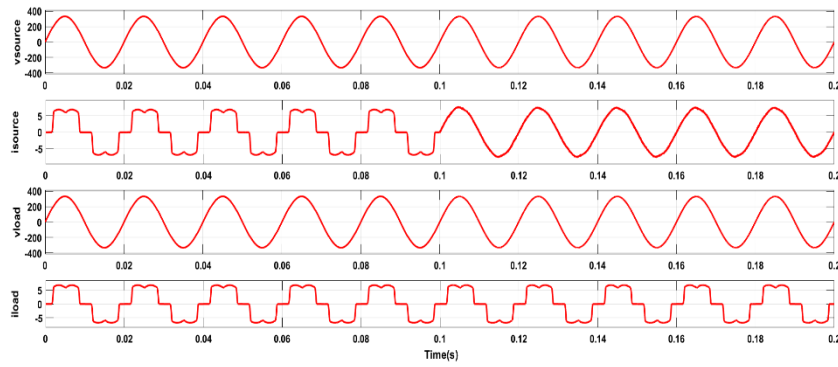


Figure 3. Simulation results for phase A before and after activation of APF

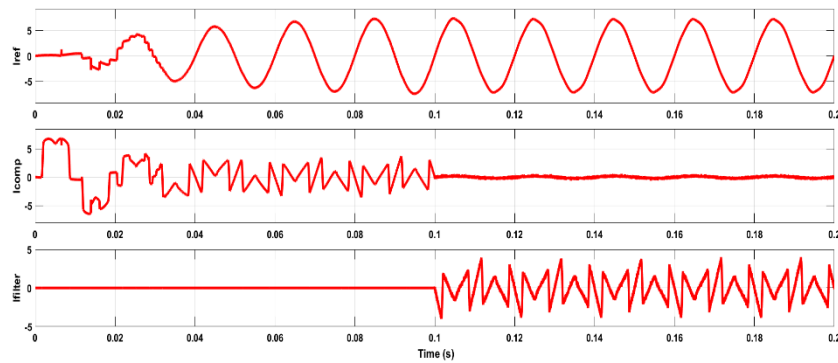


Figure 4. Simulation result for reference current, compensation current, and filter current before and after activating APF for phase a.

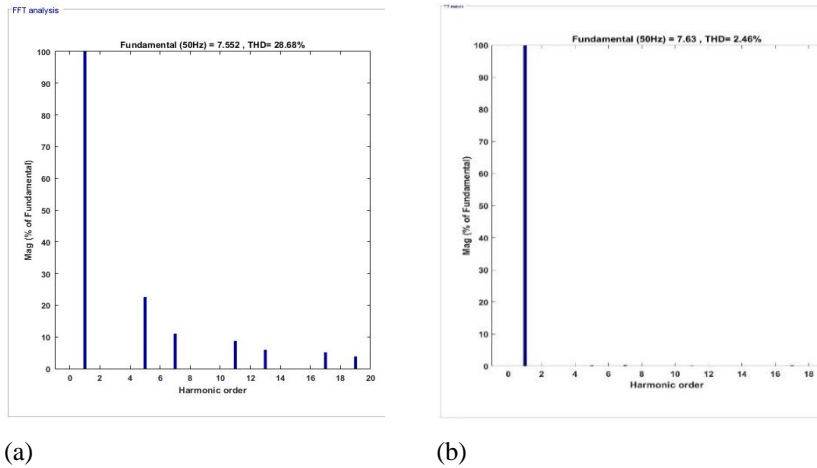


Figure 5. THD analysis for simulation of 80- Ω load (a) before connecting APF and (b) after connecting APF

Furthermore, the EFANF is simulated with two other stationary load conditions: resistive loads of 50 and 36 ohms, respectively. The waveforms of the voltage source, load current, and source current after compensation for both given loads are shown. In contrast, for investigated waveform for a single dedicated phase, a can be seen in Figure . Based on the measured waveforms shown in Figure 7, the EFANF provided the reference signal to the SAPF controller and mitigated the harmonics for all the stationary load conditions. The SAPF managed to bring down the THD from 28.29 % to 2.55% for 50- Ω load and 2.40% for 36- Ω load, respectively, as highlighted in the spectrum FFT analysis in Figure 8. The obtained results confirm the capability of the EFANF in compensation purposes for operating SPAF to mitigate harmonics produced by the non-linear load system.

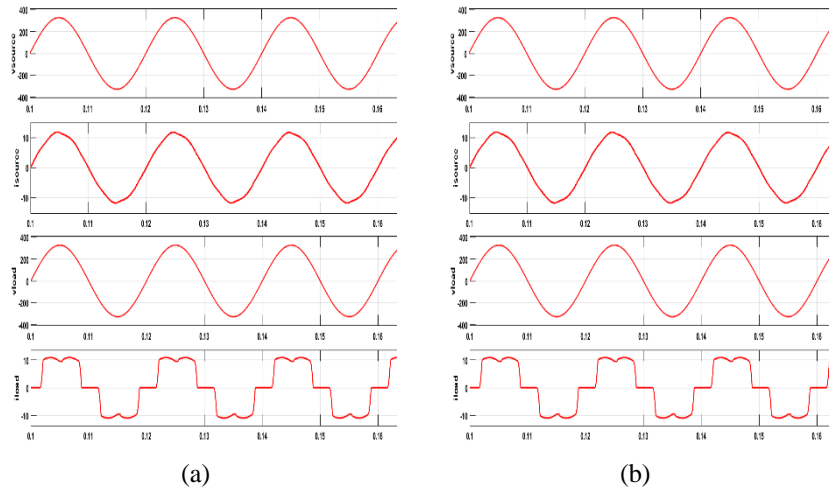


Figure 6. Simulation results of phase-a source voltage, source current, load voltage, and load current for (a) 50- Ω and (b) 36- Ω loads

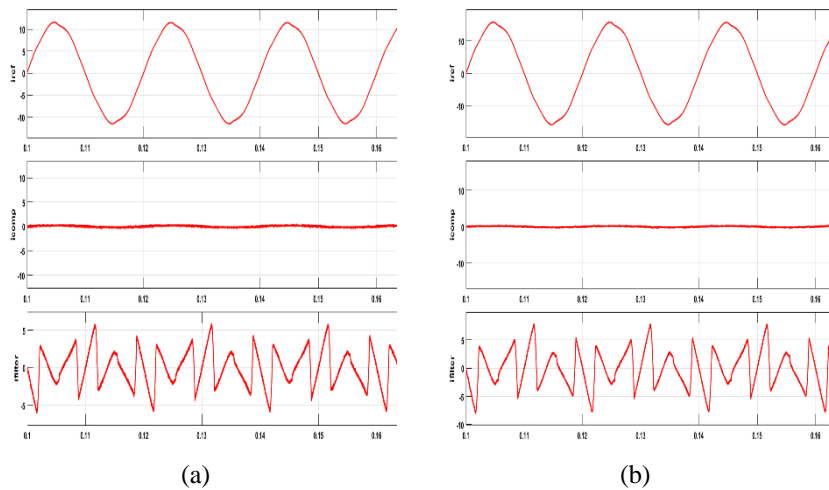


Figure 7. Simulation results of phase a reference current, compensation current, and reference current for (a) 50- Ω and (b) 36- Ω loads

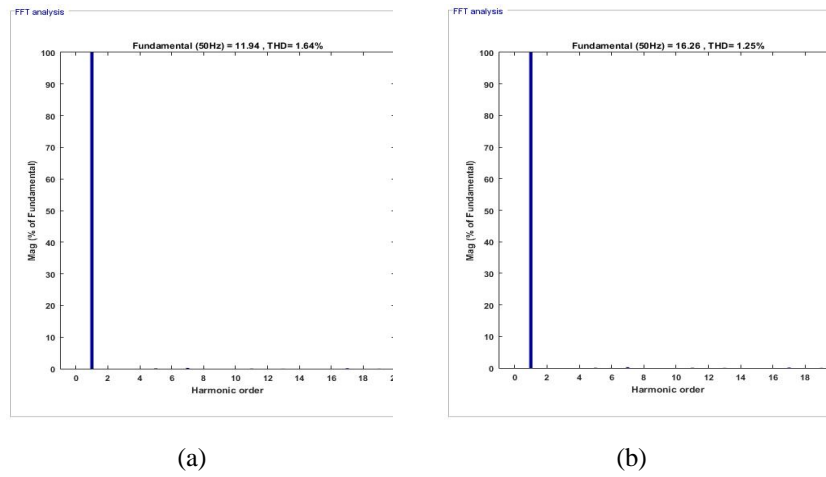


Figure 8. THD result after APF compensation for (a) 50 Ω and (b) 36 Ω loads

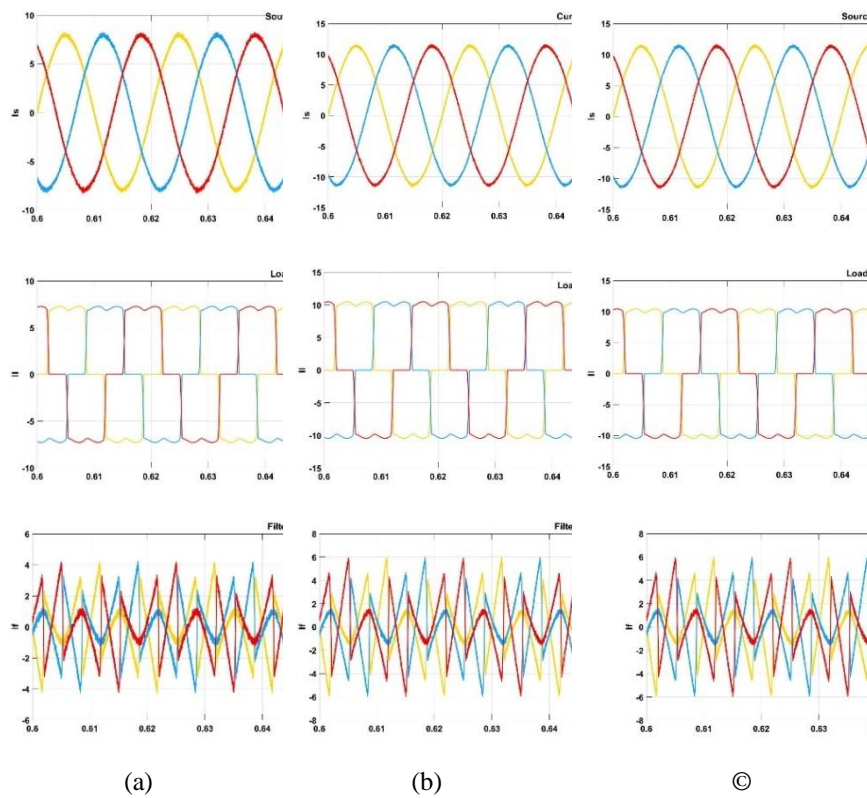


Figure 9. Simulation results of source current, load current and filter current for (a) R1L1, (b) R2L2, and (c) R3L3 loads

The proposed algorithm was also tested under different variations of loads for reactive power compensation under inductive and capacitive base loads to validate the adaptabilities of the algorithm in SAPF mitigation for the various waveform. Figure 9 shows the result of the proposed EFANF for resistive with inductive load for three different loads, which are R1L1, R2L2, and R3L3 for source current, load current and filter current. On the other hand, Figure 10 shows the source, load, and filter currents for three different resistive with capacitive loads given as R1C1, R2C2, and R3C3. Comparing the load current and source current for all three related loads, resistive with inductive and resistive with capacitive, shows that the EFANF can mitigate both reactive power compensation for resistive with inductive loads and resistive with capacitive loads.

The THD values of the current source after mitigation for all loads are given as 2.41% for R1L1, 1.73% for R2L2, 1.25% for R3L3, 1.91% for R1C1, 2.09% for R2C2, and 2.54% for R3C3. Based on the given THD values, it can be proved that the EFANF can supply the SAPF effective reference current to reach the IEEE standard for the value of the harmonic below 5%..

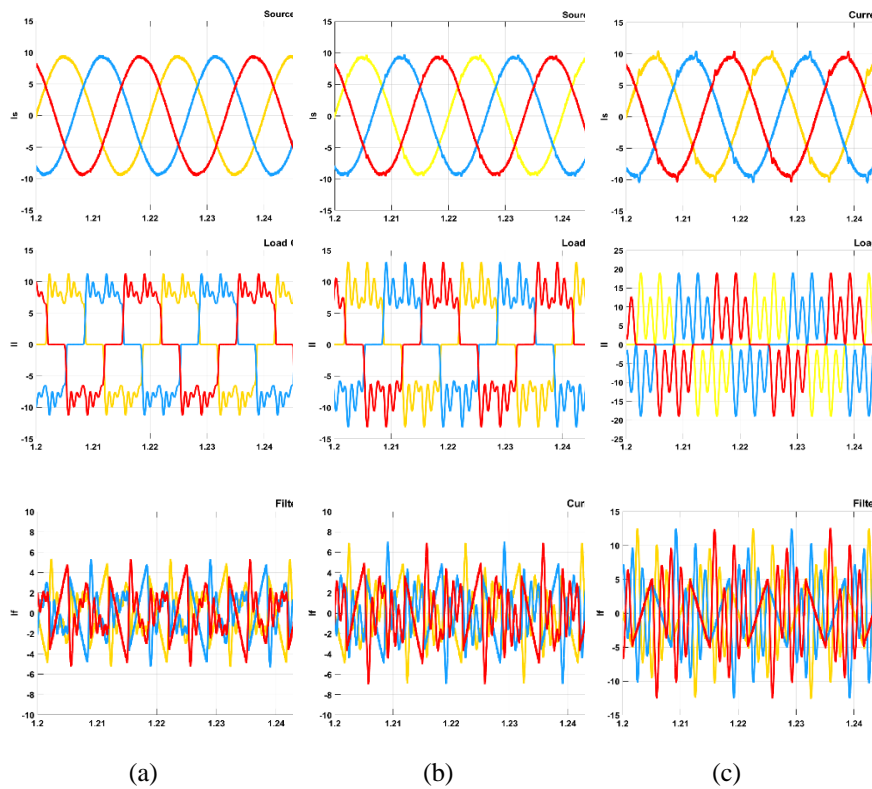


Figure 10. Simulation results of source current, load current, and filter current for (a) R1C1, (b) R2C2, and (c) R3C3 loads

Adaptableness of the EFANF is also being evaluated. The proposed algorithm is also simulated under a dynamic-state condition where the load will change between three resistivity load values that will directly affect the amount of current in the system. The dynamic changes are evaluated in changes of a resistive load from $82\text{-}\Omega$ to $50\text{-}\Omega$ and from $50\text{-}\Omega$ to $36\text{-}\Omega$, where the changes will induce the increase of current changes. Figure 11 provides simulation results for both conditions with the voltage source, load current, and current source at transition points. It is shown that the EFANF managed to cater to the changes in load and respond to them immediately, whereas based on the figure, the EFANF required 0.05s to correspond to the changes.

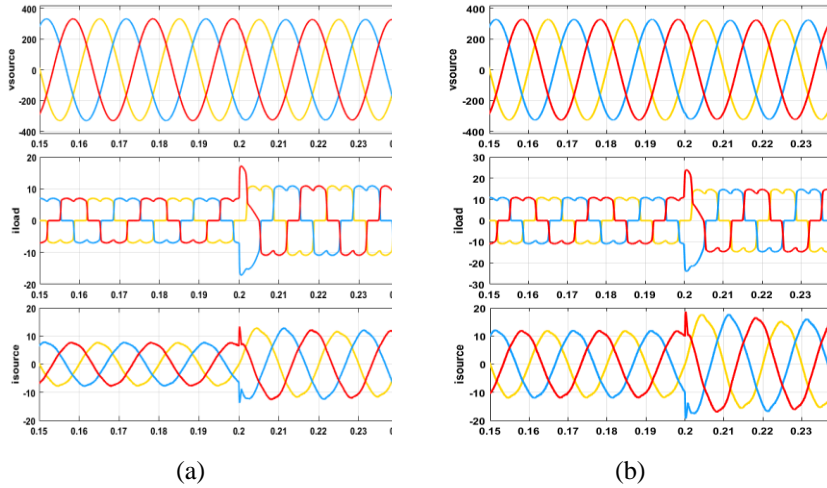


Figure 11. Simulation results of source voltage, load current, and source current under transient-state conditions for (a) $86\text{-}\Omega$ to $50\text{-}\Omega$ and (b) $50\text{-}\Omega$ to $36\text{-}\Omega$

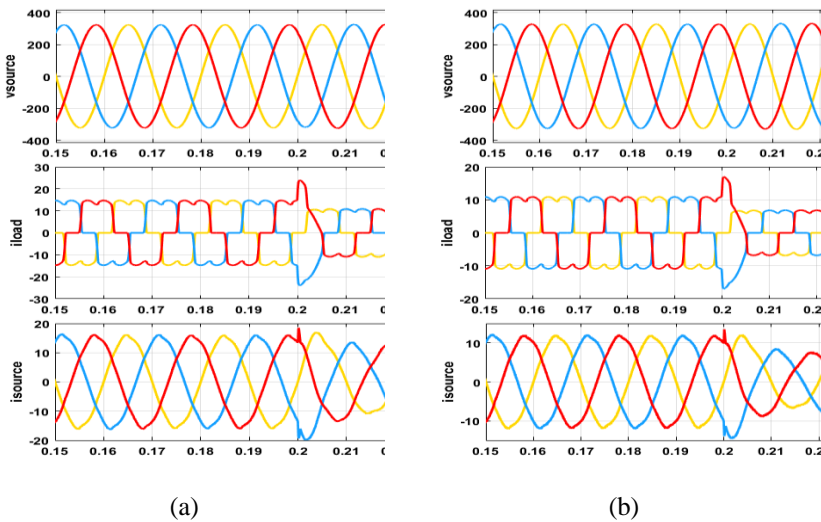


Figure 12. Simulated result of EFANF under dynamic changes for loads of (a) $36\text{-}\Omega$ to $50\text{-}\Omega$ and (b) $50\text{-}\Omega$ to $82\text{-}\Omega$

Furthermore, the EFANF adaptability to dynamic changes is also simulated for the loads' changes from 36 ohms to 50 ohms and 50 ohms to 82 ohms. The simulated waveforms are presented in Figure 12 for both conditions, where the figure illustrates source voltage, load current, and source current. The findings confirmed the capability of the EFANF to produce the corresponding reference current within both stationary and transient conditions.

4.2. Experimental Results

A laboratory hardware setup was developed to validate the proposed algorithm. The hardware consisted of measurement circuits with current and voltage sensors, a three-phase inverter connected to the filtering inductor as APF, and DSPACE RS1104 as the controller, as shown in Figure 13. A DSpace controller board is the connection point between the sensors and the output signals. For the APF, a three-phase inverter with DC-link is connected as the voltage source. The prominent role of the DSPACE is to implement the harmonics extraction algorithm, which will generate the reference current based on the EFANF. For the experiment, the supplied voltage of the system is set at 50Hz, 100 Vrms (line-to-line voltage). The experimental results of utilization of the proposed EFANF algorithm with PI DC-link control for resistive loads are shown in Figure 16. The results include source voltage v_s , source current i_s , load current i_l and filter current i_{filter} .

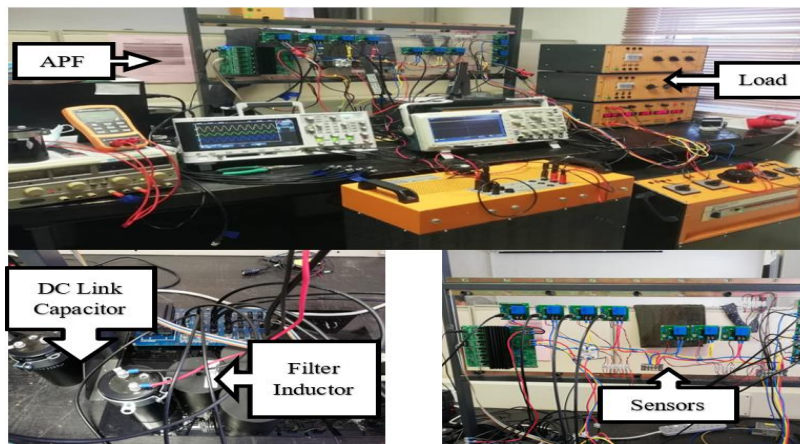


Figure 13. Laboratory hardware setup

The SAPF with EFANF effectively mitigates the harmonic current for the steady-state condition. The measurement is done using the Agilent DSO-X 2014A oscilloscope for the experimental result, covering source voltage, source current, load current, and filter current. In terms of THD calculation, the measurement is done by downloading the data from the oscilloscope. The data are then measured for harmonics decomposition using FFT analysis in MATLAB/Simulink. From the results, the algorithm managed to reduce the harmonics of the source current with THD from 62% to 3.46 % for 80 Ohms load, 28.77% to 3.73 % for 50 Ohms load, and 28.56% to 3.99 % for 36 Ohms load. All harmonics are managed to be reduced below the required IEE standard, 5%. Nevertheless, the THDs of the three-phase supply current are monitored to see the algorithm's effectiveness in the experimental work, where the THD value can be seen in Figure 14.

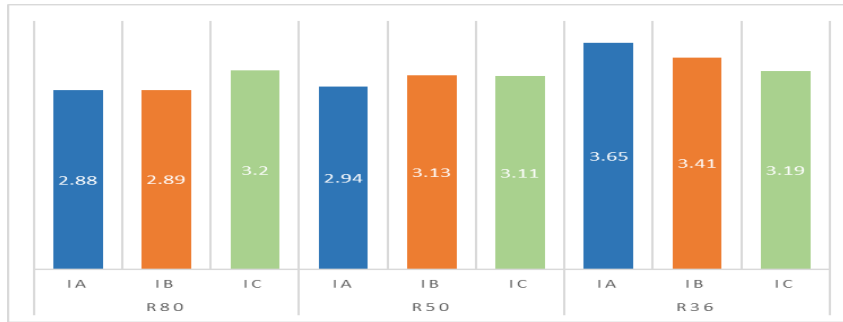


Figure 14. Experimental results of THD for three-phase source current after compensation

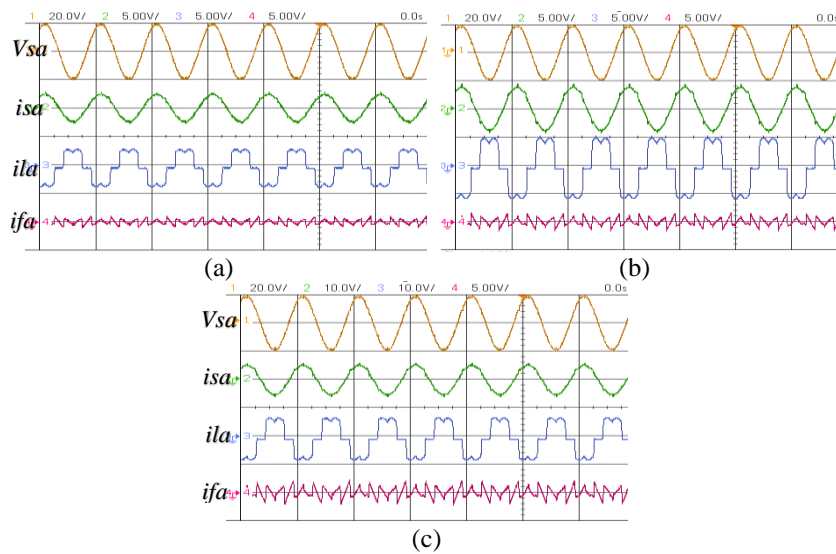


Figure 15. Experimental results of source voltage, source current, load current, filter current and THD values for (a) 82-Ω (b) 50-Ω and (c) 36-Ω loads

Figure 15 shows the waveforms of phase-a source voltage, source current, load current, and filter current in a steady-state condition obtained from experimental work. The source current waveform is sinusoidal and is in phase with the measured source voltage. Thus, THD is reduced for all the given loads, as shown in the figure.

The response of the proposed algorithm for steady-state conditions, when introduced to an inductive and capacitive load, is also confirmed with the experimental setup. The result is shown in Figure 16, where it can be verified that the proposed algorithm can mitigate resistive with inductive loads for values R1L1, R2L2, and R3L3. After mitigation, the source current loads THD are given as 2.70%, 2.63%, and 2.78%, respectively.

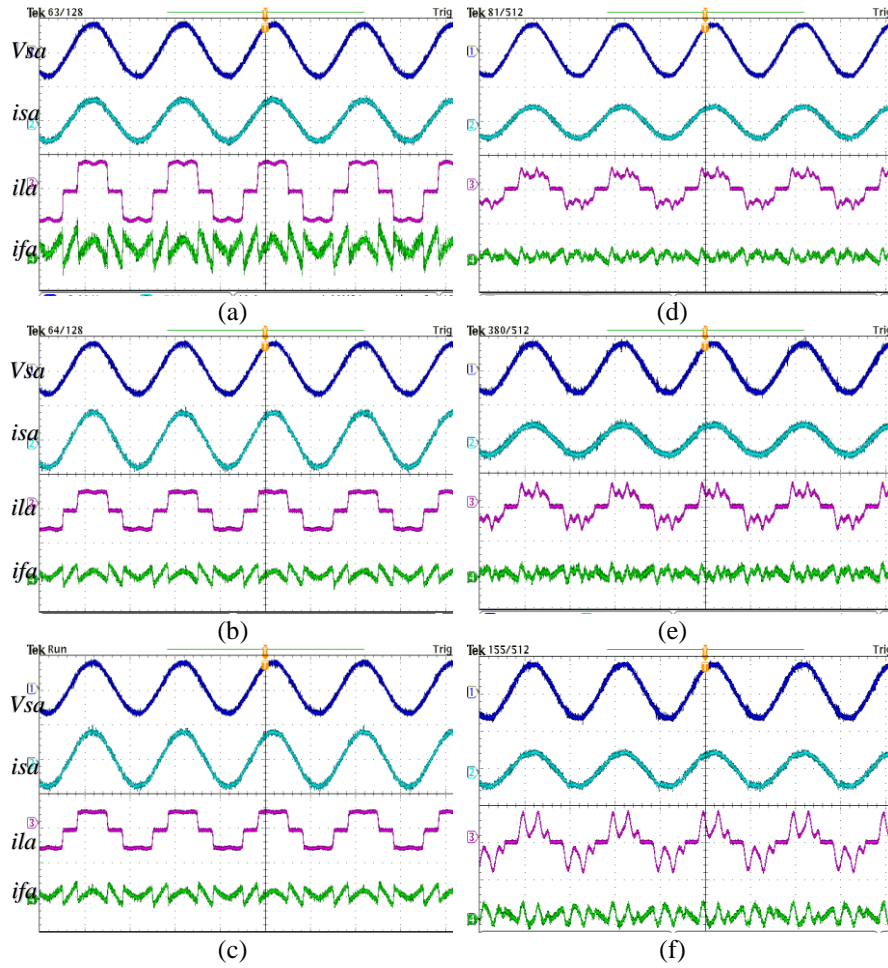


Figure 16. Experimental results of source voltage, source current, load current, filter current and THD values for (a) 67- Ω and 30H, (b) 69- Ω and 36H, (c) 76- Ω and 41H loads, (d) 60- Ω 12uF, (e) 60- Ω 17uF and (f) 60- Ω 36uF loads

The resistive with capacitive loads values of R1C1, R2C2, and R3C3. The values are within the required IEEE standard. THD's mitigated source current values are 2.52%, 2.99%, and 5.00% for each load. Based on these values, it can be concluded that the proposed EFANF algorithm can produce the appropriate reference current for the SAPF to work effectively. The SAPF also seems to have better stabilities for the resistive and inductive loads than capacitive loads. However, in terms of mitigation, the EFANF can mitigate all the different types of loads in the experimental setup.

The effectiveness and feasibility of the proposed algorithm were also verified for transient-state operation during load-changing conditions. Figure 17 shows the state for reducing load capacity, which causes ascending current state, Figure 17 also

shows the increased load capacity, which causes descending current state. In both states, the EFANF managed to mitigate within 20ms for all load changes.

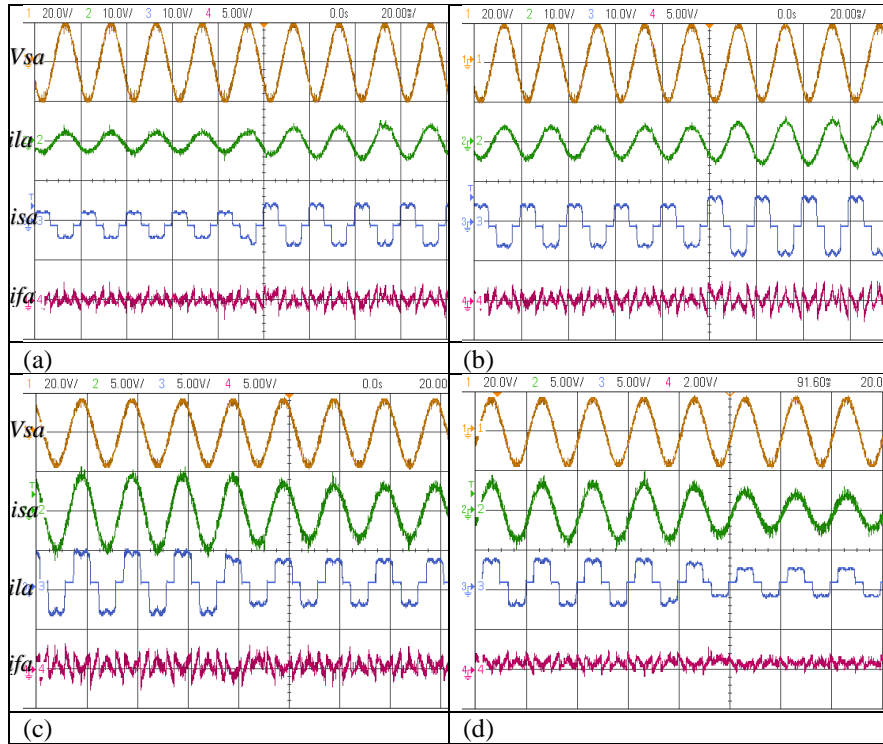


Figure 17. Experimental results of source voltage, source current, load current, filter current, and DC-Link voltage during transient-state conditions of (a) 82- Ω to 50- Ω (b) 50- Ω to 36- Ω (c) 82- Ω to 50- Ω and (d) 50- Ω to 36- Ω

5. Conclusions

This paper presents the EFANF extraction algorithm utilized in SAPF to compensate for current harmonics in the three-phase three-wire system. The proposed algorithm demonstrated its capability to generate the reference current based on the notch filtering technique, as shown in both simulation results in MATLAB/Simulink and experimental work based on the validation with DSPACE RS1104. As the EFANF is self-synchro based on frequency adaptability, PLL is not required. The algorithm extracted the fundamental component and mitigated harmonics in balanced load conditions based on the analyses of steady-state and transient state conditions. The performance of the proposed algorithm has also been verified for different types and values of reactive loads both in simulation and experimental works. The design of the EFANF also gives an optional improvement on the DC link voltage control algorithm as the losses of the DC link is provided as power losses within the system. In terms of performance, the EFANF managed to produce the THD according to the requirement of the IEE standard. Furthermore, the algorithm can adapt to the different types of loads.

Nomenclatures

v_{sa}, v_{sb}, v_{sc}	Voltage source phase a, b and c, Volt
i_{sa}, i_{sb}, i_{sc}	Current source phase a, b and c, Ampere
$\bar{i}_{refa}, \bar{i}_{refb}, \bar{i}_{refc}$	Generated reference current phase a, b and c Ampere
$3V_{e1}I_{e1}$	Fundamental effective apparent power
$3V_{eH}I_{eH}$	Harmonics power
G_e	The equivalent conductivity

Greek Symbols

ω_0	Reference frequency
θ	Estimation Frequency
γ	Accuracy coefficients
ε	Convergence speed coefficients
$\hat{\theta}$	Updated law for the frequency estimation

Abbreviations

APF	Active Power Filter
SAPF	Shunt Active Power Filter
THD	Total Harmonics Distortion
EFANF	Extended Fryze Adaptive Notch Filter

References

1. F. Zare, H. Soltani, D. Kumar, P. Davari, H.A.M. Delpino, F. Blaabjerg, Harmonic Emissions of Three-Phase Diode Rectifiers in Distribution Networks, IEEE Access. 5 (2017) 2819–2833. <https://doi.org/10.1109/ACCESS.2017.2669578>.
2. A. Alizade, J.B. Noshahr, Evaluating noise and DC offset due to inter-harmonics and supra-harmonics caused by back-to-back converter of (DFIG) in AC distribution network, CIRED - Open Access Proc. J. 2017 (2017) 629–632. <https://doi.org/10.1049/oap-cired.2017.0045>.
3. K.D. Patil, W.Z. Gandhare, Effects of harmonics in distribution systems on temperature rise and life of XLPE power cables, 2011 Int. Conf. Power Energy Syst. ICPS 2011. (2011) 1–6. <https://doi.org/10.1109/ICPES.2011.6156680>.
4. T. Toumi, A. Allali, A. Meftouhi, O. Abdelkhalek, A. Benabdelkader, M. Denai, Robust control of series active power filters for power quality enhancement in distribution grids: Simulation and experimental validation, ISA Trans. 107 (2020) 350–359. <https://doi.org/10.1016/j.isatra.2020.07.024>.
5. E. Sundaram, M. Venugopal, On design and implementation of three phase three level shunt active power filter for harmonic reduction using synchronous reference frame theory, Int. J. Electr. Power Energy Syst. 81 (2016) 40–47. <https://doi.org/10.1016/j.ijepes.2016.02.008>.
6. H. Liu, H. Hu, H. Chen, L. Zhang, Y. Xing, Fast and Flexible Selective Harmonic Extraction Methods Based on the Generalized Discrete Fourier

- Transform, IEEE Trans. Power Electron. 33 (2018) 3484–3496. <https://doi.org/10.1109/TPEL.2017.2703138>.
7. R. Panigrahi, B. Subudhi, Performance Enhancement of Shunt Active Power Filter Using a Kalman Filter-Based H^∞ Control Strategy, IEEE Trans. Power Electron. 32 (2017) 2622–2630. <https://doi.org/10.1109/TPEL.2016.2572142>.
 8. V.N. Jayasankar, U. Vinatha, Backstepping Controller with Dual Self-Tuning Filter for Single-Phase Shunt Active Power Filters under Distorted Grid Voltage Condition, IEEE Trans. Ind. Appl. 56 (2020) 7176–7184. <https://doi.org/10.1109/TIA.2020.3025520>.
 9. F. Harirchi, M.G. Simoes, Enhanced Instantaneous Power Theory Decomposition for Power Quality Smart Converter Applications, IEEE Trans. Power Electron. 33 (2018) 9344–9359. <https://doi.org/10.1109/TPEL.2018.2791954>.
 10. Y.W. Liu, S.H. Rau, C.J. Wu, W.J. Lee, Improvement of Power Quality by Using Advanced Reactive Power Compensation, IEEE Trans. Ind. Appl. 54 (2018) 18–24. <https://doi.org/10.1109/TIA.2017.2740840>.
 11. A. Chebabhi, M.K. Fellah, A. Kessal, M.F. Benkhoris, A new balancing three level three dimensional space vector modulation strategy for three level neutral point clamped four leg inverter based shunt active power filter controlling by non-linear back stepping controllers, ISA Trans. 63 (2016) 328–342. <https://doi.org/10.1016/j.isatra.2016.03.001>.
 12. A. Naderipour, Z. Abdul-Malek, V.K. Ramachandaramurthy, A. Kalam, M.R. Miveh, Hierarchical control strategy for a three-phase 4-wire microgrid under unbalanced and non-linear load conditions, ISA Trans. 94 (2019) 352–369. <https://doi.org/10.1016/j.isatra.2019.04.025>.
 13. Y. Hoon, M.A.A.M. Zainuri, A.S. Al-Ogaili, A.N. Al-Masri, J. Teh, Active Power Filtering under Unbalanced and Distorted Grid Conditions Using Modular Fundamental Element Detection Technique, IEEE Access. 9 (2021) 107502–107518. <https://doi.org/10.1109/ACCESS.2021.3101238>.
 14. S. Hou, J. Fei, C. Chen, Y. Chu, Finite-Time Adaptive Fuzzy-Neural-Network Control of Active Power Filter, IEEE Trans. Power Electron. 34 (2019) 10298–10313. <https://doi.org/10.1109/TPEL.2019.2893618>.
 15. S. Hou, J. Fei, Y. Chu, Nonsingular Terminal Sliding Mode Control of Active Power Filter, Chinese Control Conf. CCC. 2018-July (2018) 2982–2987. <https://doi.org/10.23919/ChiCC.2018.8483224>.
 16. K.H. Tan, F.J. Lin, J.H. Chen, DC-Link voltage regulation using RPFNN-AMF for Three-Phase active power filter, IEEE Access. 6 (2018) 37454–37463. <https://doi.org/10.1109/ACCESS.2018.2851250>.
 17. L. Merabet, S. Saad, D.O. Abdeslam, J. Merckle, Direct neural method for harmonic currents estimation using adaptive linear element, Electr. Power Syst. Res. 152 (2017) 61–70. <https://doi.org/10.1016/j.epsr.2017.06.018>.
 18. B. Singh, S.R. Arya, K. Kant, Notch filter-based fundamental frequency component extraction to control distribution static compensator for mitigating current-related power quality problems, IET Power Electron. 8 (2015) 1758–1766. <https://doi.org/10.1049/iet-pel.2014.0486>.

19. S. Kewat, B. Singh, Modified amplitude adaptive control algorithm for power quality improvement in multiple distributed generation system, *IET Power Electron.* 12 (2019) 2321–2329. <https://doi.org/10.1049/iet-pel.2018.5936>.
20. D. Yazdani, A. Bakhshai, P. Jain, A three-phase approach to harmonic and reactive current extraction and harmonic decomposition, *IECON Proc. (Industrial Electron. Conf.* 25 (2009) 3205–3210. <https://doi.org/10.1109/IECON.2009.5415218>.
21. R.S.R. Chilipi, N. Al Sayari, K.H. Al Hosani, A.R. Beig, Adaptive Notch Filter-Based Multipurpose Control Scheme for Grid-Interfaced Three-Phase Four-Wire DG Inverter, *IEEE Trans. Ind. Appl.* 53 (2017) 4015–4027. <https://doi.org/10.1109/TIA.2017.2676098>.
22. G. Fujita, N.D. Dinh, T. Funabashi, N.D. Tuyen, Adaptive notch filter solution under unbalanced and/or distorted point of common coupling voltage for three-phase four-wire shunt active power filter with sinusoidal utility current strategy, *IET Gener. Transm. Distrib.* 9 (2015) 1580–1596. <https://doi.org/10.1049/iet-gtd.2014.1017>.
23. N.D. Tuyen, G. Fujita, T. Funabashi, M. Nomura, Adaptive notch filter for synchronization and islanding detection using negative-sequence impedance measurement, *IEEJ Trans. Electr. Electron. Eng.* 7 (2012) 240–250. <https://doi.org/10.1002/tee.21724>.
24. M. Mojiri, A.R. Bakhshai, Stability analysis of periodic orbit of an adaptive notch filter for frequency estimation of a periodic signal, *Automatica.* 43 (2007) 450–455. <https://doi.org/10.1016/j.automatica.2006.08.018>.
25. M. Mojiri, A.R. Bakhshai, An Adaptive Notch Filter for Frequency Estimation of a Periodic Signal, *IEEE Trans. Automat. Contr.* 49 (2004) 314–318. <https://doi.org/10.1109/TAC.2003.821414>.
26. M. Mojiri, M. Karimi-Ghartemani, A. Bakhshai, Processing of harmonics and interharmonics using an adaptive notch filter, *IEEE Trans. Power Deliv.* 25 (2010) 534–542. <https://doi.org/10.1109/TPWRD.2009.2036624>.
27. X. Nie, J. Liu, Current Reference Control for Shunt Active Power Filters under Unbalanced and Distorted Supply Voltage Conditions, *IEEE Access.* 7 (2019) 177048–177055. <https://doi.org/10.1109/ACCESS.2019.2957946>.
28. D. TESHOME, T.D. Huang, K.-L. Lian, A Distinctive Load Feature Extraction Based on Fryze's Time-domain Power Theory, *IEEE Power Energy Technol. Syst. J.* 3 (2016) 1–1. <https://doi.org/10.1109/jpets.2016.2559507>.
29. S.K. Kesharvani, A. Singh, M. Badoni, Conductance based fryze algorithm for improving power quality for non-linear loads, 2014 Int. Conf. Signal Propag. Comput. Technol. ICSPCT 2014. (2014) 703–708. <https://doi.org/10.1109/ICSPCT.2014.6884965>.
30. Z. Zeng, R. Zhao, H. Yang, Coordinated control of multi-functional grid-tied inverters using conductance and susceptance limitation, *IET Power Electron.* 7 (2014) 1821–1831. <https://doi.org/10.1049/iet-pel.2013.0692>.

REVIEW FORM

Title of paper: CURRENT HARMONICS QUALITY MITIGATION TECHNIQUE FOR THREE-PHASE POWER SYSTEM BASED ON EXTENDED FRYZE ADAPTIVE NOTCH FILTER

For sections A & B, please tick a number from 0 to 5, where 0 = strongly disagree and 5 = strongly agree.

A. Technical aspects

- | | | | | | | |
|--|----------------------------|----------------------------|----------------------------|----------------------------|---------------------------------------|----------------------------|
| 1. The paper is within the scope of the Journal. | <input type="checkbox"/> 0 | <input type="checkbox"/> 1 | <input type="checkbox"/> 2 | <input type="checkbox"/> 3 | <input checked="" type="checkbox"/> 4 | <input type="checkbox"/> 5 |
| 2. The paper is original. | <input type="checkbox"/> 0 | <input type="checkbox"/> 1 | <input type="checkbox"/> 2 | <input type="checkbox"/> 3 | <input checked="" type="checkbox"/> 4 | <input type="checkbox"/> 5 |
| 3. The paper is free of technical errors. | <input type="checkbox"/> 0 | <input type="checkbox"/> 1 | <input type="checkbox"/> 2 | <input type="checkbox"/> 3 | <input checked="" type="checkbox"/> 4 | <input type="checkbox"/> 5 |

B. Communications aspects

- | | | | | | | |
|--|----------------------------|----------------------------|----------------------------|----------------------------|---------------------------------------|----------------------------|
| 1. The paper is clearly readable. | <input type="checkbox"/> 0 | <input type="checkbox"/> 1 | <input type="checkbox"/> 2 | <input type="checkbox"/> 3 | <input checked="" type="checkbox"/> 4 | <input type="checkbox"/> 5 |
| 2. The figures are clear & do clearly convey the intended message. | <input type="checkbox"/> 0 | <input type="checkbox"/> 1 | <input type="checkbox"/> 2 | <input type="checkbox"/> 3 | <input checked="" type="checkbox"/> 4 | <input type="checkbox"/> 5 |
| 3. The length of the paper is appropriate. | <input type="checkbox"/> 0 | <input type="checkbox"/> 1 | <input type="checkbox"/> 2 | <input type="checkbox"/> 3 | <input checked="" type="checkbox"/> 4 | <input type="checkbox"/> 5 |

C. Comments to the authors (You may use another sheet of paper.)

1. In the conclusion of the abstract section state the most significant THD improvement of the source current with the proposed method using either the results of Matlab simulations or the results of laboratory experiments.
2. Use italic models to write quantities and units in Table 1 (use Microsoft Equation).
3. Create Figure 6a and Figure 6b in two rows of the figures table respectively (not in the double-column model).
4. Create Figure 7a and Figure 7b in two rows of the figures table respectively (not in the column model).
5. Create Figure 9a, Figure 9b, and Figure 9c in three rows of the figures table respectively (not in the three-column model)
6. Create Figure 10a, Figure 10b, and Figure 10c in three rows of the figures table respectively (not in the three-column model)
7. Create Figure 11a and Figure 11b in two rows of the figures table respectively (not in the double column model)
8. Create Figure 12a and Figure 12b in two rows of the figures table respectively (not in the double column model)
9. Figure 14 not only shows a bar diagram of THD source current after compensation, but also before compensation on the non-linear load ($R = 80 \text{ ohm}$, $R = 50 \text{ ohm}$, and $R = 36 \text{ ohm}$). This revised figure will help the readers understand that your proposed method has better performance after compensation. After that, you have to make a clear analysis of the new figure.
10. Make Fig 15a, Fig 15b, and Fig 15c in the form of a three-row table respectively. Fig 15a and Fig 15b are too short for a two-column form because the two figures will be truncated.

11. Create Figure 16a to Figure 16f in six rows of the figures table respectively (not in the double column model).
12. Make Fig 17a, Fig 17b, Fig 17c, and Fig 17d in the form of a four-row table respectively (not in the double column model).
13. Describe in detail the weaknesses of your method and the future work needed to improve these weaknesses. Explain in a last single paragraph in the conclusion section.

D. Recommendation (Tick one)

1. Accepted without modifications. ☐
2. Accepted with minor corrections. ☒
3. Accepted with major modification. ☐
4. Rejected. ☐

E. Comments to the editors (These comments will not be sent to the authors)

CURRENT HARMONICS QUALITY MITIGATION TECHNIQUE FOR THREE-PHASE POWER SYSTEM BASED ON EXTENDED FRYZE ADAPTIVE NOTCH FILTER

Abstract

The power quality problem, especially regarding harmonics contamination, has dramatically affected the overall power system stability. In response to this, using an Active Power Filter (APF) is considered one of the compelling methods to overcome harmonics issues. This paper presents the implementation of Shunt APF with an improved adaptive notch filter known as Extended Fryze Adaptive Notch Filter (EFANF) for fundamental signal extraction. The adaptive notch filter has improved the utilization from a single-phase to three-phase application for direct fundamental signal extraction and is designed to cater DC link voltage regulation controllers based on the power loss equation. This extraction algorithm inherits simple design construction and frequency tracking, eliminating PLL reliance on synchronization. The algorithm's effectiveness in operation for the Shunt APF is validated through simulation using MATLAB/Simulink and experiment work by integrating the algorithm with DSPACE RS1104. Based on both evaluations, the results obtained show a satisfactory and reasonable agreement in mitigating the harmonics for multi-load conditions. Simulation and experimentally proven harmonics mitigation managed to reduce under 5% following the IEE standard, and the algorithm function within expectation for both steady and transient state conditions. Furthermore, the DC link also tended to be maintained by the algorithm.

Keywords: Adaptive notch filter, Fryze, shunt active power filter, Harmonics.

Commented [WU1]: 1. In the conclusion of the abstract section state the most significant THD improvement of the source current with the proposed method using either the results of Matlab simulations or the results of laboratory experiments.

1. Introduction

The development of power systems has shaped multiple power generation, transmission, distribution, and application segments. All the advancements are often polluting and distorting the power system by increasing the utilization of non-linear loads, mainly contributed by power-electronics devices [1–3]. The need for power electronics devices can exponentially increase within the industrial and consumer sectors. Based on the extensive use of sensitive loads, such as computers and microprocessor-based industrial controllers, and now with the emergence of renewable energy such as solar and wind and the growth of electric vehicles, there is a growing need for effective harmonic measurement and compensation systems. Although conventional solutions have been used to mitigate power quality, such as passive filters in terms of harmonics, the solution is deemed ineffective, especially when involving load changes. As implementation of standard regulation in power flow is becoming more rigid such as IEEE519 and IEC 61000-3-2, active power compensation is seen as a better choice in realizing power quality (PQ) control.

Active power compensation offers better PQ compensation, especially harmonics, power factor, and active-reactive power control. Furthermore, the protection, management, performance, and efficiency of active power compensation are realized through continuous development in developing signal processing, detection, and extraction within mathematical algorithms and hardware throughout the past years. One of the apparatuses demonstrating a solid ability to eliminate harmonics is the Active Power Filter (APF) system. Such filters are an excellent way to reduce harmonic disturbances of voltage and current, sudden voltage fluctuations, transient disturbances, and current and voltage faults. Currently, there are multiple topologies of active power compensation available for additional compensation, such as series active power filter [4], shunt active power filter (SAPF), hybrid active power filter, and Unified Power Quality Conditioner (UPQC). Effective and efficient compensations are compulsory when dealing with harmonics' power quality. Hence, a precise algorithm is essential for extracting harmonics elements in controlling the power system's active power filter (APF). Over the years, various identification and extraction techniques have been developed; the methods can be divided into time and frequency domains.

The methods used in the frequency-based domain vary from commonly used fast Fourier and discrete Fourier algorithms, Kalman Filtering algorithm to wavelet transformation algorithm [5–7]. When using the mentioned techniques, most of the algorithms designed in the frequency domain require transformation, which is a little tedious to be applied in the time domain and usually incongruous with changing load in the power system. Another drawback of the frequency domain method is that it requires numerous cycles for better current estimation. In applying APF, the commonly used extraction method is usually within the time domain to cater to the changing waveform of loads in real-time situations, especially when involved with data acquisition. The time-domain techniques are divided into a few categories: classical methods derived from instantaneous power theory [8–10] and synchronous power theory [11–13], such as PQ, PQR, etc. DQ method. However, these methods usually involve multi-conversion planes and require additional filters to extract the information.

Another emerging method is the intelligent algorithms, which vary from the neural network, adaptive neural network, and adaptive linear neuron, where all these algorithms require training within the process [14–17]. Besides these three methods, another method used in the APF is the notch filter method, which is simple in design and can accommodate changes in loads [18]. The work introduced adaptive notch filters as harmonics, interharmonics processing methods, and time-domain signal analysis [19]. However, the method is limited to only processing information due to the algorithm's lack of a controlling method for DC link control. Yazdani et al. also proposed the ANF for three-phase application [20], which performed harmonic reactive current extraction and harmonic decomposition. However, the work was limited to monitoring and extraction only. In some other works, the ANF replaces the lowpass filter function in the PQ algorithm for shunt APF [21–23] with a three-phase four-wire system.

Although the strategy takes advantage of the transformation of the frame for instantaneous power flow, the application of ANF has increased the algorithm's complexity as the method includes the transformation process and integration of the ANF for filtering purposes. This strategy undermines the ANF's capability to directly filter the system's fundamental signal.

To utilize the potential of the ANF in shunt APF application. This paper presents an extended ANF application for harmonics extraction, DC link control, and current control. Within this method, three elements are focused on as the APF control system: the computational algorithm of reference current, the voltage regulation for the DC link control, and the generation of the firing pulse of the voltage source inverter (VSI). The main section of the paper is the proposed Extended Fryze Adaptive Notch Filter (EFANF) as the main algorithm component. The algorithm implements the Adaptive Notch Filter (ANF) extraction algorithm and the Fryze algorithm as system power control. Adjacent to the adaptive capability of the ANF, the algorithm also provides self-synchronization for the EFANF. This section also discusses the implementation of DC link voltage regulation, where the PI method is introduced as stability control within the EFANF, all highlighted in sections 2 and 3. The simulation and experimental works results are explained in section 4 of the paper. Finally, section 5 concludes the research contribution and highlights the overall significance of the impact of the work.

2. Principle operation of shunt APF

Shunt APF is implemented using a current control-voltage source inverter (CC-VSI), as shown in figure 1. The CC-VSI are connected in parallel with the non-linear loads through filter inductance. The CC-VSI performs the main task within the power quality system: inject (opposite magnitude) any unwanted harmonics current components produced due to the load current in the supply system at the point of common coupling (PCC).

The instantaneous current source of the overall system is given in equation 1 where $i_s(t)$ is the source current, $i_L(t)$ is the load current and $i_c(t)$ is the compensation current.

$$i_s(t) = i_L(t) - i_c(t) \quad (1)$$

Meanwhile, the instantaneous voltage source $v_s(t)$ is given in equation 2, and the non-linear load current can be considered as the embodiment of fundamental current component and harmonics current components, as shown in equation 3

$$v_s(t) = V_m \sin \omega t \quad (2)$$

$$i_L(t) = \sum_{n=1}^{\infty} I_n \sin(n\omega t + \phi_n) \\ = I_1 \sin(\omega t + \phi_1) + \sum_{n=2}^{\infty} I_n \sin(n\omega t + \phi_n) \quad (3)$$

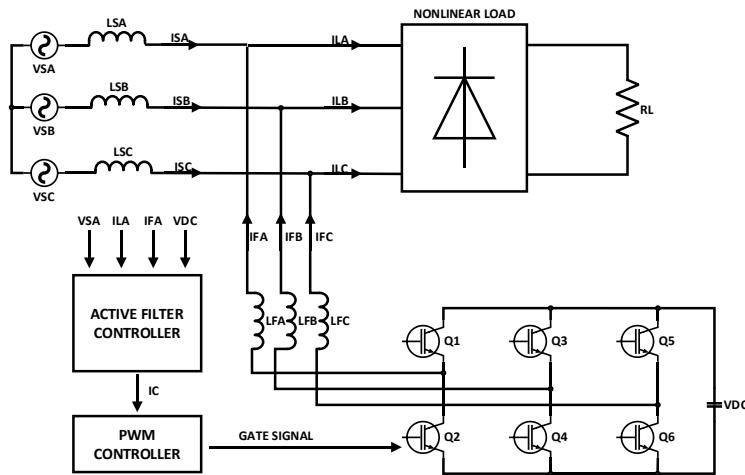


Fig. 1. Shunt APF System

The instantaneous power of the load $p_L(t)$ can be figured out based on equation 4 given as

$$p_L(t) = i_s(t) \times v_s(t) \\ = V_m \sin^2 \omega t \times \cos \phi_1 + V_m I_1 \sin \omega t \times \cos \omega t \times \sin \phi_1 \\ + V_m \sin \omega t \left(\sum_{n=2}^{\infty} I_n \sin(n\omega t + \phi_n) \right) \\ = p_f(t) + p_r(t) + p_h(t) \quad (4)$$

The equation consists of active power $p_f(t)$, reactive power $p_r(t)$, and harmonics-induced power $p_h(t)$. Based on this, the real power drawn from the load is given in equation 5.

$$p_f(t) = V_m I_1 \sin^2 \omega t \times \cos \phi_1 \quad (5)$$

3. Principle Of Current Control System

The structure of the current control system is shown in figure 1. The system can be divided into three major components. The first part is the computation of the reference current using an extended fryze adaptive notch filter (EFANF), the second part is the self-synchronization of the EFANF, and the third component is the DC link voltage regulation and the firing pulses for the APF.

3.1. Adaptive Notch Filter

Ideally, an adaptive notch filter (ANF) works in the concept of a linear gain applied for all the frequencies except a specified frequency where the frequency gain is zero. Based on this characteristic, the filter can withdraw an implicit signal of the sinusoidal waveform from the specified frequency's measured component of an electrical power system. ANF has well been researched in removing noises within the sinusoidal waveform[24]. Originally, ANF is based on an IIR filter[25]; however, with improvement in the notch frequency, the filter can adapt to notch frequency change with time by tracking the input signal frequency variation. This tracking capability eliminates the need for the signal frequency to be consistent, as is usually required for the typical notch filter to work efficiently. The ANF's dynamic operation can refer to the following set of differential equations.

$$\ddot{x} + \theta^2 x = 2\varepsilon\theta e(t) \quad (6)$$

$$\dot{\theta} = -\gamma x \theta e(t) \quad (7)$$

$$e(t) = u(t) - \dot{x} \quad (8)$$

The ANF can be composed of the following elements based on the differential equations. The input signal of the ANF is given by $u(t)$. The estimation frequency of the ANF system is given by θ . The accuracy and convergence speed are determined by two coefficients within the ANF known as γ and ε . The two coefficients, however, must compensate each other for the ANF to work effectively and most efficiently, $\dot{\theta}$ represents the updated law for the frequency estimation [26].

In a functional single sinusoidal input $u(t) = A_1 \sin(\omega_0 t + \varphi_1)$, the used ANF has an explicit characteristic where it has a unique periodic orbit located at O as shown in equation 9. For a single ANF system, three functional outputs will be produced by the ANF, which are the filtered cos signal noted by \bar{x} but in negative magnitude, filtered sin signal noted as $\bar{\dot{x}}$ which is identified as the input signal and finally $\bar{\theta}$ as the frequency of the signal.

$$O = \begin{pmatrix} \bar{x} \\ \bar{\dot{x}} \\ \bar{\theta} \end{pmatrix} = \begin{pmatrix} -A_1 \cos(\omega_0 t + \varphi_1) / \omega_0 \\ A_1 \sin \omega_0 (\omega_0 t + \varphi_1) \\ \omega_0 \end{pmatrix} \quad (9)$$

When involving a three-phase power system, for a shunt active power filter, the measurement of the waveform will apply three-phase waveforms of voltage and

current for supply and load. Any three-phase sinusoidal voltage or current can be represented based on equation 10.

$$u(t) = \begin{pmatrix} u_a(t) \\ u_b(t) \\ u_c(t) \end{pmatrix} = \begin{pmatrix} A_a \sin(\omega t + \phi_a) \\ A_b \sin(\omega t + \phi_b) \\ A_c \sin(\omega t + \phi_c) \end{pmatrix} \quad (10)$$

For the three-phase application, improvement can be applied to the ANF in terms of frequency tracking as the filter shares the common frequency ω_0 in the same electrical power system. Based on this, the frequency law of triple ANF can be shared, thus reducing the complexity of the ANF from the 9th order to the 7th order integration function. The ANF will work in parallel order in extracting the fundamental components by sharing the standard frequency over time. The fundamental equation of the ANF for a three-phase system can be nominated in equations 11, 12, and 13, where the phase is represented as n for phases a , b , and c . Meanwhile, the updated law of frequency is based on the summation of the error signal of all three phases.

$$\ddot{x}_n + \theta^2 x_n = 2\varepsilon\theta e_n(t) \quad (11)$$

$$\dot{\theta} = -\gamma\theta \sum x_n e_n(t) \quad (12)$$

$$e_n(t) = u_n(t) - \dot{x}_n \quad (13)$$

When the equation is expanded to the respective phase, the ANF phase error equation is given as equation 14, the error for each phase is inserted into equation 12, where the ANF phase update law is given as equation 15.

$$e_n(t) = \begin{pmatrix} e_a(t) \\ e_b(t) \\ e_c(t) \end{pmatrix} = \begin{pmatrix} u_a(t) - \dot{x}_a \\ u_b(t) - \dot{x}_b \\ u_c(t) - \dot{x}_c \end{pmatrix} \quad (14)$$

$$\begin{aligned} \dot{\theta} &= -\gamma\theta \sum x_n e_n(t) = -\gamma\theta (x_a e_a(t) + x_b e_b(t) + x_c e_c(t)) \\ &= -\gamma\theta (x_a (u_a(t) - \dot{x}_a) + x_b (u_b(t) - \dot{x}_b) + x_c (u_c(t) - \dot{x}_c)) \\ &= -\gamma(\theta x_a (u_a(t) - \dot{x}_a) + \theta x_b (u_b(t) - \dot{x}_b) + \theta x_c (u_c(t) - \dot{x}_c)) \end{aligned} \quad (15)$$

The ANF for each phase is given as equation 16, where θ is obtained from the integration of $\dot{\theta}$ and x obtained from the double integration of \ddot{x} .

$$\begin{pmatrix} ANF_a \\ ANF_b \\ ANF_c \end{pmatrix} = \begin{pmatrix} \ddot{x}_a + \theta^2 x_a = 2\varepsilon\theta e_a(t) \\ \ddot{x}_b + \theta^2 x_b = 2\varepsilon\theta e_b(t) \\ \ddot{x}_c + \theta^2 x_c = 2\varepsilon\theta e_c(t) \end{pmatrix} \quad (16)$$

3.2. Reference current estimation

In a three-phase power system, based on equation 4, the power flow within the system usually consists of absolute power, reactive power, and harmonics power. Therefore, the power term containing all efficient and non-efficient powers terms in the three-phase system is defined as eq 17.

$$S_e^2 = (3V_{e1}I_{e1})^2 + (3V_{e1}I_{eH})^2 + (3V_{eH}I_{e1})^2 + (3V_{eH}I_{eH})^2 \quad (17)$$

Where $(3V_{e1}I_{e1})^2$ refers to the fundamental effective apparent power and $(3V_{e1}I_{eH})^2 + (3V_{eH}I_{e1})^2 + (3V_{eH}I_{eH})^2$ refers to nonfundamental effective apparent power. By applying ANF for the measured voltage and current, their fundamental components can be extracted, and the fundamental power for the system can be obtained based on the extracted components. Based on this, the estimation of the reference supply current will be produced. However, to ensure the successful task of SAPF, the DC link voltage needs to be controlled to ensure that it is maintained at the reference value. As the DC link of a SAPF acquires its power from the line and is accustomed to losses due to switches and active power transfer, the DC link voltage is exposed to various disturbances, leading to instability of the voltage. To be overwhelmed with this condition, a DC link control is essential to the SAPF. The DC-link reference is determined and compared with this system's measured DC link voltage. The error between the reference and measured DC link voltage is passed into the proportional-integral controller (PI). Loss is integrated into the instantaneous power equation, as in equation 18.

$$\bar{p}_{3\phi} = v_a i_a + v_b i_b + v_c i_c + P_{dc} \quad (18)$$

The error or difference obtained from DC link voltage measurement is shown in equation 19, and the PI controller is applied towards the error to get the value as power losses of DC-link shown in equation 20 below.

$$e_{vdc}(t) = v_{dcref} - v_{dcsense} \quad (19)$$

$$P_{dc} = P_{dc}(t-1) + K_p(e_{vdc}(t) - e_{vdc}(n-1)) + K_i e_{vdc}(t) \quad (20)$$

Meanwhile, the three-phase reference supply is obtained through the fryze equation [27–30], where this method determines the reference current based on the average value of three-phase instantaneous power. The equivalent conductivity calculates the average current, and the average admittance is determined based on the concept of aggregate voltage as follows,

$$G_e = \frac{\bar{p}_{3\phi}}{V_e^2}, \quad \text{where } V_e^2 = \sqrt{v_a^2 + v_b^2 + v_c^2} \quad (22)$$

When the equation is expanded, the reference current can be given as,

$$\bar{i}_{refk} = G_e v_k, \quad k = (a, b, c) \quad (23)$$

$$\vec{i}_{refk} = \begin{bmatrix} \overline{i_{refa}} \\ \overline{i_{refb}} \\ \overline{i_{refc}} \end{bmatrix} = \begin{bmatrix} \frac{(v_a i_a + v_b i_b + v_c i_c + P_{dc}) \times v_a}{\sqrt{v_a^2 + v_b^2 + v_c^2}} \\ \frac{(v_a i_a + v_b i_b + v_c i_c + P_{dc}) \times v_b}{\sqrt{v_a^2 + v_b^2 + v_c^2}} \\ \frac{(v_a i_a + v_b i_b + v_c i_c + P_{dc}) \times v_c}{\sqrt{v_a^2 + v_b^2 + v_c^2}} \end{bmatrix} \quad (24)$$

The individual reference current for each phase sequence can be obtained from equation 24.

4. Result and Analysis

The performance of the proposed EFANF is verified by simulation and experimental works. Table 1 describes the parameters of design that are being applied in the simulation.

Table 1. Simulation Parameters

Parameter	Value
Source Voltage	415 V (RMS), 50 Hz
Source Impedance	1Ω, 1mH
DC Link Capacitance	3300 μF
DC Link Reference Voltage	700 V
Filtering Inductor	5 mH
ANF Gains	$\varepsilon = 0.16$, $\gamma = 180$
Non-linear load (3 Phase rectifier with 3 load conditions)	Resistive Load
	R1 = 80 Ω, R2 = 50 Ω and R3 = 36 Ω
	Resistive with Inductive Load
	R1L1 = 77Ω 30H, R2L2 = 69Ω 36H
	R3L3 = 41Ω 41H
	Resistive with Capacitive Load
	R1C1 = 65Ω 12uF, R2C2 = 65Ω 19uF and R3C3 = 65Ω 36uF

Commented [WU2]: 2. Use italic models to write quantities and units in Table 1 (use Microsoft Equation).

4.1. Simulation Results

The performance, reliability, and efficiency of the EFANF for a balanced three-phase SAPF are initially simulated and evaluated using MATLAB-Simulink. According to the circuit shown in figure 1, inputs for the EFANF algorithm are based on the measured i_{sa} , i_{sb} , i_{sc} , i_{la} , i_{lb} , i_{lc} and the three-phase source voltage v_{sa} , v_{sb} , v_{sc} to come out with currents references $\overline{i_{refa}}$, $\overline{i_{refb}}$, $\overline{i_{refc}}$ for the APF. Evaluation is based on resistive load for three load conditions and tested for sudden changes of load for increasing and decreasing current and the keenness of the EFANF to succumb to the changes. The operation is tested to activate the APF after reaching a simulation time of 0.1s.

The system will be subjected to a non-linear rectifier with three different resistivity values for the output. Figure 2 shows the output waveform of the power system connected with SAPF at the point of PCC. The measurement is taken before the PCC for source voltage (V_s) and sources current (I_s) and after the PCC for load voltage (V_l) and load current (I_l). As shown in Figure 2, the system's voltage is a pure sinusoidal waveform, and the load is a distorted waveform due to the rectifier. Figure 5 focuses on phase-A waveforms for source voltage, source current, load voltage, and load current. Based on the Fast Fourier Transform (FFT) analysis, it can be shown that the harmonics due to non-linear load are given in figure 7, where the THD value is 28.29 percent.

Based on figure 3, the current source waveform is being mitigated from the distortion by the SAPF. From point 0.1s, the load waveform has become sinusoidal, and at the same time, no distortion occurred within the source voltage and load voltage, and there is not also change that happened towards the load current. The APF is successfully mitigating the harmonics at the PCC. To evaluate the APF currents, details of the reference current, compensation current, and filter current are given in figure 4. It is shown that the EFANF managed to extract the fundamental current after three cycles of the waveform, and the compensation current is provided in the equation below.

$$i_{comp} = i_{source} - i_{ref} \quad (22)$$

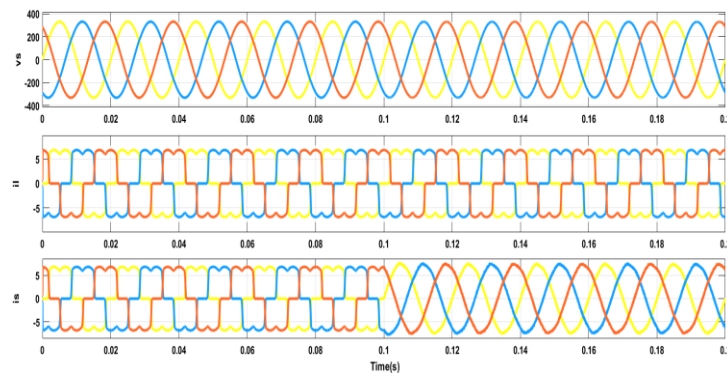


Figure 2. Simulation results of 80 Ω load for source voltage, load current, and source current before and after activation of APF.

Figure 4 shows the waveform for the reference current, compensation current, and filter current for phase a. The ANF produces the reference current and inputs it into the APF current control. The difference between the reference and source current will have the required compensation current for the APF to mitigate the harmonics. At simulation time 0.1s, the APF is activated, and the filtering current follows the required harmonics mitigation value for the load. The total harmonics distortion value of the source current after connecting APF is seen to reduce to 3.20 % due to the compensation current, as shown in Figure 5.

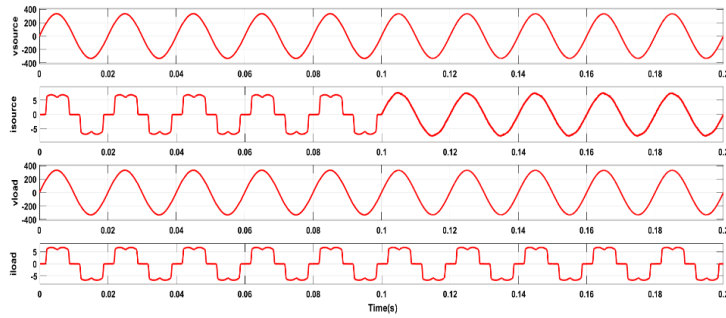


Figure 3. Simulation results for phase A before and after activation of APF

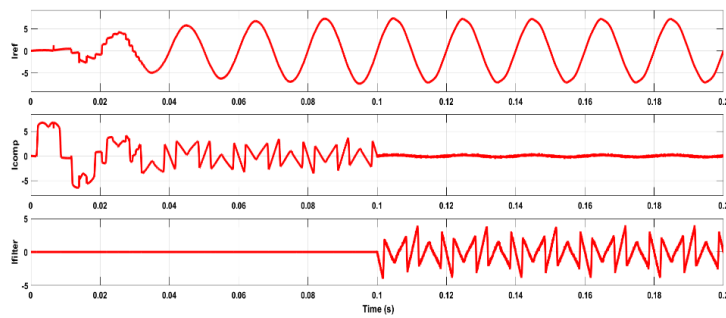


Figure 4. Simulation result for reference current, compensation current, and filter current before and after activating APF for phase a.

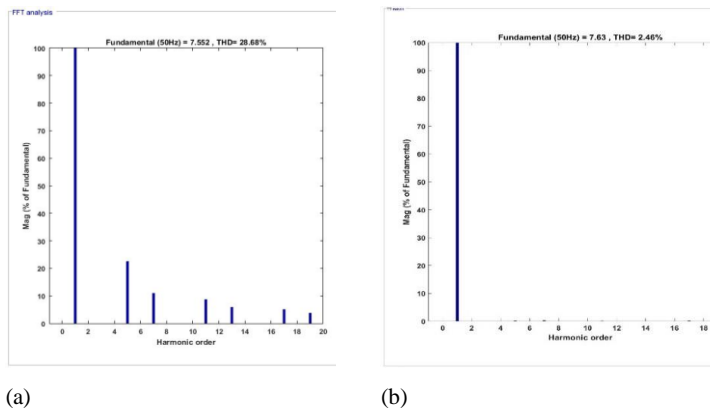


Figure 5. THD analysis for simulation of 80-Ω load (a) before connecting APF and (b) after connecting APF

Furthermore, the EFANF is simulated with two other stationary load conditions: resistive loads of 50 and 36 ohms, respectively. The waveforms of the voltage source, load current, and source current after compensation for both given loads are shown. In contrast, for investigated waveform for a single dedicated phase, a can be seen in Figure . Based on the measured waveforms shown in Figure 7, the EFANF provided the reference signal to the SAPF controller and mitigated the harmonics for all the stationary load conditions. The SAPF managed to bring down the THD from 28.29 % to 2.55% for 50- Ω load and 2.40% for 36- Ω load, respectively, as highlighted in the spectrum FFT analysis in Figure 8. The obtained results confirm the capability of the EFANF in compensation purposes for operating SPAF to mitigate harmonics produced by the non-linear load system.

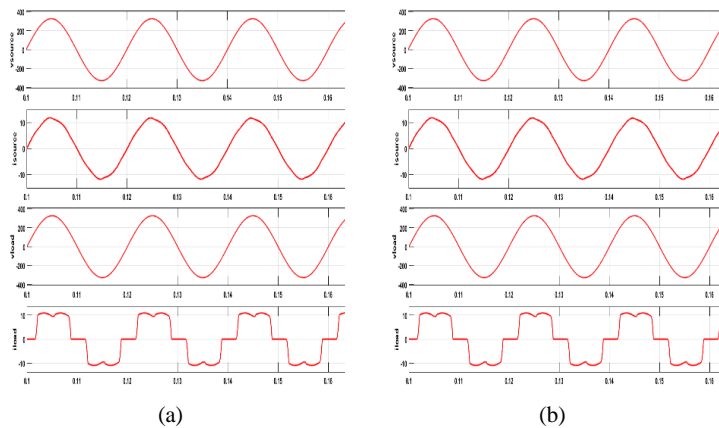


Figure 6. Simulation results of phase-a source voltage, source current, load voltage, and load current for (a) 50- Ω and (b) 36- Ω loads

Commented [WU3]: 3. Create Figure 6a and Figure 6b in two rows of the figures table respectively (not in the double-column model)

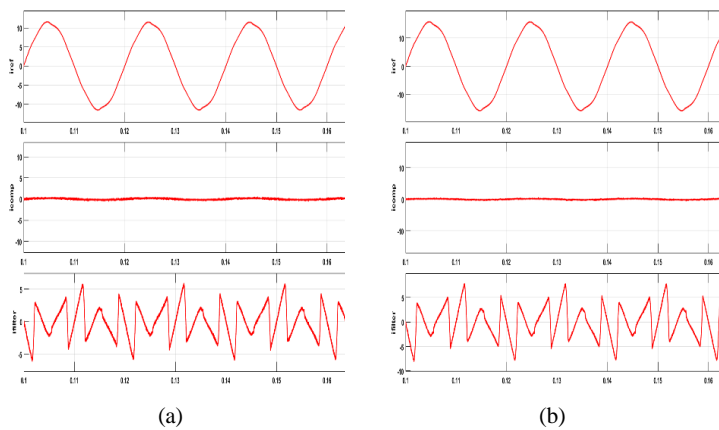


Figure 7. Simulation results of phase a reference current, compensation current, and reference current for (a) 50- Ω and (b) 36- Ω loads

Commented [WU4]: 4. Create Figure 7a and Figure 7b in two rows of the figures table respectively (not in the double-column model)

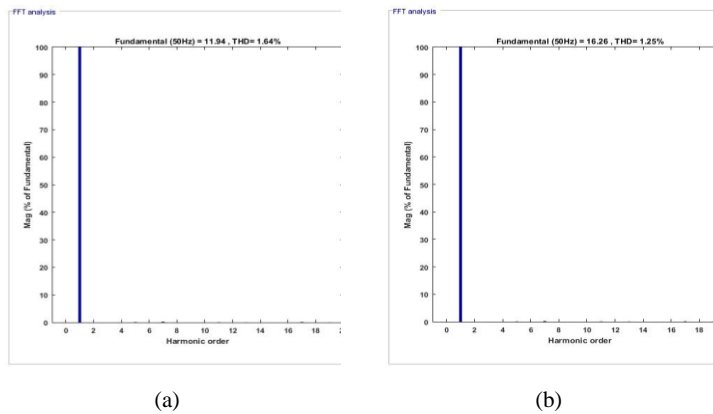


Figure 8. THD result after APF compensation for (a) 50 Ω and (b) 36 Ω loads

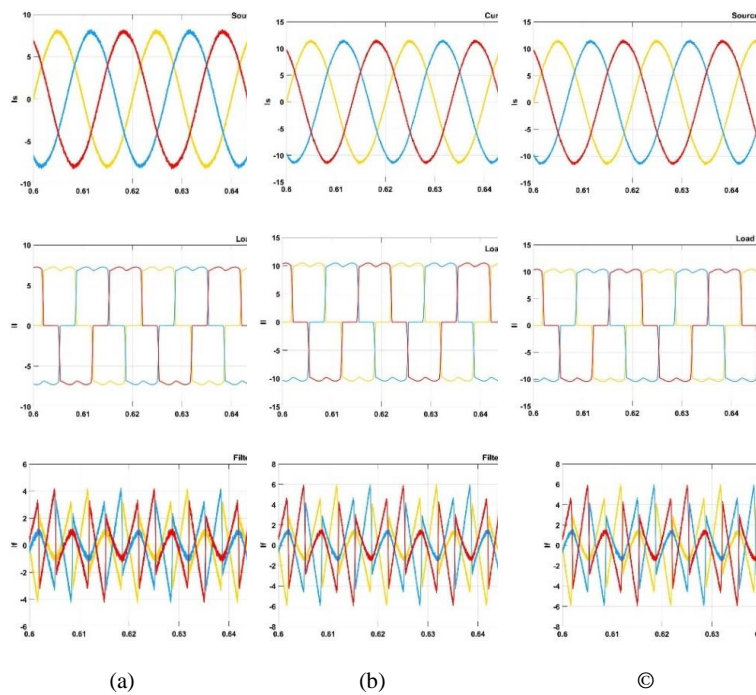


Figure 9. Simulation results of source current, load current and filter current for (a) R1L1, (b) R2L2, and (c) R3L3 loads

Commented [WU5]: 5. Create Figure 9a Figure 9b and Figure 9c in three rows of the figures table respectively (not in the three-column model)

The proposed algorithm was also tested under different variations of loads for reactive power compensation under inductive and capacitive base loads to validate the adaptabilities of the algorithm in SAPF mitigation for the various waveform. Figure 9 shows the result of the proposed EFANF for resistive with inductive load for three different loads, which are R1L1, R2L2, and R3L3 for source current, load current and filter current. On the other hand, Figure 10 shows the source, load, and filter currents for three different resistive with capacitive loads given as R1C1, R2C2, and R3C3. Comparing the load current and source current for all three related loads, resistive with inductive and resistive with capacitive, shows that the EFANF can mitigate both reactive power compensation for resistive with inductive loads and resistive with capacitive loads.

The THD values of the current source after mitigation for all loads are given as 2.41% for R1L1, 1.73% for R2L2, 1.25% for R3L3, 1.91% for R1C1, 2.09% for R2C2, and 2.54% for R3C3. Based on the given THD values, it can be proved that the EFANF can supply the SAPF effective reference current to reach the IEEE standard for the value of the harmonic below 5%..

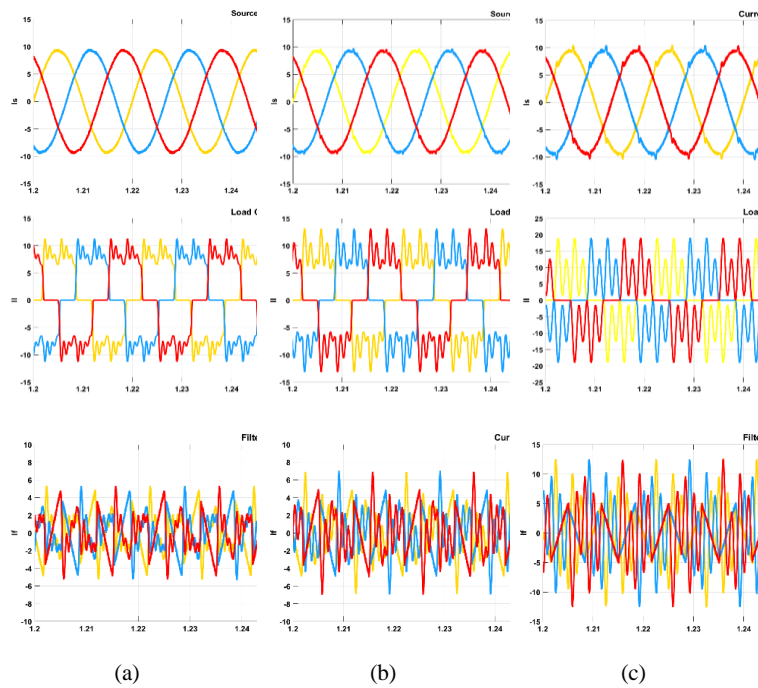


Figure 10. Simulation results of source current, load current, and filter current for (a) R1C1, (b) R2C2, and (c) R3C3 loads

Commented [WU6]: 6. Create Figure 10a Figure 10b and Figure 10c in three rows of the figures table respectively (not in the three-column model)

Adaptableness of the EFANF is also being evaluated. The proposed algorithm is also simulated under a dynamic-state condition where the load will change between three resistivity load values that will directly affect the amount of current in the system. The dynamic changes are evaluated in changes of a resistive load from $82\text{-}\Omega$ to $50\text{-}\Omega$ and from $50\text{-}\Omega$ to $36\text{-}\Omega$, where the changes will induce the increase of current changes. Figure 11 provides simulation results for both conditions with the voltage source, load current, and current source at transition points. It is shown that the EFANF managed to cater to the changes in load and respond to them immediately, whereas based on the figure, the EFANF required 0.05s to correspond to the changes.

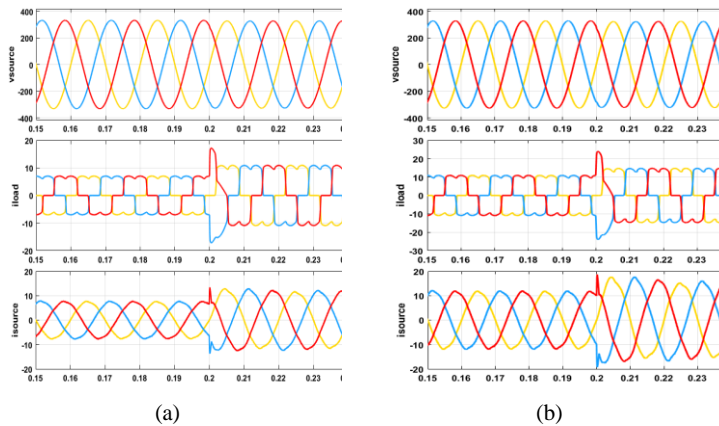


Figure 11. Simulation results of source voltage, load current, and source current under transient-state conditions for (a) $86\text{-}\Omega$ to $50\text{-}\Omega$ and (b) $50\text{-}\Omega$ to $36\text{-}\Omega$

Commented [WU7]: 7.Create Figure 11a and Figure 11b in two rows of the figures table respectively (not in the double column model)

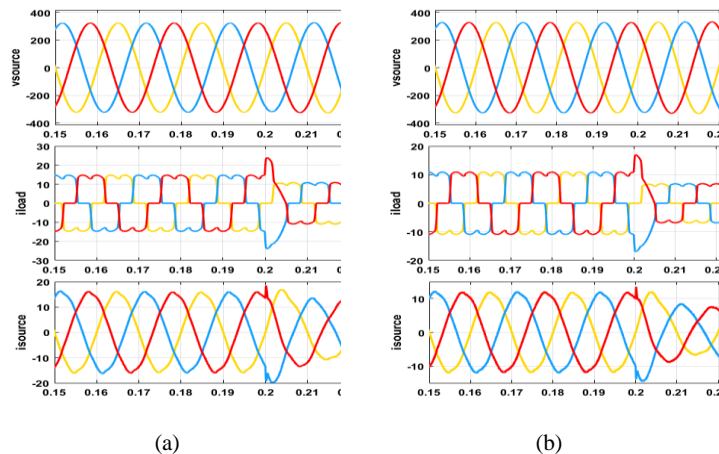


Figure 12. Simulated result of EFANF under dynamic changes for loads of (a) $36\text{-}\Omega$ to $50\text{-}\Omega$ and (b) $50\text{-}\Omega$ to $82\text{-}\Omega$

Commented [WU8]: 8.Create Figure 12a and Figure 12b in two rows of the figures table respectively (not in the double-column model).

Furthermore, the EFANF adaptability to dynamic changes is also simulated for the loads' changes from 36 ohms to 50 ohms and 50 ohms to 82 ohms. The simulated waveforms are presented in Figure 12 for both conditions, where the figure illustrates source voltage, load current, and source current. The findings confirmed the capability of the EFANF to produce the corresponding reference current within both stationary and transient conditions.

4.2. Experimental Results

A laboratory hardware setup was developed to validate the proposed algorithm. The hardware consisted of measurement circuits with current and voltage sensors, a three-phase inverter connected to the filtering inductor as APF, and DSPACE RS1104 as the controller, as shown in Figure 13. A DSpace controller board is the connection point between the sensors and the output signals. For the APF, a three-phase inverter with DC-link is connected as the voltage source. The prominent role of the DSPACE is to implement the harmonics extraction algorithm, which will generate the reference current based on the EFANF. For the experiment, the supplied voltage of the system is set at 50Hz, 100 Vrms (line-to-line voltage). The experimental results of utilization of the proposed EFANF algorithm with PI DC-link control for resistive loads are shown in Figure 16. The results include source voltage v_s , source current i_s , load current i_l and filter current i_{filter} .

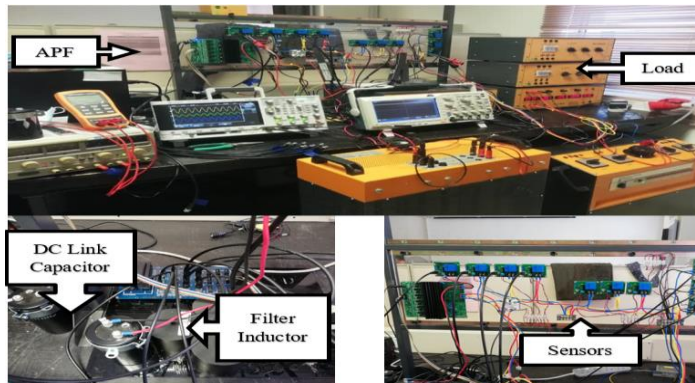


Figure 13. Laboratory hardware setup

The SAPF with EFANF effectively mitigates the harmonic current for the steady-state condition. The measurement is done using the Agilent DSO-X 2014A oscilloscope for the experimental result, covering source voltage, source current, load current, and filter current. In terms of THD calculation, the measurement is done by downloading the data from the oscilloscope. The data are then measured for harmonics decomposition using FFT analysis in MATLAB/Simulink. From the results, the algorithm managed to reduce the harmonics of the source current with THD from 62% to 3.46 % for 80 Ohms load, 28.77% to 3.73 % for 50 Ohms load, and 28.56% to 3.99 % for 36 Ohms load. All harmonics are managed to be reduced below the required IEE standard, 5%. Nevertheless, the THDs of the three-phase supply current are monitored to see the algorithm's effectiveness in the experimental work, where the THD value can be seen in Figure 14.

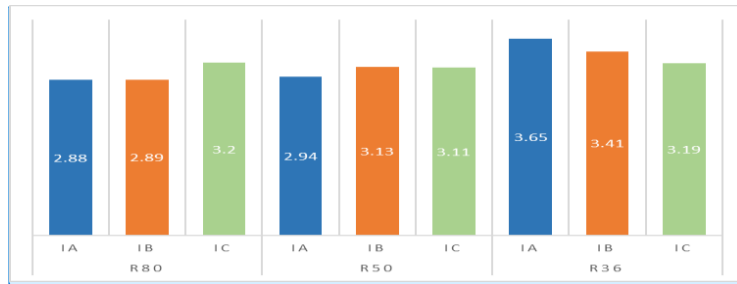


Figure 14. Experimental results of THD for three-phase source current after compensation

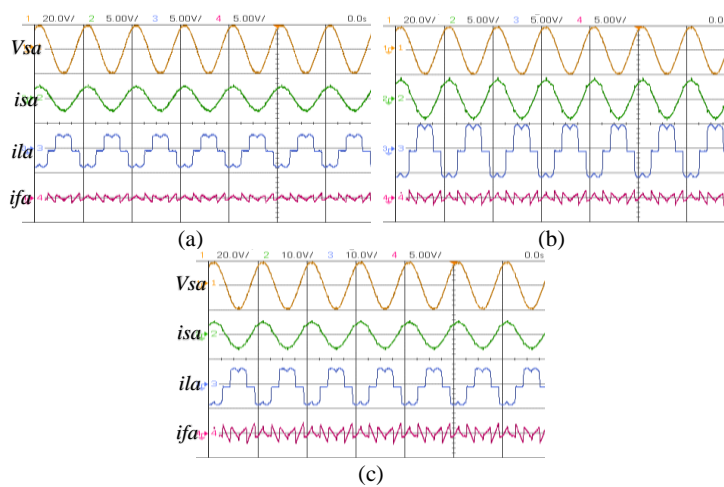


Figure 15. Experimental results of source voltage, source current, load current, filter current and THD values for (a) 82-Ω (b) 50-Ω and (c) 36-Ω loads

Figure 15 shows the waveforms of phase-a source voltage, source current, load current, and filter current in a steady-state condition obtained from experimental work. The source current waveform is sinusoidal and is in phase with the measured source voltage. Thus, THD is reduced for all the given loads, as shown in the figure.

The response of the proposed algorithm for steady-state conditions, when introduced to an inductive and capacitive load, is also confirmed with the experimental setup. The result is shown in Figure 16, where it can be verified that the proposed algorithm can mitigate resistive with inductive loads for values R1L1, R2L2, and R3L3. After mitigation, the source current loads THD are given as 2.70%, 2.63%, and 2.78%, respectively.

Commented [WU9]: 9. Figure 14 not only shows a bar diagram of THD source current after compensation, but also before compensation on the non-linear load ($R = 80$ ohm, $R = 50$ ohm, and $R = 36$ ohm). This revised figure will help the readers understand that your proposed method has better performance after compensation. After that, you have to make a clear analysis of the new figure.

Commented [WU10]: 10. Make Fig 15a, Fig 15b, and Fig 15c in the form of a three-row table respectively. Fig 15a and Fig 15b are too short for a two-column form because the two figures will be truncated.

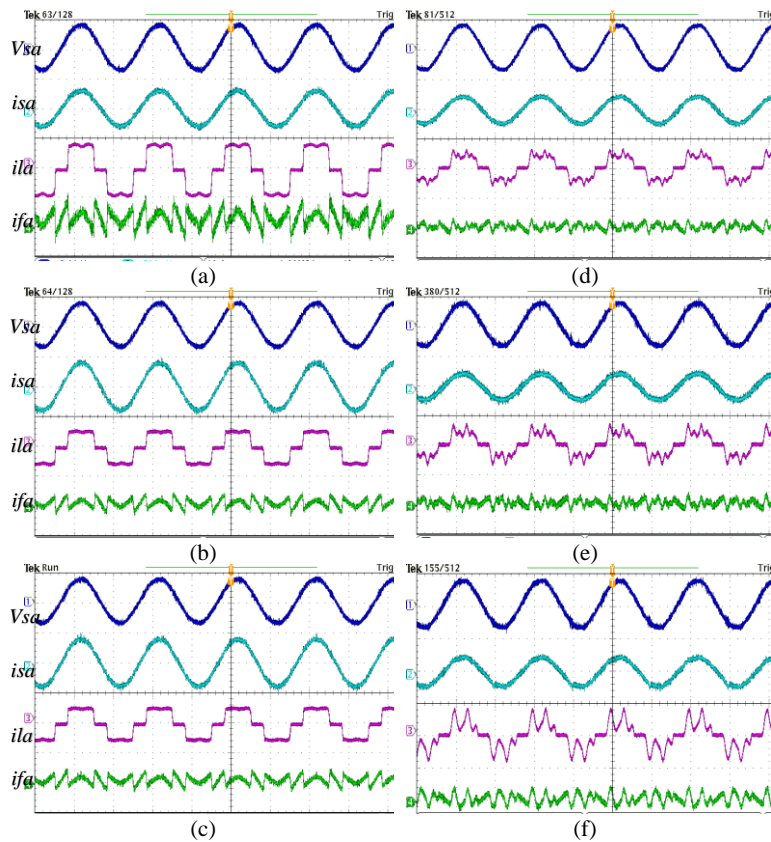


Figure 16. Experimental results of source voltage, source current, load current, filter current and THD values for (a) 67- Ω and 30H, (b) 69- Ω and 36H, (c) 76- Ω and 41H loads, (d) 60- Ω 12uF, (e) 60- Ω 17uF and (f) 60- Ω 36uF loads

The resistive with capacitive loads values of R1C1, R2C2, and R3C3. The values are within the required IEEE standard. THD's mitigated source current values are 2.52%, 2.99%, and 5.00% for each load. Based on these values, it can be concluded that the proposed EFANF algorithm can produce the appropriate reference current for the SAPF to work effectively. The SAPF also seems to have better stabilities for the resistive and inductive loads than capacitive loads. However, in terms of mitigation, the EFANF can mitigate all the different types of loads in the experimental setup.

The effectiveness and feasibility of the proposed algorithm were also verified for transient-state operation during load-changing conditions. Figure 17 shows the state for reducing load capacity, which causes ascending current state, Figure 17 also

Commented [WU11]: 11. Create Figure 16a to Figure 16f in six rows of the figures table respectively (not in the double-column model).

shows the increased load capacity, which causes descending current state. In both states, the EFANF managed to mitigate within 20ms for all load changes.

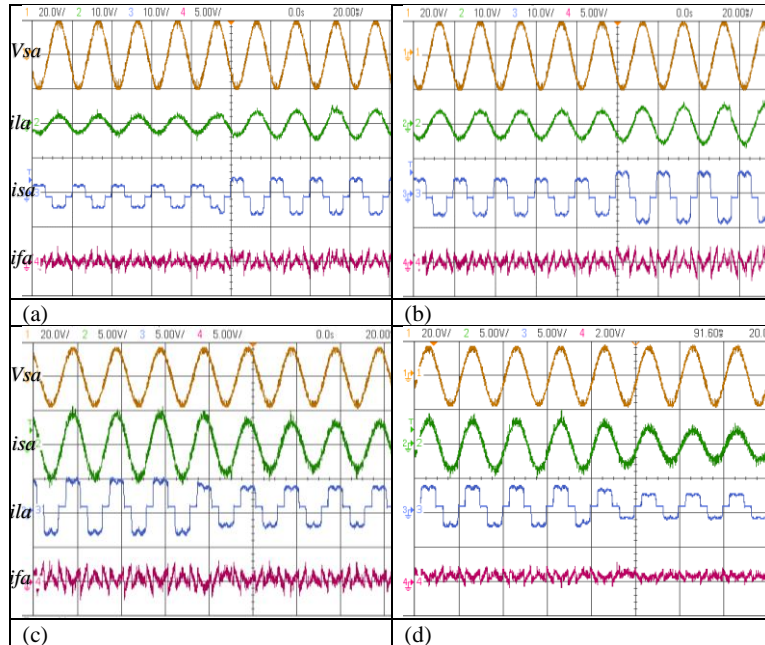


Figure 17. Experimental results of source voltage, source current, load current, filter current, and DC-Link voltage during transient-state conditions of (a) 82- Ω to 50- Ω (b) 50- Ω to 36- Ω (c) 82- Ω to 50- Ω and (d) 50- Ω to 36- Ω

5. Conclusions

This paper presents the EFANF extraction algorithm utilized in SAPF to compensate for current harmonics in the three-phase three-wire system. The proposed algorithm demonstrated its capability to generate the reference current based on the notch filtering technique, as shown in both simulation results in MATLAB/Simulink and experimental work based on the validation with DSPACE RS1104. As the EFANF is self-synchro based on frequency adaptability, PLL is not required. The algorithm extracted the fundamental component and mitigated harmonics in balanced load conditions based on the analyses of steady-state and transient state conditions. The performance of the proposed algorithm has also been verified for different types and values of reactive loads both in simulation and experimental works. The design of the EFANF also gives an optional improvement on the DC link voltage control algorithm as the losses of the DC link is provided as power losses within the system. In terms of performance, the EFANF managed to produce the THD according to the requirement of the IEE standard. Furthermore, the algorithm can adapt to the different types of loads.

Commented [WU12]: 12. Make Fig 17a, Fig 17b, Fig 17c, and Fig 17d in the form of a four-row table respectively (not in the double -column model)

Commented [WU13]: Describe in detail the weaknesses of your method and the future work needed to improve these weaknesses. Explain in a last single paragraph in the conclusion section.

Nomenclatures

v_{sa}, v_{sb}, v_{sc}	Voltage source phase a, b and c, Volt
i_{sa}, i_{sb}, i_{sc}	Current source phase a, b and c, Ampere
$i_{refa}, i_{refb}, i_{refc}$	Generated reference current phase a, b and c Ampere
$3V_{e1}I_{e1}$	Fundamental effective apparent power
$3V_{eH}I_{eH}$	Harmonics power
G_e	The equivalent conductivity

Greek Symbols

ω_0	Reference frequency
θ	Estimation Frequency
γ	Accuracy coefficients
ε	Convergence speed coefficients
$\dot{\theta}$	Updated law for the frequency estimation

Abbreviations

APF	Active Power Filter
SAPF	Shunt Active Power Filter
THD	Total Harmonics Distortion
EFANF	Extended Fryze Adaptive Notch Filter

References

1. F. Zare, H. Soltani, D. Kumar, P. Davari, H.A.M. Delpino, F. Blaabjerg, Harmonic Emissions of Three-Phase Diode Rectifiers in Distribution Networks, IEEE Access. 5 (2017) 2819–2833. <https://doi.org/10.1109/ACCESS.2017.2669578>.
2. A. Alizade, J.B. Noshahr, Evaluating noise and DC offset due to inter-harmonics and supra-harmonics caused by back-to-back converter of (DFIG) in AC distribution network, CIRED - Open Access Proc. J. 2017 (2017) 629–632. <https://doi.org/10.1049/oap-cired.2017.0045>.
3. K.D. Patil, W.Z. Gandhare, Effects of harmonics in distribution systems on temperature rise and life of XLPE power cables, 2011 Int. Conf. Power Energy Syst. ICPS 2011. (2011) 1–6. <https://doi.org/10.1109/ICPES.2011.6156680>.
4. T. Toumi, A. Allali, A. Meftouhi, O. Abdelkhalek, A. Benabdelkader, M. Denai, Robust control of series active power filters for power quality enhancement in distribution grids: Simulation and experimental validation, ISA Trans. 107 (2020) 350–359. <https://doi.org/10.1016/j.isatra.2020.07.024>.
5. E. Sundaram, M. Venugopal, On design and implementation of three phase three level shunt active power filter for harmonic reduction using synchronous reference frame theory, Int. J. Electr. Power Energy Syst. 81 (2016) 40–47. <https://doi.org/10.1016/j.ijepes.2016.02.008>.
6. H. Liu, H. Hu, H. Chen, L. Zhang, Y. Xing, Fast and Flexible Selective Harmonic Extraction Methods Based on the Generalized Discrete Fourier

- Transform, *IEEE Trans. Power Electron.* 33 (2018) 3484–3496. <https://doi.org/10.1109/TPEL.2017.2703138>.
7. R. Panigrahi, B. Subudhi, Performance Enhancement of Shunt Active Power Filter Using a Kalman Filter-Based H^∞ Control Strategy, *IEEE Trans. Power Electron.* 32 (2017) 2622–2630. <https://doi.org/10.1109/TPEL.2016.2572142>.
 8. V.N. Jayasankar, U. Vinatha, Backstepping Controller with Dual Self-Tuning Filter for Single-Phase Shunt Active Power Filters under Distorted Grid Voltage Condition, *IEEE Trans. Ind. Appl.* 56 (2020) 7176–7184. <https://doi.org/10.1109/TIA.2020.3025520>.
 9. F. Harirchi, M.G. Simoes, Enhanced Instantaneous Power Theory Decomposition for Power Quality Smart Converter Applications, *IEEE Trans. Power Electron.* 33 (2018) 9344–9359. <https://doi.org/10.1109/TPEL.2018.2791954>.
 10. Y.W. Liu, S.H. Rau, C.J. Wu, W.J. Lee, Improvement of Power Quality by Using Advanced Reactive Power Compensation, *IEEE Trans. Ind. Appl.* 54 (2018) 18–24. <https://doi.org/10.1109/TIA.2017.2740840>.
 11. A. Chebabhi, M.K. Fellah, A. Kessal, M.F. Benkhoris, A new balancing three level three dimensional space vector modulation strategy for three level neutral point clamped four leg inverter based shunt active power filter controlling by non-linear back stepping controllers, *ISA Trans.* 63 (2016) 328–342. <https://doi.org/10.1016/j.isatra.2016.03.001>.
 12. A. Naderipour, Z. Abdul-Malek, V.K. Ramachandramurthy, A. Kalam, M.R. Miveh, Hierarchical control strategy for a three-phase 4-wire microgrid under unbalanced and non-linear load conditions, *ISA Trans.* 94 (2019) 352–369. <https://doi.org/10.1016/j.isatra.2019.04.025>.
 13. Y. Hoon, M.A.A.M. Zainuri, A.S. Al-Ogaili, A.N. Al-Masri, J. Teh, Active Power Filtering under Unbalanced and Distorted Grid Conditions Using Modular Fundamental Element Detection Technique, *IEEE Access.* 9 (2021) 107502–107518. <https://doi.org/10.1109/ACCESS.2021.3101238>.
 14. S. Hou, J. Fei, C. Chen, Y. Chu, Finite-Time Adaptive Fuzzy-Neural-Network Control of Active Power Filter, *IEEE Trans. Power Electron.* 34 (2019) 10298–10313. <https://doi.org/10.1109/TPEL.2019.2893618>.
 15. S. Hou, J. Fei, Y. Chu, Nonsingular Terminal Sliding Mode Control of Active Power Filter, *Chinese Control Conf. CCC. 2018-July* (2018) 2982–2987. <https://doi.org/10.23919/ChiCC.2018.8483224>.
 16. K.H. Tan, F.J. Lin, J.H. Chen, DC-Link voltage regulation using RPFNN-AMF for Three-Phase active power filter, *IEEE Access.* 6 (2018) 37454–37463. <https://doi.org/10.1109/ACCESS.2018.2851250>.
 17. L. Merabet, S. Saad, D.O. Abdeslam, J. Merckle, Direct neural method for harmonic currents estimation using adaptive linear element, *Electr. Power Syst. Res.* 152 (2017) 61–70. <https://doi.org/10.1016/j.epsr.2017.06.018>.
 18. B. Singh, S.R. Arya, K. Kant, Notch filter-based fundamental frequency component extraction to control distribution static compensator for mitigating current-related power quality problems, *IET Power Electron.* 8 (2015) 1758–1766. <https://doi.org/10.1049/iet-pel.2014.0486>.

19. S. Kewat, B. Singh, Modified amplitude adaptive control algorithm for power quality improvement in multiple distributed generation system, *IET Power Electron.* 12 (2019) 2321–2329. <https://doi.org/10.1049/iet-pel.2018.5936>.
20. D. Yazdani, A. Bakhshai, P. Jain, A three-phase approach to harmonic and reactive current extraction and harmonic decomposition, *IECON Proc. (Industrial Electron. Conf.* 25 (2009) 3205–3210. <https://doi.org/10.1109/IECON.2009.5415218>.
21. R.S.R. Chilipi, N. Al Sayari, K.H. Al Hosani, A.R. Beig, Adaptive Notch Filter-Based Multipurpose Control Scheme for Grid-Interfaced Three-Phase Four-Wire DG Inverter, *IEEE Trans. Ind. Appl.* 53 (2017) 4015–4027. <https://doi.org/10.1109/TIA.2017.2676098>.
22. G. Fujita, N.D. Dinh, T. Funabashi, N.D. Tuyen, Adaptive notch filter solution under unbalanced and/or distorted point of common coupling voltage for three-phase four-wire shunt active power filter with sinusoidal utility current strategy, *IET Gener. Transm. Distrib.* 9 (2015) 1580–1596. <https://doi.org/10.1049/iet-gtd.2014.1017>.
23. N.D. Tuyen, G. Fujita, T. Funabashi, M. Nomura, Adaptive notch filter for synchronization and islanding detection using negative-sequence impedance measurement, *IEEJ Trans. Electr. Electron. Eng.* 7 (2012) 240–250. <https://doi.org/10.1002/tee.21724>.
24. M. Mojiri, A.R. Bakhshai, Stability analysis of periodic orbit of an adaptive notch filter for frequency estimation of a periodic signal, *Automatica.* 43 (2007) 450–455. <https://doi.org/10.1016/j.automatica.2006.08.018>.
25. M. Mojiri, A.R. Bakhshai, An Adaptive Notch Filter for Frequency Estimation of a Periodic Signal, *IEEE Trans. Automat. Contr.* 49 (2004) 314–318. <https://doi.org/10.1109/TAC.2003.821414>.
26. M. Mojiri, M. Karimi-Ghartemani, A. Bakhshai, Processing of harmonics and interharmonics using an adaptive notch filter, *IEEE Trans. Power Deliv.* 25 (2010) 534–542. <https://doi.org/10.1109/TPWRD.2009.2036624>.
27. X. Nie, J. Liu, Current Reference Control for Shunt Active Power Filters under Unbalanced and Distorted Supply Voltage Conditions, *IEEE Access.* 7 (2019) 177048–177055. <https://doi.org/10.1109/ACCESS.2019.2957946>.
28. D. TESHOME, T.D. Huang, K.-L. Lian, A Distinctive Load Feature Extraction Based on Fryze's Time-domain Power Theory, *IEEE Power Energy Technol. Syst. J.* 3 (2016) 1–1. <https://doi.org/10.1109/jpets.2016.2559507>.
29. S.K. Kesharvani, A. Singh, M. Badoni, Conductance based fryze algorithm for improving power quality for non-linear loads, 2014 Int. Conf. Signal Propag. Comput. Technol. ICSPCT 2014. (2014) 703–708. <https://doi.org/10.1109/ICSPCT.2014.6884965>.
30. Z. Zeng, R. Zhao, H. Yang, Coordinated control of multi-functional grid-tied inverters using conductance and susceptance limitation, *IET Power Electron.* 7 (2014) 1821–1831. <https://doi.org/10.1049/iet-pel.2013.0692>.

OUTLINING HOW THE ISSUES ARE ADDRESSED

Title of paper: CURRENT HARMONICS QUALITY MITIGATION TECHNIQUE FOR THREE-PHASE POWER SYSTEM BASED ON EXTENDED FRYZE ADAPTIVE NOTCH FILTER

1. Address all the concerns/recommendations of the reviewers.
2. All amendments made are to be highlighted in red color in the revised paper.

Reviewer # 1

Final Recommendation Please tick	Accepted without modification <input type="checkbox"/>	Accepted with minor corrections <input type="checkbox"/>	Accepted with major modification <input type="checkbox"/>	Rejected <input type="checkbox"/>
Comments	Addressed (Y/N)	Reply/Action taken		
<ul style="list-style-type: none">• Frequency of a power system may fluctuate based on the loads connected and faults occur. What is the effect of frequency variation in the adaptive notch filter? Is frequency regulation is considered in the constraints of the filter?	Y	The filter can adapt to notch frequency change with time by tracking the input signal frequency variation. This tracking capability eliminates the need for the signal frequency to be consistent, as is usually required for the typical notch filter to work efficiently. With the characteristic of the applied adaptive notch filter, the frequency regulation problem can be accounted for.		
<ul style="list-style-type: none">• The FFT algorithm to obtain THD value is missing in the methodology. Kindly justify why FFT is chosen rather than other time-frequency signal processing algorithms since other TFD methods may produce better THD results.	Y	The FFT used to obtain the THD value is based on the toolbox of the Simulink. The reason of applying FFT is mentioned in the methodology. The FFT is used compared to other methods due to the accessibility of the FFT within the Simulink. The method for applying the FFT analysis for harmonic order are added in the methodology.		
<ul style="list-style-type: none">• Any worst-case scenario with worst THD result? This is to highlight the impact or effect of THD towards the power system.	Y	Throughout the power system, when there is trend of rising harmonics attribution, there will be possibility of detrimental impact towards various components within the system itself. The complications that arise within the harmonics are considered to have direct effect towards signal contamination of the		

		current flow. Abnormal heating of materials and interruption of operations are two of the keys issued accustomed with the current harmonics.
<ul style="list-style-type: none"> What is the difference of the results performed by the proposed method in both IEC and IEEE standards? What is the limitation to achieve the harmonic limit set by both standards? 	Y	<p>IEEE Standard 519-1992 is used to address harmonic issues in electrical power systems. Basically, the IEEE standard is applied at the PCC and should not be applied at equipment or location within user facilities. Based IEEE standard 519-2022, it specifies the current distortion for TDD should not exceed 5% in electrical power systems. Meanwhile, the IEC standard is more to wide design targets that are separated based on medium voltage (MV), high voltage (HV) and extra-high voltage (EHV). Based on IEC, the standard of harmonics is set as 6.5% for MV and 3% for HV/EHV. For the limitation to achieve the harmonics limit set by both standards, as the standard for harmonics value in IEEE is lower than IEC, then the IEEE standard is fulfilled. Referring to the standards, the result acquired by the proposed method achieved to satisfy the requirement for both</p>

(Please add more rows if needed)

Reviewer # 2				
Final Recommendation Please tick	Accepted without modification <input type="checkbox"/>	Accepted with minor corrections <input type="checkbox"/>	Accepted with major modification <input type="checkbox"/>	Rejected <input type="checkbox"/>
Comments	Addressed (Y/N)	Reply/Action taken		
<ul style="list-style-type: none"> The contribution of the paper has to be explained clearly in the abstract, introduction, and methodology sections. 	Y	<p>The main contribution of the algorithm is highlighted in the abstract. In the introduction section the contribution of the algorithm is mentioned; however, the contribution is emphasized more.</p>		

<ul style="list-style-type: none"> How the proposed approach is developed comparing with the following paper? S.H. Mohamad et al, Adaptive notch filter under indirect and direct current controls for active power filter, Bulletin of Electrical Engineering and Informatics, Vol. 9, No. 5, October 2020, pp. 1794-1802. The differences need to be highlighted in the introduction. 	Y	The proposed method that is currently explained is a continuation of the following paper. In the following paper, the algorithm used is pure ANF reference generation using basic generation without any current control. In comparison to the EFANF, it is applied to have a full SAPF control, where the algorithm is having current reference generation and DC link Voltage Control. Explicit characteristic of the current method is explained in the algorithm's equation and process.
<ul style="list-style-type: none"> The simulation diagrams need to be included in the section 4 	Y	Diagram developed in MATLAB Simulation is included in the paper.
<ul style="list-style-type: none"> The proposed approach has to be applied to unbalance three phase system to verify the robustness and effectiveness of the proposed approach 	Y	For the current paper, the scope of the paper has been set for a three phase – three wire balanced system. In terms of robustness, it is currently done by applying transient response of different types of loads and different values of loads. However, the suggestion that the approach must be applied to unbalance three phase system to verify the robustness and effectiveness of the proposed approach will be taken in consideration for improvement in the future.
<ul style="list-style-type: none"> Section 3 needs to be explained using flowchart. 	Y	To summarize the SAPF process in terms of visualization, a flowchart explaining the flow of the process is included.
<ul style="list-style-type: none"> The results of the simulation and experimental sections need to be compared particularly the figures. 	Y	The result of both of simulation and experimental are summarizes the implication of the results toward each other at the result section.
<ul style="list-style-type: none"> It is better to change the title of the paper to “Mitigation of Harmonic Current for Three-Phase Power System Based on Extended Fryze Adaptive Notch Filter” 	Y	The title of the paper is changed to “Mitigation of Harmonic Current for Balanced Three-Phase Power System Based on Extended Fryze Adaptive Notch Filter”

(Please add more rows if needed)

Reviewer # 3

**Final
Recommendation**
Please tick

**Accepted without
modification**
☒

**Accepted with minor
corrections**
☐

**Accepted with major
modification**
☐

Rejected
☐

Comments	Addressed (Y/N)	Reply/Action taken
<ul style="list-style-type: none"> In the conclusion of the abstract section state the most significant THD improvement of the source current with the proposed method using either the results of Matlab simulations or the results of laboratory experiments. 	Y	The conclusion for the significant results of simulation and experiment is included within the abstract section.
<ul style="list-style-type: none"> Use italic models to write quantities and units in Table 1 (use Microsoft Equation). 	Y	All quantities and units in Table 1 are changed to italic models (using Microsoft Equation).
<ul style="list-style-type: none"> Create Figure 6a and Figure 6b in two rows of the figures table respectively (not in the double-column model). 	Y	The figure has been adjusted in two rows as mentioned
<ul style="list-style-type: none"> Create Figure 7a and Figure 7b in two rows of the figures table respectively (not in the column model). 	Y	The figure has been adjusted in two rows as mentioned
<ul style="list-style-type: none"> Create Figure 9a, Figure 9b, and Figure 9c in three rows of the figures table respectively (not in the three-column model) 	Y	The figure has been adjusted in three rows as mentioned
<ul style="list-style-type: none"> Create Figure 10a, Figure 10b, and Figure 10c in three rows of the figures table respectively (not in the three-column model) 	Y	The figure has been adjusted in three rows as mentioned
<ul style="list-style-type: none"> Create Figure 11a and Figure 11b in two rows of the figures table respectively (not in the double column model) 	Y	The figure has been adjusted in two rows as mentioned
<ul style="list-style-type: none"> Create Figure 12a and Figure 12b in two rows of the figures table respectively (not in the double column model) 	Y	The figure has been adjusted in two rows as mentioned
<ul style="list-style-type: none"> Figure 14 not only shows a bar diagram of THD source current after compensation, but also before compensation on the non-linear load ($R = 80 \text{ ohm}$, $R = 50 \text{ ohm}$, and $R = 36 \text{ ohm}$). This revised figure will help the readers understand that your proposed method has better performance after compensation. After that, you have to make a clear analysis of the new figure. 	Y	The figure has been revised and the THD analysis before and after the application of SAPF in the system is highlighted.
<ul style="list-style-type: none"> Make Fig 15a, Fig 15b, and Fig 15c in the form of a three-row table respectively. Fig 15a and Fig 15b are too short for a two-column form because the two figures will be truncated. 	Y	The figure has been adjusted in three rows as mentioned

<ul style="list-style-type: none"> • Create Figure 16a to Figure 16f in six rows of the figures table respectively (not in the double column model). 	Y	The figure has been adjusted in six rows as mentioned
<ul style="list-style-type: none"> • Make Fig 17a, Fig 17b, Fig 17c, and Fig 17d in the form of a four-row table respectively (not in the double column model). 	Y	The figure has been adjusted in four rows as mentioned
<ul style="list-style-type: none"> • Describe in detail the weaknesses of your method and the future work needed to improve these weaknesses. Explain in a last single paragraph in the conclusion section. 	Y	The algorithm is still dependent on two coefficients γ and ϵ for the algorithm to be working effectively. In the current work, the coefficients are obtained through empirical method. To improve the effectiveness of coefficients, future works are recommended to obtain the best possible coefficients values through optimization method. This has been added in the conclusion section.

(Please add more rows if needed)

Reviewer # 4

Final Recommendation Please tick	Accepted without modification <input type="checkbox"/>	Accepted with minor corrections <input type="checkbox"/>	Accepted with major modification <input type="checkbox"/>	Rejected <input type="checkbox"/>
--	--	--	---	---

Comments	Addressed (Y/N)	Reply/Action taken
•		
•		
•		

(Please add more rows if needed)

Reviewer # 5

Final Recommendation Please tick	Accepted without modification <input type="checkbox"/>	Accepted with minor corrections <input type="checkbox"/>	Accepted with major modification <input type="checkbox"/>	Rejected <input type="checkbox"/>
--	--	--	---	---

Comments	Addressed (Y/N)	Reply/Action taken
•		
•		
•		
•		

(Please add more rows if needed)

Reviewer # 6

Final Recommendation Please tick	Accepted without modification <input type="checkbox"/>	Accepted with minor corrections <input type="checkbox"/>	Accepted with major modification <input type="checkbox"/>	Rejected <input type="checkbox"/>
--	--	--	---	---

Comments	Addressed (Y/N)	Reply/Action taken
•		
•		
•		
•		

(Please add more rows if needed)

Reviewer # 7				
Final Recommendation Please tick	Accepted without modification <input type="checkbox"/>	Accepted with minor corrections <input type="checkbox"/>	Accepted with major modification <input type="checkbox"/>	Rejected <input type="checkbox"/>

Comments	Addressed (Y/N)	Reply/Action taken
•		
•		
•		
•		

(Please add more rows if needed)

Reviewer # 8				
Final Recommendation Please tick	Accepted without modification <input type="checkbox"/>	Accepted with minor corrections <input type="checkbox"/>	Accepted with major modification <input type="checkbox"/>	Rejected <input type="checkbox"/>

Comments	Addressed (Y/N)	Reply/Action taken
•		
•		
•		
•		

(Please add more rows if needed)

Reviewer # 9				
Final Recommendation Please tick	Accepted without modification <input type="checkbox"/>	Accepted with minor corrections <input type="checkbox"/>	Accepted with major modification <input type="checkbox"/>	Rejected <input type="checkbox"/>

Comments	Addressed (Y/N)	Reply/Action taken
•		
•		

•		
•		

(Please add more rows if needed)

Reviewer # 10

Final Recommendation Please tick	Accepted without modification <input type="checkbox"/>	Accepted with minor corrections <input type="checkbox"/>	Accepted with major modification <input type="checkbox"/>	Rejected <input type="checkbox"/>
---	---	---	--	--

Comments	Addressed (Y/N)	Reply/Action taken
•		
•		
•		
•		

(Please add more rows if needed)

MITIGATION OF HARMONIC CURRENT FOR BALANCED THREE-PHASE POWER SYSTEM BASED ON EXTENDED FRYZE ADAPTIVE NOTCH FILTER

Commented [TSHBM@AR1]: Reviewer 2
Mitigation of Harmonic Current for Balanced Three-Phase Power System Based on Extended Fryze Adaptive Notch Filter

Commented [TSHBM@AR2R1]: The title of the paper is changed and added for Balanced system.

Abstract

The power quality problem, especially regarding harmonics contamination, has dramatically affected the overall power system stability. In response to this, using an Active Power Filter (APF) is considered one of the compelling methods to overcome harmonics issues. This paper presents the implementation of Shunt APF with an improved adaptive notch filter known as Extended Fryze Adaptive Notch Filter (EFANF) for fundamental signal extraction. The adaptive notch filter has improved the utilization from a single-phase to three-phase application for direct fundamental signal extraction and is designed to cater DC link voltage regulation controllers based on the power loss equation by applying Fryze current control power. This extraction algorithm inherits simple design construction and frequency tracking, eliminating PLL reliance on synchronization. **The proposed algorithm also improved the design by eliminating the needs of low pass filter as others time domain algorithms.** The algorithm's effectiveness in operation for the Shunt APF is validated through simulation using MATLAB/Simulink and experiment work by integrating the algorithm with DSPACE RS1104. Based on both evaluations, the results obtained show a satisfactory and reasonable agreement in mitigating the harmonics for multi-load conditions. Simulation and experimentally proven harmonics mitigation managed to reduce under 5% following the IEE standard, and the algorithm function within expectation for both steady and transient state conditions. In comparison between the simulation and experimental results, both results show almost similar results in terms of waveform for source voltage, source current, load current, and filter current in both steady state and transient state. **In terms of THD values, both simulations and experimental results recorded that the THD values for both conditions are below 5%, where the range is 1.45% to 2.46% for simulation and 2.88% to 3.65% for experimental results.** Furthermore, the DC link also tended to be maintained by the algorithm.

Keywords: Adaptive notch filter, Fryze, shunt active power filter, Harmonics.

Commented [TSHBM@AR3]: Reviewer 2
For the main contribution of the algorithm is highlighted into the abstract, in the introduction section the contribution of the algorithm is mentioned however the contribution will be emphasizing more.

Commented [TSHBM@AR4R3]: Additional contribution of algorithm is added prior to existing ones in the abstract.

Commented [TSHBM@AR5]: Reviewer 3
1. In the conclusion of the abstract section state the most significant THD improvement of the source current with the proposed method using either the results of Matlab simulations or the results of laboratory experiments.

Commented [TSHBM@AR6R5]: The result are mentioned

1. Introduction

The development of power systems has shaped multiple power generation, transmission, distribution, and application segments. All the advancements are often polluting and distorting the power system by increasing the utilization of non-linear loads, mainly contributed by power-electronics devices [1–3]. The need for power electronics devices can exponentially increase within the industrial and consumer sectors. Based on the extensive use of sensitive loads, such as computers and microprocessor-based industrial controllers, and now with the emergence of renewable energy such as solar and wind and the growth of electric vehicles, there is a growing need for effective harmonic measurement and compensation systems. Although conventional solutions have been used to mitigate power quality, such as passive filters in terms of harmonics, the solution is deemed ineffective, especially when involving load changes. As implementation of standard regulation in power flow is becoming more rigid such as IEEE519 and IEC 61000-3-2, active power compensation is seen as a better choice in realizing power quality (PQ) control.

Active power compensation offers better PQ compensation, especially harmonics, power factor, and active-reactive power control. Furthermore, the protection, management, performance, and efficiency of active power compensation are realized through continuous development in developing signal processing, detection, and extraction within mathematical algorithms and hardware throughout the past years. One of the apparatuses demonstrating a solid ability to eliminate harmonics is the Active Power Filter (APF) system. Such filters are an excellent way to reduce harmonic disturbances of voltage and current, sudden voltage fluctuations, transient disturbances, and current and voltage faults. Currently, there are multiple topologies of active power compensation available for additional compensation, such as series active power filter [4], shunt active power filter (SAPF), hybrid active power filter, and Unified Power Quality Conditioner (UPQC). Effective and efficient compensations are compulsory when dealing with harmonics' power quality. Hence, a precise algorithm is essential for extracting harmonics elements in controlling the power system's active power filter (APF). Over the years, various identification and extraction techniques have been developed; the methods can be divided into time and frequency domains.

The methods used in the frequency-based domain vary from commonly used fast Fourier and discrete Fourier algorithms, Kalman Filtering algorithm to wavelet transformation algorithm [5–7]. When using the mentioned techniques, most of the algorithms designed in the frequency domain require transformation, which is a little tedious to be applied in the time domain and usually incongruous with changing load in the power system. Another drawback of the frequency domain method is that it requires numerous cycles for better current estimation. In applying APF, the commonly used extraction method is usually within the time domain to cater to the changing waveform of loads in real-time situations, especially when involved with data acquisition. The time-domain techniques are divided into a few categories: classical methods derived from instantaneous power theory [8–10] and synchronous power theory [11–13], such as PQ, PQR, etc. DQ method. However, these methods usually involve multi-conversion planes and require additional filters to extract the information.

Another emerging method is the intelligent algorithms, which vary from the neural network, adaptive neural network, and adaptive linear neuron, where all these algorithms require training within the process [14–17]. Besides these three methods, another method used in the APF is the notch filter method, which is simple in design and can accommodate changes in loads [18]. The work introduced adaptive notch filters as harmonics, interharmonics processing methods, and time-domain signal analysis [19]. However, the method is limited to only processing information due to the algorithm's lack of a controlling method for DC link control. Yazdani et al. also proposed the ANF for three-phase application [20], which performed harmonic reactive current extraction and harmonic decomposition. However, the work was limited to monitoring and extraction only. **The ANF also been applied for ICC and DCC current control, but within this research also the DC Link control is not accounted for [21].** In some other works, the ANF replaces the lowpass filter function in the PQ algorithm for shunt APF [22–24] with a three-phase four-wire system. Although the strategy takes advantage of the transformation of the frame for instantaneous power flow, the application of ANF has increased the algorithm's complexity as the method includes the transformation process and integration of the ANF for filtering purposes. This strategy undermines the ANF's capability to directly filter the system's fundamental signal.

To utilize the potential of the ANF in shunt APF application. This paper presents an extended ANF application for harmonics extraction, DC link control, and current control. Within this method, three elements are focused on as the APF control system: the computational algorithm of reference current, the voltage regulation for the DC link control, and the generation of the firing pulse of the voltage source inverter (VSI). The main section of the paper is the proposed Extended Fryze Adaptive Notch Filter (EFANF) as the main algorithm component. **The algorithm implements the Adaptive Notch Filter (ANF) as three-phase extraction algorithm where each block extract individual phase and the algorithm is implementing Fryze algorithm as current control and reference current generation where there this method applied minimization method in finding active and nonactive current calculation.** Adjacent to the adaptive capability of the ANF, the algorithm also provides self-synchronization for the EFANF. This section also discusses the implementation of DC link voltage regulation, where the PI method is introduced as stability control within the EFANF, all highlighted in sections 2 and 3. The simulation and experimental works results are explained in section 4 of the paper. Finally, section 5 concludes the research contribution and highlights the overall significance of the impact of the work.

2. Principle operation of shunt APF

Shunt APF is implemented using a current control-voltage source inverter (CC-VSI), as shown in Fig. 1. The CC-VSI are connected in parallel with the non-linear loads through filter inductance. The CC-VSI performs the main task within the power quality system: inject (opposite magnitude) any unwanted harmonics current components produced due to the load current in the supply system at the point of common coupling (PCC). The instantaneous current source of the overall system is given in equation 1 where $i_s(t)$ is the source current, $i_L(t)$ is the load current and $i_c(t)$ is the compensation current.

$$i_s(t) = i_L(t) - i_c(t) \quad (1)$$

Commented [TSHBM@AR7]: Reviewer 2

How the proposed approach is developed comparing with the following paper? S.H. Mohamad et al, Adaptive notch filter under indirect and direct current controls for active power filter, Bulletin of Electrical Engineering and Informatics, Vol. 9, No. 5, October 2020, pp. 1794-1802. The differences need to be highlighted in the introduction.

Commented [TSHBM@AR8R7]: The proposed method that is currently explained is a continuation of the following paper. In the following paper, the algorithm used is pure ANF reference generation using basic generation without any current control. In comparison to the EFANF, it is applied to have a full SAPF control, where the algorithm is having current reference generation and DC link Voltage Control. Explicit characteristic of the current method is explained in the algorithm's equation and process.

Commented [TSHBM@AR9]: Reviewer 2

For the main contribution of the algorithm is highlighted into the abstract, in the introduction section the contribution of the algorithm is mentioned however the contribution will be emphasizing more.

Commented [TSHBM@AR10R9]: Contribution of the algorithms is highlighted

Meanwhile, the instantaneous voltage source $v_s(t)$ is given in equation 2, and the non-linear load current can be considered as the embodiment of fundamental current component and harmonics current components, as shown in equation 3

$$v_s(t) = V_m \sin \omega t \quad (2)$$

$$i_L(t) = \sum_{n=1}^{\infty} I_n \sin(n\omega t + \phi_n) \\ = I_1 \sin(\omega t + \phi_1) + \sum_{n=2}^{\infty} I_n \sin(n\omega t + \phi_n) \quad (3)$$

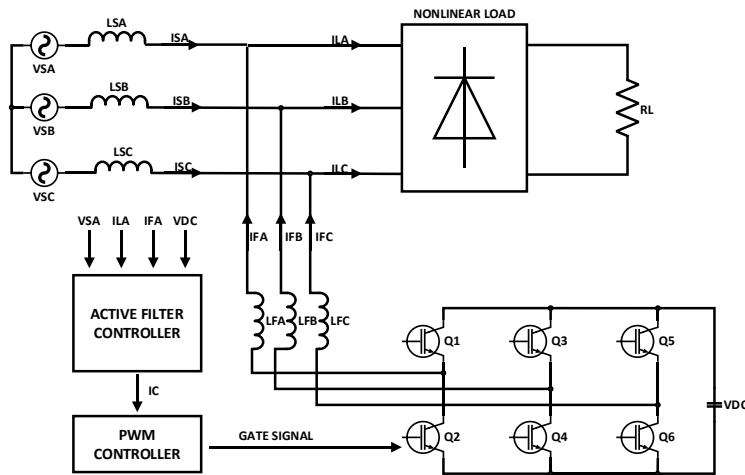


Fig. 1. Shunt APF System

The instantaneous power of the load $p_L(t)$ can be Fig.d out based on equation 4 given as

$$p_L(t) = i_s(t) \times v_s(t) \\ = V_m \sin^2 \omega t \times \cos \phi_1 + V_m I_1 \sin \omega t \times \cos \omega t \times \sin \phi_1 \\ + V_m \sin \omega t \left(\sum_{n=2}^{\infty} I_n \sin(n\omega t + \phi_n) \right) \\ = p_f(t) + p_r(t) + p_h(t) \quad (4)$$

The equation consists of active power $p_f(t)$, reactive power $p_r(t)$, and harmonics-induced power $p_h(t)$. Based on this, the real power drawn from the load is given in equation 5.

$$p_f(t) = V_m I_1 \sin^2 \omega t \times \cos \phi_1 \quad (5)$$

3.Principle Of Current Control System

The structure of the current control system is shown in Fig. 2. The system can be divided into three major components. The first part is the computation of the reference current using an extended fryze adaptive notch filter (EFANF), the second part is the self-synchronization of the EFANF, and the third component is the DC link voltage regulation and the firing pulses for the APF.

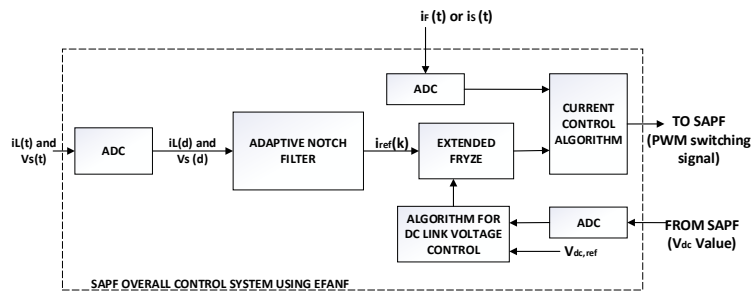


Fig. 2. Shunt APF System Flow Diagram

Commented [TSHBM@AR11]: Reviewer 2
Section 3 needs to be explained using flowchart.

Commented [TSHBM@AR12R11]: A flow diagram is being added to explain the process of the system

3.1. Adaptive Notch Filter

Ideally, an adaptive notch filter (ANF) works in the concept of a linear gain applied for all the frequencies except a specified frequency where the frequency gain is zero. Based on this characteristic, the filter can withdraw an implicit signal of the sinusoidal waveform from the specified frequency's measured component of an electrical power system. ANF has well been researched in removing noises within the sinusoidal waveform[24]. Originally, ANF is based on an IIR filter[26]; however, with improvement in the notch frequency, the filter can adapt to notch frequency change with time by tracking the input signal frequency variation. This tracking capability eliminates the need for the signal frequency to be consistent, as is usually required for the typical notch filter to work efficiently. The ANF's dynamic operation can refer to the following set of differential equations.

$$\ddot{x} + \theta^2 x = 2\varepsilon\theta e(t) \quad (6)$$

$$\dot{\theta} = -\gamma x \theta e(t) \quad (7)$$

$$e(t) = u(t) - \dot{x} \quad (8)$$

The ANF can be composed of the following elements based on the differential equations. The input signal of the ANF is given by $u(t)$. The estimation frequency of the ANF system is given by θ . The accuracy and convergence speed are determined by two coefficients within the ANF known as γ and ε . The two coefficients, however, must compensate each other for the ANF to work effectively and most efficiently, $\dot{\theta}$ represents the updated law for the frequency estimation [27].

In a functional single sinusoidal input $u(t) = A_1 \sin(\omega_0 t + \phi_1)$, the used ANF has an explicit characteristic where it has a unique periodic orbit located at O as shown in equation 9. For a single ANF system, three functional outputs will be produced by the ANF, which are the filtered cos signal noted by \bar{x} but in negative magnitude, filtered sin signal noted as $\dot{\bar{x}}$ which is identified as the input signal and finally $\bar{\theta}$ as the frequency of the signal.

$$O = \begin{pmatrix} \bar{x} \\ \dot{\bar{x}} \\ \bar{\theta} \end{pmatrix} = \begin{pmatrix} -A_1 \cos(\omega_0 t + \phi_1) / \omega_0 \\ A_1 \sin \omega_0 (\omega_0 t + \phi_1) \\ \omega_0 \end{pmatrix} \quad (9)$$

When involving a three-phase power system, for a shunt active power filter, the measurement of the waveform will apply three-phase waveforms of voltage and current for supply and load. Any three-phase sinusoidal voltage or current can be represented based on equation 10.

$$u(t) = \begin{pmatrix} u_a(t) \\ u_b(t) \\ u_c(t) \end{pmatrix} = \begin{pmatrix} A_a \sin(\omega t + \phi_a) \\ A_b \sin(\omega t + \phi_b) \\ A_c \sin(\omega t + \phi_c) \end{pmatrix} \quad (10)$$

For the three-phase application, improvement can be applied to the ANF in terms of frequency tracking as the filter shares the common frequency ω_0 in the same electrical power system. Based on this, the frequency law of triple ANF can be shared, thus reducing the complexity of the ANF from the 9th order to the 7th order integration function. The ANF will work in parallel order in extracting the fundamental components by sharing the standard frequency over time. The fundamental equation of the ANF for a three-phase system can be nominated in equations 11, 12, and 13, where the phase is represented as n for phases a , b , and c . Meanwhile, the updated law of frequency is based on the summation of the error signal of all three phases.

$$\ddot{x}_n + \theta^2 x_n = 2\varepsilon \theta e_n(t) \quad (11)$$

$$\dot{\theta} = -\gamma \theta \sum x_n e_n(t) \quad (12)$$

$$e_n(t) = u_n(t) - \dot{x}_n \quad (13)$$

When the equation is expanded to the respective phase, the ANF phase error equation is given as equation 14, the error for each phase is inserted into equation 12, where the ANF phase update law is given as equation 15.

$$e_n(t) = \begin{pmatrix} e_a(t) \\ e_b(t) \\ e_c(t) \end{pmatrix} = \begin{pmatrix} u_a(t) - \dot{x}_a \\ u_b(t) - \dot{x}_b \\ u_c(t) - \dot{x}_c \end{pmatrix} \quad (14)$$

$$\begin{aligned}
\dot{\theta} &= -y\theta \sum x_n e_n(t) = -y\theta(x_a e_a(t) + x_b e_b(t) + x_c e_c(t)) \\
&= -y\theta(x_a(u_a(t) - \dot{x}_a) + x_b(u_b(t) - \dot{x}_b) + x_b(u_c(t) - \dot{x}_c)) \\
&= -y(\theta x_a(u_a(t) - \dot{x}_a) + \theta x_b(u_b(t) - \dot{x}_b) + \theta x_b(u_c(t) - \dot{x}_c)) \quad (15)
\end{aligned}$$

The ANF for each phase is given as equation 16, where θ is obtained from the integration of $\dot{\theta}$ and x obtained from the double integration of \ddot{x} .

$$\begin{pmatrix} ANF_a \\ ANF_b \\ ANF_c \end{pmatrix} = \begin{pmatrix} \ddot{x}_a + \theta^2 x_a = 2\varepsilon\theta e_a(t) \\ \ddot{x}_b + \theta^2 x_b = 2\varepsilon\theta e_b(t) \\ \ddot{x}_c + \theta^2 x_c = 2\varepsilon\theta e_c(t) \end{pmatrix} \quad (16)$$

3.2. Reference current estimation

In a three-phase power system, based on equation 4, the power flow within the system usually consists of absolute power, reactive power, and harmonics power. Therefore, the power term containing all efficient and non-efficient powers terms in the three-phase system is defined as eq 17.

$$S_e^2 = (3V_{e1}I_{e1})^2 + (3V_{e1}I_{eH})^2 + (3V_{eH}I_{e1})^2 + (3V_{eH}I_{eH})^2 \quad (17)$$

Where $(3V_{e1}I_{e1})^2$ refers to the fundamental effective apparent power and $(3V_{e1}I_{eH})^2 + (3V_{eH}I_{e1})^2 + (3V_{eH}I_{eH})^2$ refers to nonfundamental effective apparent power. By applying ANF for the measured voltage and current, their fundamental components can be extracted, and the fundamental power for the system can be obtained based on the extracted components. Based on this, the estimation of the reference supply current will be produced. However, to ensure the successful task of SAPF, the DC link voltage needs to be controlled to ensure that it is maintained at the reference value. As the DC link of a SAPF acquires its power from the line and is accustomed to losses due to switches and active power transfer, the DC link voltage is exposed to various disturbances, leading to instability of the voltage. To be overwhelmed with this condition, a DC link control is essential to the SAPF. The DC-link reference is determined and compared with this system's measured DC link voltage. The error between the reference and measured DC link voltage is passed into the proportional-integral controller (PI). Loss is integrated into the instantaneous power equation, as in equation 18. Where this is on the improvement point compared to previous works for ANF application SAPF.

$$\bar{p}_{3\phi} = v_a i_a + v_b i_b + v_c i_c + P_{dc} \quad (18)$$

The error or difference obtained from DC link voltage measurement is shown in equation 19, and the PI controller is applied towards the error to get the value as power losses of DC-link shown in equation 20 below.

$$e_{vdc}(t) = v_{dcref} - v_{dcense} \quad (19)$$

$$P_{dc} = P_{dc}(t-1) + K_p(e_{vdc}(t) - e_{vdc}(n-1)) + K_i e_{vdc}(t) \quad (20)$$

Meanwhile, the three-phase reference supply is obtained through the fryze equation [28–31], where this method determines the reference current based on the average value of three-phase instantaneous power. The equivalent conductivity calculates the average current, and the average admittance is determined based on the concept of aggregate voltage as follows,

$$G_e = \frac{\bar{p}_{3\phi}}{V_s^2}, \quad \text{where } V_s^2 = \sqrt{v_a^2 + v_b^2 + v_c^2} \quad (22)$$

When the equation is expanded, the reference current can be given as,

$$\bar{i}_{refk} = G_e v_k, \quad k = (a, b, c) \quad (23)$$

$$\bar{i}_{refk} = \begin{bmatrix} \bar{i}_{refa} \\ \bar{i}_{refb} \\ \bar{i}_{refc} \end{bmatrix} = \begin{bmatrix} \frac{(v_a i_a + v_b i_b + v_c i_c + P_{dc}) \times v_a}{\sqrt{v_a^2 + v_b^2 + v_c^2}} \\ \frac{(v_a i_a + v_b i_b + v_c i_c + P_{dc}) \times v_b}{\sqrt{v_a^2 + v_b^2 + v_c^2}} \\ \frac{(v_a i_a + v_b i_b + v_c i_c + P_{dc}) \times v_c}{\sqrt{v_a^2 + v_b^2 + v_c^2}} \end{bmatrix} \quad (24)$$

The individual reference current for each phase sequence can be obtained from equation 24.

4. Result and Analysis

The performance of the proposed EFANF is verified by simulation and experimental works. Table 1 describes the parameters of design that are being applied in the simulation.

Table 1. Simulation Parameters

Parameter	Value
Source Voltage	415 V (RMS), 50 Hz
Source Impedance	1 Ω , 1 mH
DC Link Capacitance	3300 μ F
DC Link Reference Voltage	700V
Filtering Inductor	500 mH
ANF Gains	$\varepsilon = 0.16, \gamma = 180$
	Resistive Load
	$R1 = 80 \Omega, R2 = 50 \Omega$ and $R3 = 36 \Omega$
	Resistive with Inductive Load
	$R1L1 = 77 \Omega$ 30mH,
	$R2L2 = 69 \Omega$ 36mH and
	$R3L3 = 41 \Omega$ 41mH
	Resistive with Capacitive Load
	$R1C1 = 65 \Omega$ 12 μ F, $R2C2$
	$= 65 \Omega$ 19 μ F and $R3C3 = 65 \Omega$ 36 μ F

Commented [TSHBM@AR13]: Reviewer 3
2. Use italic models to write quantities and units in Table 1 (use Microsoft Equation).

4.1. Simulation Results

The performance, reliability, and efficiency of the EFANF for a balanced three-phase SAPF are initially simulated and evaluated using MATLAB-Simulink. According to the circuit shown in Fig. 3, inputs for the EFANF algorithm are based on the measured $i_{sa}, i_{sb}, i_{sc}, i_{la}, i_{lb}, i_{lc}$ and the three-phase source voltage v_{sa}, v_{sb}, v_{sc} to come out with currents references $i_{refa}, i_{refb}, i_{refc}$ for the APF. Evaluation is based on resistive load for three load conditions and tested for sudden changes of load for increasing and decreasing current and the keenness of the EFANF to succumb to the changes. The operation is tested to activate the APF after reaching a simulation time of 0.1s.

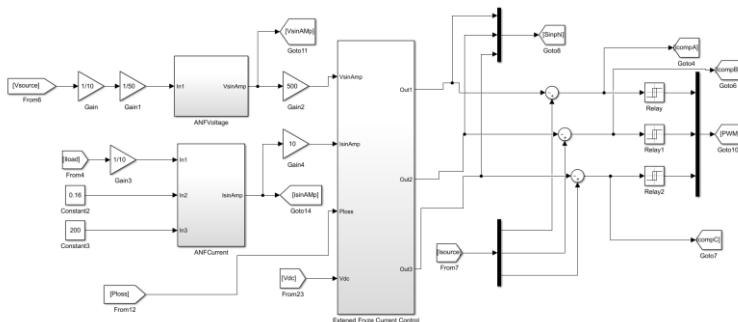


Fig. 3. MATLAB Simulation diagram for EFANF Control System.

The system will be subjected to a non-linear rectifier with three different resistivity values for the output. Fig. 4 shows the output waveform of the power system connected with SAPF at the point of PCC. The measurement is taken before the PCC for source voltage (Vs) and source current (Is) and after the PCC for load voltage (VL) and load current (IL). As shown in Fig. 2, the system's voltage is a pure sinusoidal waveform, and the load is a distorted waveform due to the rectifier. Fig. 5 focuses on phase-A waveforms for source voltage, source current, load voltage, and load current. **To obtain the THD for the simulation, PowerGui FFT Analysis Tool** **MATLAB Simulink is used for immediate result.** Based on the Fast Fourier Transform (FFT) analysis, it can be shown that the harmonics due to non-linear load are given in Fig. 7, where the THD value is 28.29 percent.

Based on Fig. 5, the current source waveform is being mitigated from the distortion by the SAPF. From point 0.1s, the load waveform has become sinusoidal, and at the same time, no distortion occurred within the source voltage and load voltage, and there is not also change that happened towards the load current. The APF is successfully mitigating the harmonics at the PCC. To evaluate the APF currents, details of the reference current, compensation current, and filter current are given in Fig. 6. It is shown that the EFANF managed to extract the fundamental current after three cycles of the waveform, and the compensation current is provided in the equation below.

$$i_{comp} = i_{source} - i_{ref} \quad (22)$$

Commented [TSHBM@AR14]: Reviewer 3
The simulation diagrams need to be included in the section 4

Commented [TSHBM@AR15R14]: MATLAB Simulation Diagram is included

Commented [TSHBM@AR16]: Reviewer 1
The FFT algorithm to obtain THD value is missing in the methodology. Kindly justify why FFT is chosen rather than other time-frequency signal processing algorithms since other TFD methods may produce better THD results.

Commented [TSHBM@AR17R16]: The FFT used to obtain the THD value is based on the toolbox of the Simulink. The reason of application of FFT is mentioned in the methodology. The FFT is used compared to other method due the accessibility of the FFT within the Simulink. The method for applying the FFT analysis for harmonic order are added in the methodology.

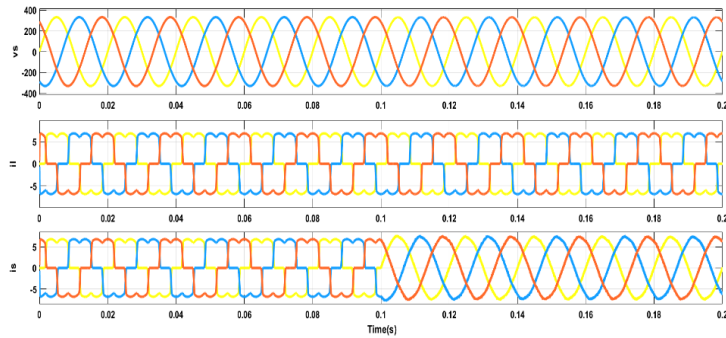


Fig. 4. Simulation results of 80 Ω load for source voltage, load current, and source current before and after activation of APF.

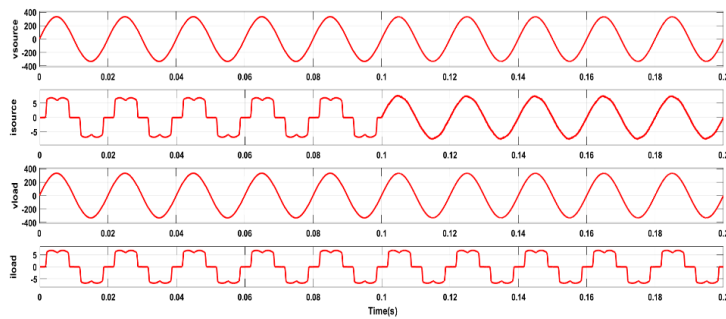


Fig. 5. Simulation results for phase A before and after activation of APF

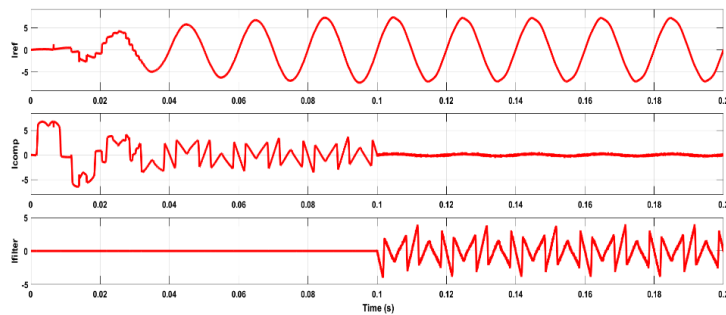


Fig. 6. Simulation result for reference current, compensation current, and filter current before and after activating APF for phase a.

Fig. 6 shows the waveform for the reference current, compensation current, and filter current for phase a. The ANF produces the reference current and inputs it into the APF current control. The difference between the reference and source current will

have the required compensation current for the APF to mitigate the harmonics. At simulation time 0.1s, the APF is activated, and the filtering current follows the required harmonics mitigation value for the load. The total harmonics distortion value of the source current after connecting APF is seen to reduce to 3.20 % due to the compensation current, as shown in Fig. 7.

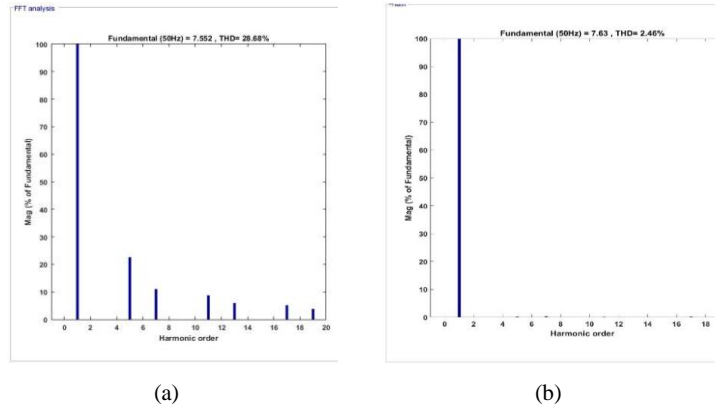


Fig. 7. THD analysis for simulation of 80-Ω load (a) before connecting APF and (b) after connecting APF

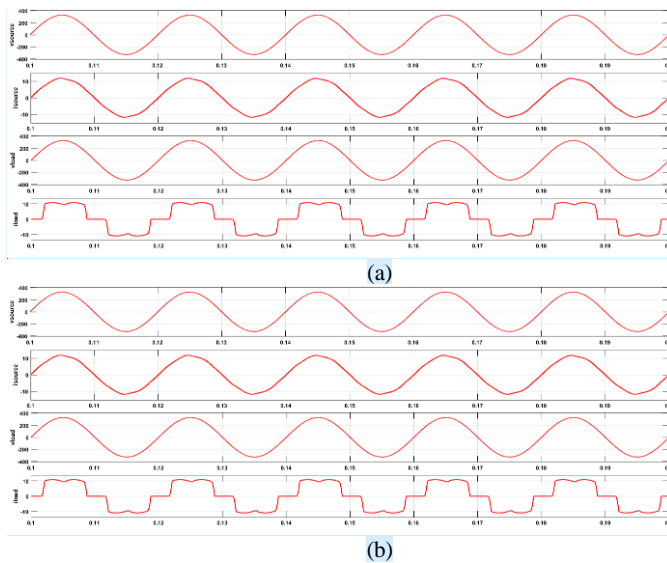


Fig. 8. Simulation results of phase-a source voltage, source current, load voltage, and load current for (a) 50-Ω and (b) 36-Ω loads

Commented [TSHBM@AR18]: Reviewer 3
Create Figure 6a and Figure 6b in two rows of the figures table respectively (not in the double-column model) - (figure changed to fig 8)

Furthermore, the EFANF is simulated with two other stationary load conditions: resistive loads of 50 and 36 ohms, respectively. The waveforms of the voltage source, load current, and source current after compensation for both given loads are shown. In contrast, for investigated waveform for a single dedicated phase, a can be seen in Fig. 8. Based on the measured waveforms shown in Fig. 9, the EFANF provided the reference signal to the SAPF controller and mitigated the harmonics for all the stationary load conditions. The SAPF managed to bring down the THD from 28.29 % to 2.55% for 50- Ω load and 2.40% for 36- Ω load, respectively, as highlighted in the spectrum FFT analysis in Fig. 10. The obtained results confirm the capability of the EFANF in compensation purposes for operating SPAPF to mitigate harmonics produced by the non-linear load system.

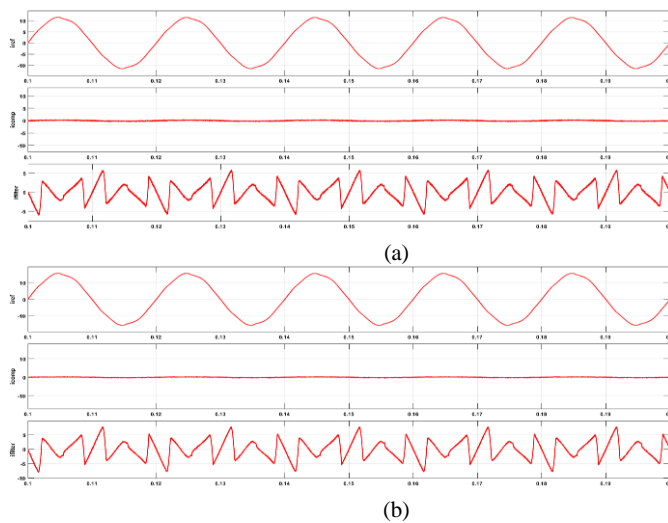


Fig. 9. Simulation results of phase a reference current, compensation current, and reference current for (a) 50- Ω and (b) 36- Ω loads

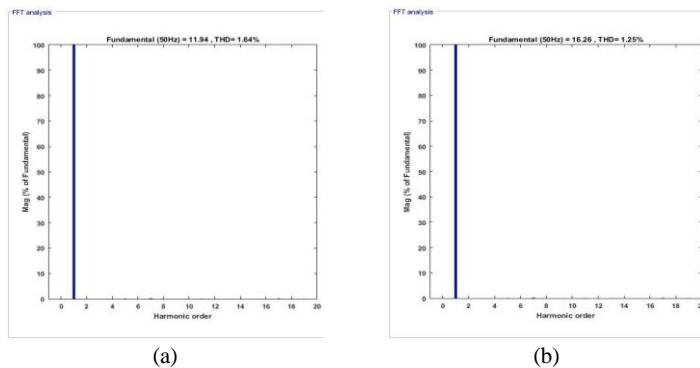


Fig. 10. THD result after APF compensation for (a) 50 Ω and (b) 36 Ω loads

Commented [TSHBM@AR19]: Reviewer 3
Create Figure 7a and Figure 7b in two rows of the figures table respectively (not in the double-column model) - (Figure change to Figure 9)

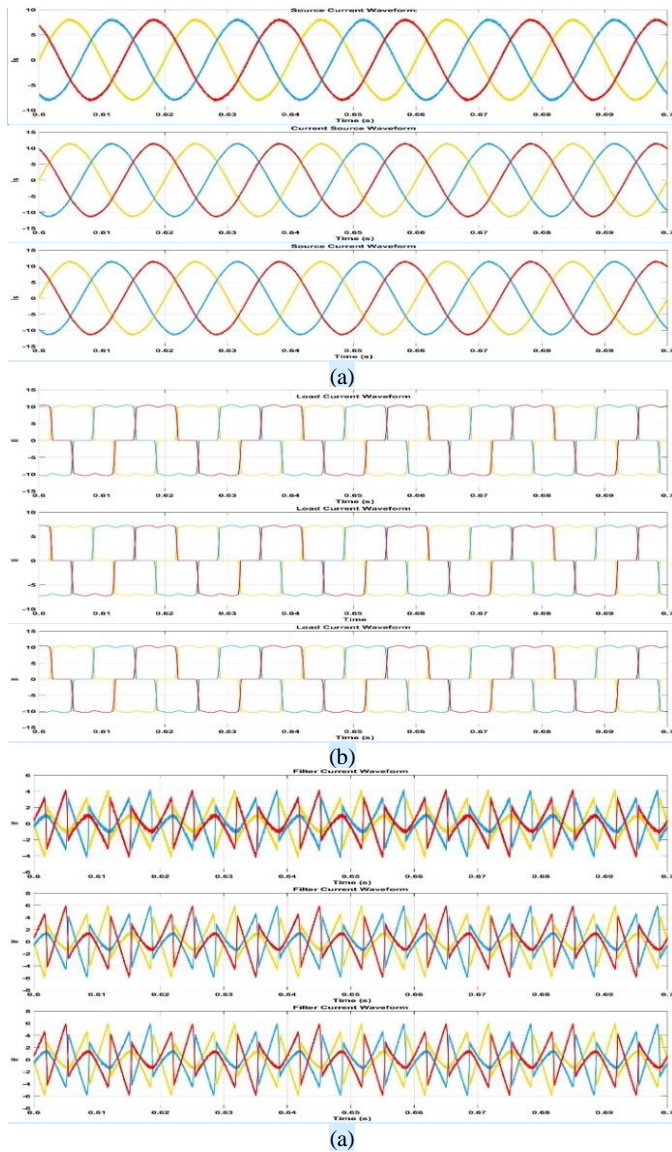


Fig. 11. Simulation results of source current, load current and filter current for (a) R1L1, (b) R2L2, and (c) R3L3 loads

Commented [TSHBM@AR20]: Reviewer 3
Create Figure 9a Figure 9b and Figure 9c in three rows of the figures table respectively (not in the three-column model) - (figure change to figure 11)

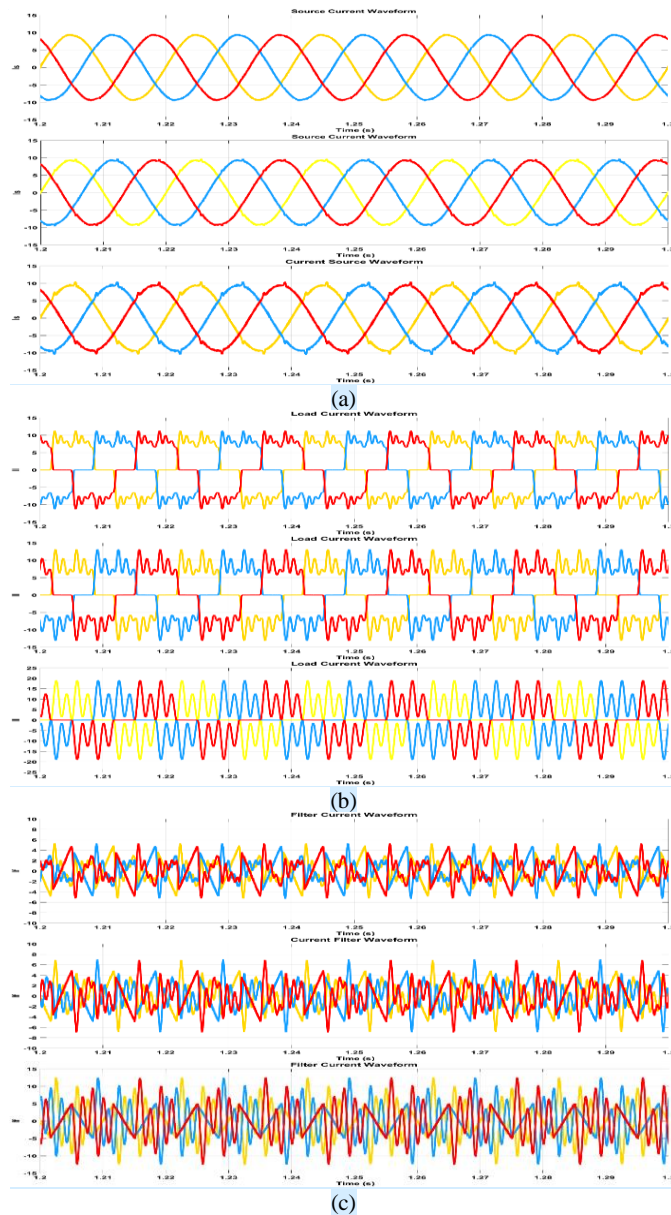


Fig. 12. Simulation results of source current, load current, and filter current for (a) R1C1, (b) R2C2, and (c) R3C3 loads

Commented [TSHBM@AR21]: Reviewer 3
Create Figure 10a Figure 10b and Figure 10c in three rows of the figures table respectively (not in the three-column model) - Figure change to figure 12

The proposed algorithm was also tested under different variations of loads for reactive power compensation under inductive and capacitive base loads to validate the adaptabilities of the algorithm in SAPF mitigation for the various waveform. Fig. 11 shows the result of the proposed EFANF for resistive with inductive load for three different loads, which are R1L1, R2L2, and R3L3 for source current, load current and filter current. On the other hand, Fig. 12 shows the source, load, and filter currents for three different resistive with capacitive loads given as R1C1, R2C2, and R3C3. Comparing the load current and source current for all three related loads, resistive with inductive and resistive with capacitive, shows that the EFANF can mitigate both reactive power compensation for resistive with inductive loads and resistive with capacitive loads. The THD values of the current source after mitigation for all loads are given as 2.41% for R1L1, 1.73% for R2L2, 1.25% for R3L3, 1.91% for R1C1, 2.09% for R2C2, and 2.54% for R3C3. Based on the given THD values, it can be proved that the EFANF can supply the SAPF effective reference current to reach the IEEE standard for the value of the harmonic below 5%.

Adaptableness of the EFANF is also being evaluated. The proposed algorithm is also simulated under a dynamic-state condition where the load will change between three resistivity load values that will directly affect the amount of current in the system. The dynamic changes are evaluated in changes of a resistive load from 82- Ω to 50- Ω and from 50- Ω to 36- Ω , where the changes will induce the increase of current changes. Fig. 13 provides simulation results for both conditions with the voltage source, load current, and current source at transition points. It is shown that the EFANF managed to cater to the changes in load and respond to them immediately, whereas based on the Fig., the EFANF required 0.05s to correspond to the changes.

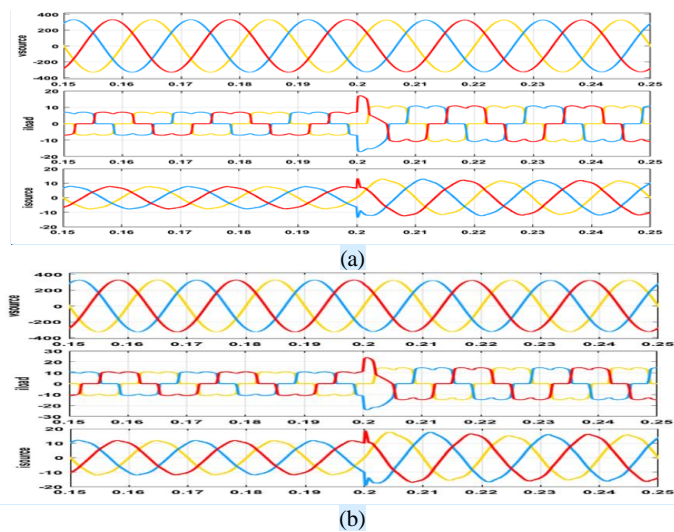


Fig. 13. Simulation results of source voltage, load current, and source current under transient-state conditions for (a) 86- Ω to 50- Ω and (b) 50- Ω to 36- Ω

Commented [TSHBM@AR22]: Reviewer 13
Create Figure 11a and Figure 11b in two rows of the figures table respectively (not in the double column model) - Figure change to Fig 13

Furthermore, the EFANF adaptability to dynamic changes is also simulated for the loads' changes from 36 ohms to 50 ohms and 50 ohms to 82 ohms. The simulated waveforms are presented in Fig. 14 for both conditions, where the Fig. illustrates source voltage, load current, and source current. The findings confirmed the capability of the EFANF to produce the corresponding reference current within both stationary and transient conditions.

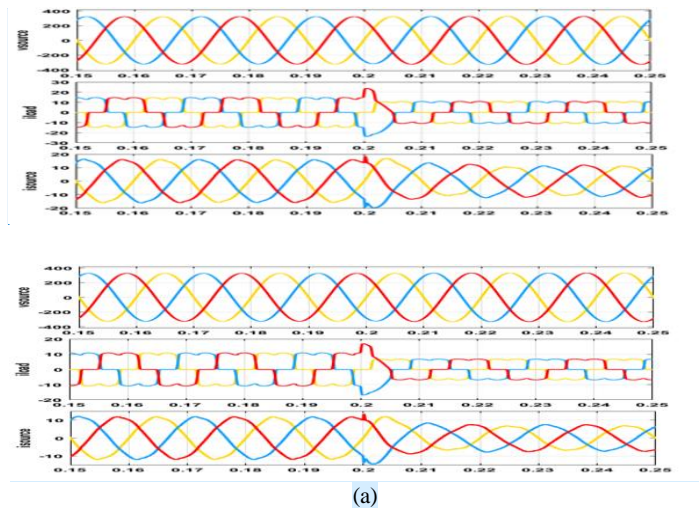


Fig. 14. Simulated result of EFANF under dynamic changes for loads of (a) 36- Ω to 50- Ω and (b) 50- Ω to 82- Ω Re

4.2. Experimental Results

A laboratory hardware setup was developed to validate the proposed algorithm. The hardware consisted of measurement circuits with current and voltage sensors, a three-phase inverter connected to the filtering inductor as APF, and DSPACE RS1104 as the controller, as shown in Fig. 15. A DSpace controller board is the connection point between the sensors and the output signals. For the APF, a three-phase inverter with DC-link is connected as the voltage source. The prominent role of the DSPACE is to implement the harmonics extraction algorithm, which will generate the reference current based on the EFANF. For the experiment, the supplied voltage of the system is set at 50Hz, 100 Vrms (line-to-line voltage). The experimental results of utilization of the proposed EFANF algorithm with PI DC-link control for resistive loads are shown in Fig. 16. The results include source voltage v_s , source current i_s , load current i_l and filter current i_{filter} .

The SAPF with EFANF effectively mitigates the harmonic current for the steady-state condition. The measurement is done using the Agilent DSO-X 2014A oscilloscope for the experimental result, covering source voltage, source current, load current, and filter current. In terms of THD calculation, the measurement is done by downloading the data from the oscilloscope. The data are then measured for harmonics decomposition using FFT analysis in MATLAB/Simulink.

Commented [TSHBM@AR23]: Reviewer 3
Create Figure 12a and Figure 12b in two rows of the figures table respectively (not in the double-column model). - Figure change to Figure 14

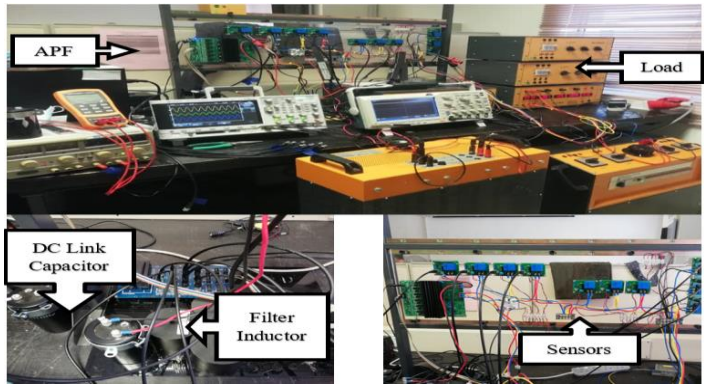


Fig. 15. Laboratory hardware setup

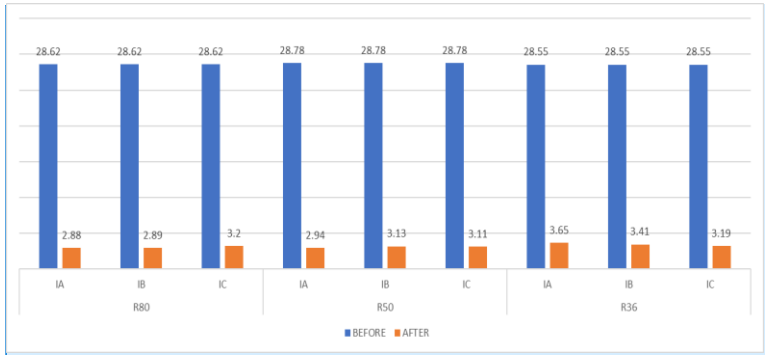


Fig. 16. Experimental results of THD for three-phase source current after compensation

All harmonics are managed to be reduced below the required IEE standard, 5%. Nevertheless, the THDs of the three-phase supply current are monitored to see the algorithm's effectiveness in the experimental work, where the THD value can be seen in Fig. 16. From the results, the algorithm managed to reduce the harmonics of the source current with THD from 28.62% to 2.88%, 2.89% and 3.2% for 80 Ohms load, 28.77% to 2.94%, 3.13% and 3.11% for 50 Ohms load, lastly from 28.56% to 3.65%, 3.14% and 3.19% for 36 Ohms load regards to phase IA, IB and IC.

Fig. 17 shows the waveforms of phase-a source voltage, source current, load current, and filter current in a steady-state condition obtained from experimental work. The source current waveform is sinusoidal and is in phase with the measured source voltage. Thus, THD is reduced for all the given loads, as shown in the Fig.17. The response of the proposed algorithm for steady-state conditions, when introduced to an inductive and capacitive load, is also confirmed with the experimental setup. The result is shown in Fig. 18, where it can be verified that the

Commented [TSHBM@AR24]: Reviewer 3
Figure 14 not only shows a bar diagram of THD source current after compensation, but also before compensation on the non-linear load (R = 80 ohm, R = 50 ohm, and R = 36 ohm). This revised figure will help the readers understand that your proposed method has better performance after compensation. After that, you have to make a clear analysis of the new figure

Commented [TSHBM@AR25R24]: Figure updated and analysis is included

proposed algorithm can mitigate resistive with inductive loads for values R1L1, R2L2, and R3L3. After mitigation, the source current loads THD are given as 2.70%, 2.63%, and 2.78%, respectively.

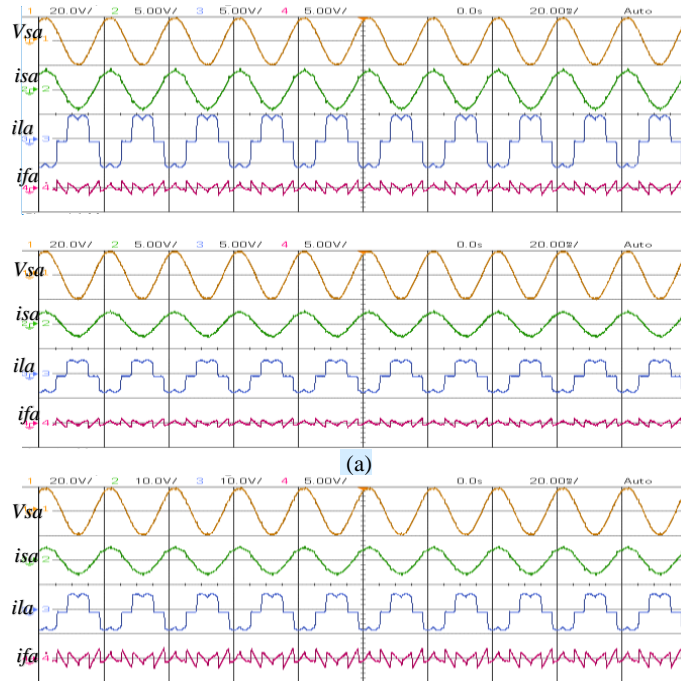


Fig. 17. Experimental results of source voltage, source current, load current, filter current and THD values for (a) 82-Ω (b) 50-Ω and (c) 36-Ω loads

The resistive with capacitive loads values of R1C1, R2C2, and R3C3. The values are within the required IEEE standard. THD's mitigated source current values are 2.52%, 2.99%, and 5.00% for each load. Based on these values, it can be concluded that the proposed EFANF algorithm can produce the appropriate reference current for the SAPF to work effectively. The SAPF also seems to have better stabilities for the resistive and inductive loads than capacitive loads. However, in terms of mitigation, the EFANF can mitigate all the different types of loads in the experimental setup.

The effectiveness and feasibility of the proposed algorithm were also verified for transient-state operation during load-changing conditions. Fig. 19 shows the state for reducing load capacity, which causes ascending current state, Fig. 19 also shows the increased load capacity, which causes descending current state. In both states, the EFANF managed to mitigate within 20ms for all load changes.

Commented [TSHBM@AR26]: Reviewer 3
Make Fig 15a, Fig 15b, and Fig 15c in the form of a three-row table respectively. Fig 15a and Fig 15b are too short for a two-column form because the two figures will be truncated.

Commented [TSHBM@AR27R26]: Figure updated and figure number is changed to fig 17

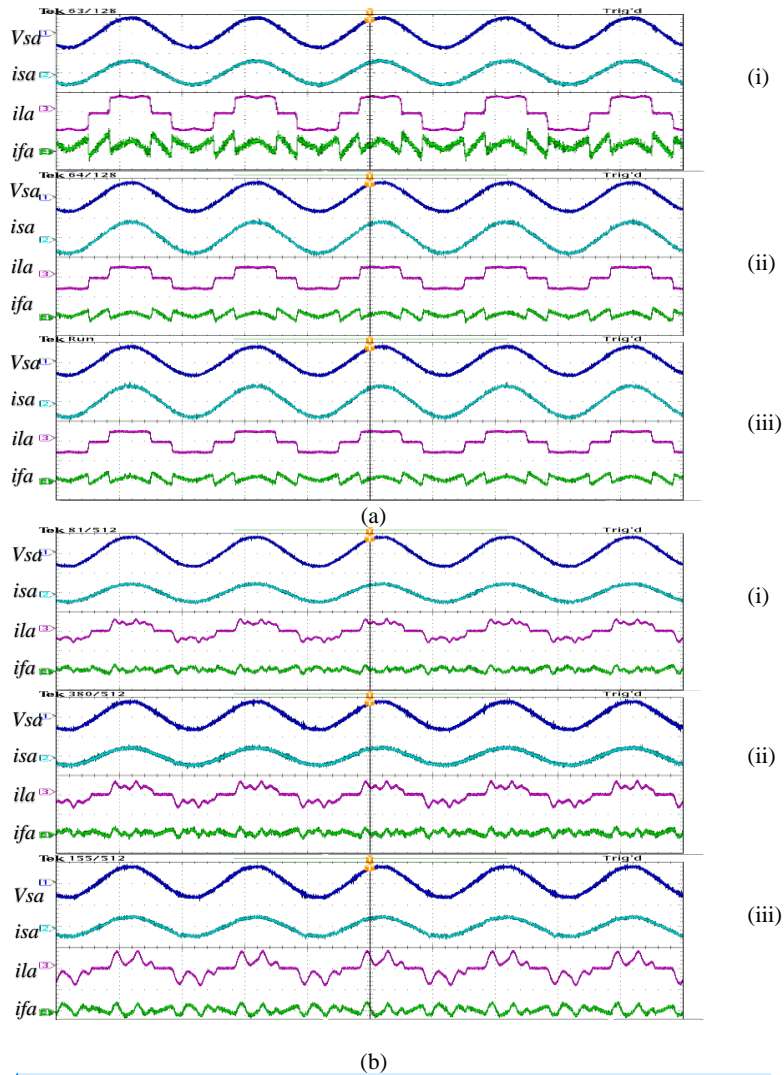


Fig. 18. Experimental results of source voltage, source current, load current, filter current and THD values for (a-i) 67- Ω and 30H, (a-ii) 69- Ω and 36H, (a-iii) 76- Ω and 41H loads, (b-i) 60- Ω 12uF, (b-ii) 60- Ω 17uF and (b-iii) 60- Ω 36uF loads

Commented [TSHBM@AR28]: Review 3
Create Figure 16a to Figure 16f in six rows of the figures table respectively (not in the double column model).

Commented [TSHBM@AR29R28]: Figure updated and changed to figure 18

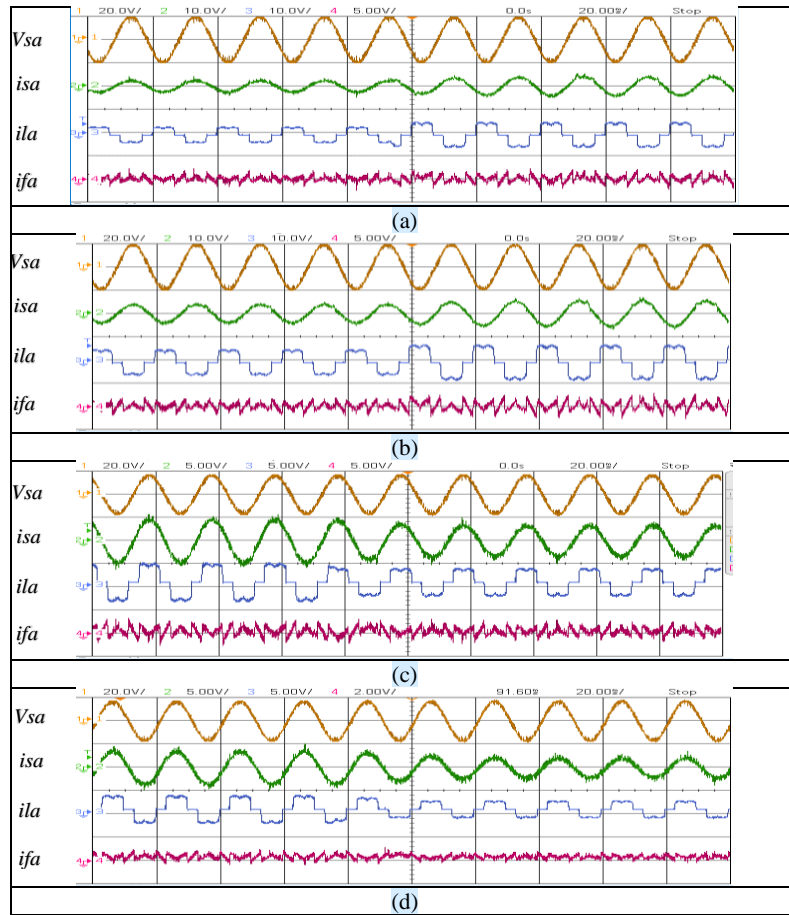


Fig. 19. Experimental results of source voltage, source current, load current, filter current, and DC-Link voltage during transient-state conditions of (a) 82-Ω to 50-Ω (b) 50-Ω to 36-Ω (c) 82-Ω to 50-Ω and (d) 50-Ω to 36-Ω

In comparison between the simulation and experimental results, both results show almost similar results in terms of waveform for source voltage, source current, load current, and filter current in both steady state and transient state. In terms of THD values, both simulations and experimental results recorded that the THD values for both conditions are below 5%, where the range is 1.45% to 2.46% for simulation and 2.88% to 3.65% for experimental results.

5. Conclusions

This paper presents the EFANF extraction algorithm utilized in SAPF to compensate for current harmonics in the three-phase three-wire system. The

Commented [TSHBM@AR30]: Review 3
Make Fig 17a, Fig 17b, Fig 17c, and Fig 17d in the form of a four-row table respectively (not in the double column model).

Commented [TSHBM@AR31R30]: Figure updated and change to figure 19

Commented [TSHBM@AR32]: Reviewer 2
The results of the simulation and experimental sections need to be compared particularly the figures.

Commented [TSHBM@AR33R32]: The result of both of simulation and experimental are summarizes the implication of the results toward each other at the result section.

proposed algorithm demonstrated its capability to generate the reference current based on the notch filtering technique, as shown in both simulation results in MATLAB/Simulink and experimental work based on the validation with DSPACE RS1104. As the EFANF is self-synchro based on frequency adaptability, PLL is not required. The algorithm extracted the fundamental component and mitigated harmonics in balanced load conditions based on the analyses of steady-state and transient state conditions. The performance of the proposed algorithm has also been verified for different types and values of reactive loads both in simulation and experimental works. The design of the EFANF also gives an optional improvement on the DC link voltage control algorithm as the losses of the DC link is provided as power losses within the system. In terms of performance, the EFANF managed to produce the THD according to the requirement of the IEE standard. Furthermore, the algorithm can adapt to the different types of loads. However, in the adaptation of EFANF, the algorithm is still dependent on two coefficients γ and ε for the algorithm to be working effectively. In current works, the coefficients are obtaining through empirical method. To improve the effectiveness of coefficients, future works are recommended to obtain the best possible coefficients values through optimization method.

Nomenclatures

v_{sa}, v_{sb}, v_{sc}	Voltage source phase a, b and c, Volt
i_{sa}, i_{sb}, i_{sc}	Current source phase a, b and c, Ampere
$i_{refa}, i_{refb}, i_{refc}$	Generated reference current phase a, b and c Ampere
i_{refa}	
$3V_{e1}I_{e1}$	Fundamental effective apparent power
$3V_{eH}I_{eH}$	Harmonics power
G_e	The equivalent conductivity

Greek Symbols

ω_0	Reference frequency
θ	Estimation Frequency
γ	Accuracy coefficients
ε	Convergence speed coefficients
$\hat{\theta}$	Updated law for the frequency estimation

Abbreviations

APF	Active Power Filter
SAPF	Shunt Active Power Filter
THD	Total Harmonics Distortion
EFANF	Extended Fryze Adaptive Notch Filter

References

1. F. Zare, H. Soltani, D. Kumar, P. Davari, H.A.M. Delpino, F. Blaabjerg, Harmonic Emissions of Three-Phase Diode Rectifiers in Distribution

Commented [TSHBM@AR34]: Reviewer 3

Describe in detail the weaknesses of your method and the future work needed to improve these weaknesses. Explain in a last single paragraph in the conclusion section.

Commented [TSHBM@AR35R34]: Added weakness and future work suggestion.

- Networks, IEEE Access. 5 (2017) 2819–2833. <https://doi.org/10.1109/ACCESS.2017.2669578>.
2. A. Alizade, J.B. Noshahr, Evaluating noise and DC offset due to inter-harmonics and supra-harmonics caused by back-to-back converter of (DFIG) in AC distribution network, CIREN - Open Access Proc. J. 2017 (2017) 629–632. <https://doi.org/10.1049/oap-cired.2017.0045>.
 3. K.D. Patil, W.Z. Gandhare, Effects of harmonics in distribution systems on temperature rise and life of XLPE power cables, 2011 Int. Conf. Power Energy Syst. ICPS 2011. (2011) 1–6. <https://doi.org/10.1109/ICPES.2011.6156680>.
 4. T. Toumi, A. Allali, A. Meftouhi, O. Abdelkhalek, A. Benabdelkader, M. Denai, Robust control of series active power filters for power quality enhancement in distribution grids: Simulation and experimental validation, ISA Trans. 107 (2020) 350–359. <https://doi.org/10.1016/j.isatra.2020.07.024>.
 5. E. Sundaram, M. Venugopal, On design and implementation of three phase three level shunt active power filter for harmonic reduction using synchronous reference frame theory, Int. J. Electr. Power Energy Syst. 81 (2016) 40–47. <https://doi.org/10.1016/j.ijepes.2016.02.008>.
 6. H. Liu, H. Hu, H. Chen, L. Zhang, Y. Xing, Fast and Flexible Selective Harmonic Extraction Methods Based on the Generalized Discrete Fourier Transform, IEEE Trans. Power Electron. 33 (2018) 3484–3496. <https://doi.org/10.1109/TPEL.2017.2703138>.
 7. R. Panigrahi, B. Subudhi, Performance Enhancement of Shunt Active Power Filter Using a Kalman Filter-Based H^∞ Control Strategy, IEEE Trans. Power Electron. 32 (2017) 2622–2630. <https://doi.org/10.1109/TPEL.2016.2572142>.
 8. V.N. Jayasankar, U. Vinatha, Backstepping Controller with Dual Self-Tuning Filter for Single-Phase Shunt Active Power Filters under Distorted Grid Voltage Condition, IEEE Trans. Ind. Appl. 56 (2020) 7176–7184. <https://doi.org/10.1109/TIA.2020.3025520>.
 9. F. Harirchi, M.G. Simoes, Enhanced Instantaneous Power Theory Decomposition for Power Quality Smart Converter Applications, IEEE Trans. Power Electron. 33 (2018) 9344–9359. <https://doi.org/10.1109/TPEL.2018.2791954>.
 10. Y.W. Liu, S.H. Rau, C.J. Wu, W.J. Lee, Improvement of Power Quality by Using Advanced Reactive Power Compensation, IEEE Trans. Ind. Appl. 54 (2018) 18–24. <https://doi.org/10.1109/TIA.2017.2740840>.
 11. A. Chebabhi, M.K. Fellah, A. Kessal, M.F. Benkhoris, A new balancing three level three dimensional space vector modulation strategy for three level neutral point clamped four leg inverter based shunt active power filter controlling by non-linear back stepping controllers, ISA Trans. 63 (2016) 328–342. <https://doi.org/10.1016/j.isatra.2016.03.001>.
 12. A. Naderipour, Z. Abdul-Malek, V.K. Ramachandramurthy, A. Kalam, M.R. Miveh, Hierarchical control strategy for a three-phase 4-wire microgrid under unbalanced and non-linear load conditions, ISA Trans. 94 (2019) 352–369. <https://doi.org/10.1016/j.isatra.2019.04.025>.
 13. Y. Hoon, M.A.A.M. Zainuri, A.S. Al-Ogaili, A.N. Al-Masri, J. Teh, Active Power Filtering under Unbalanced and Distorted Grid Conditions Using

- Modular Fundamental Element Detection Technique, *IEEE Access*. 9 (2021) 107502–107518. <https://doi.org/10.1109/ACCESS.2021.3101238>.
14. S. Hou, J. Fei, C. Chen, Y. Chu, Finite-Time Adaptive Fuzzy-Neural-Network Control of Active Power Filter, *IEEE Trans. Power Electron.* 34 (2019) 10298–10313. <https://doi.org/10.1109/TPEL.2019.2893618>.
15. S. Hou, J. Fei, Y. Chu, Nonsingular Terminal Sliding Mode Control of Active Power Filter, *Chinese Control Conf. CCC*. 2018-July (2018) 2982–2987. <https://doi.org/10.23919/ChiCC.2018.8483224>.
16. K.H. Tan, F.J. Lin, J.H. Chen, DC-Link voltage regulation using RPFNN-AMF for Three-Phase active power filter, *IEEE Access*. 6 (2018) 37454–37463. <https://doi.org/10.1109/ACCESS.2018.2851250>.
17. L. Merabet, S. Saad, D.O. Abdeslam, J. Merckle, Direct neural method for harmonic currents estimation using adaptive linear element, *Electr. Power Syst. Res.* 152 (2017) 61–70. <https://doi.org/10.1016/j.epsr.2017.06.018>.
18. B. Singh, S.R. Arya, K. Kant, Notch filter-based fundamental frequency component extraction to control distribution static compensator for mitigating current-related power quality problems, *IET Power Electron.* 8 (2015) 1758–1766. <https://doi.org/10.1049/iet-pel.2014.0486>.
19. S. Kewat, B. Singh, Modified amplitude adaptive control algorithm for power quality improvement in multiple distributed generation system, *IET Power Electron.* 12 (2019) 2321–2329. <https://doi.org/10.1049/iet-pel.2018.5936>.
20. D. Yazdani, A. Bakhshai, P. Jain, A three-phase approach to harmonic and reactive current extraction and harmonic decomposition, *IECON Proc. (Industrial Electron. Conf.* 25 (2009) 3205–3210. <https://doi.org/10.1109/IECON.2009.5415218>.
21. S.H. Mohamad, M.A.M. Radzi, N.F. Mailah, N.I.A. Wahab, A. Jidin, M.Y. Lada, Adaptive notch filter under indirect and direct current controls for active power filter, *Bull. Electr. Eng. Informatics.* 9 (2020) 1794–1802. <https://doi.org/10.11591/eei.v9i5.2165>.
22. R.S.R. Chilipi, N. Al Sayari, K.H. Al Hosani, A.R. Beig, Adaptive Notch Filter-Based Multipurpose Control Scheme for Grid-Interfaced Three-Phase Four-Wire DG Inverter, *IEEE Trans. Ind. Appl.* 53 (2017) 4015–4027. <https://doi.org/10.1109/TIA.2017.2676098>.
23. G. Fujita, N.D. Dinh, T. Funabashi, N.D. Tuyen, Adaptive notch filter solution under unbalanced and/or distorted point of common coupling voltage for three-phase four-wire shunt active power filter with sinusoidal utility current strategy, *IET Gener. Transm. Distrib.* 9 (2015) 1580–1596. <https://doi.org/10.1049/iet-gtd.2014.1017>.
24. N.D. Tuyen, G. Fujita, T. Funabashi, M. Nomura, Adaptive notch filter for synchronization and islanding detection using negative-sequence impedance measurement, *IEEE Trans. Electr. Electron. Eng.* 7 (2012) 240–250. <https://doi.org/10.1002/tee.21724>.
25. M. Mojiri, A.R. Bakhshai, Stability analysis of periodic orbit of an adaptive notch filter for frequency estimation of a periodic signal, *Automatica*. 43 (2007) 450–455. <https://doi.org/10.1016/j.automatica.2006.08.018>.

26. M. Mojiri, A.R. Bakhshai, An Adaptive Notch Filter for Frequency Estimation of a Periodic Signal, *IEEE Trans. Automat. Contr.* 49 (2004) 314–318. <https://doi.org/10.1109/TAC.2003.821414>.
27. M. Mojiri, M. Karimi-Ghartemani, A. Bakhshai, Processing of harmonics and interharmonics using an adaptive notch filter, *IEEE Trans. Power Deliv.* 25 (2010) 534–542. <https://doi.org/10.1109/TPWRD.2009.2036624>.
28. X. Nie, J. Liu, Current Reference Control for Shunt Active Power Filters under Unbalanced and Distorted Supply Voltage Conditions, *IEEE Access.* 7 (2019) 177048–177055. <https://doi.org/10.1109/ACCESS.2019.2957946>.
29. D. TESHOME, T.D. Huang, K.-L. Lian, A Distinctive Load Feature Extraction Based on Fryze's Time-domain Power Theory, *IEEE Power Energy Technol. Syst. J.* 3 (2016) 1–1. <https://doi.org/10.1109/jpets.2016.2559507>.
30. S.K. Kesharvani, A. Singh, M. Badoni, Conductance based fryze algorithm for improving power quality for non-linear loads, 2014 Int. Conf. Signal Propag. Comput. Technol. ICSPCT 2014. (2014) 703–708. <https://doi.org/10.1109/ICSPCT.2014.6884965>.
31. Z. Zeng, R. Zhao, H. Yang, Coordinated control of multi-functional grid-tied inverters using conductance and susceptance limitation, *IET Power Electron.* 7 (2014) 1821–1831. <https://doi.org/10.1049/iet-pel.2013.0692>.

Friday, 30 December, 2022

Reviewer's Task No.: 3

Dear **Dr. Amirullah Ubhara Surabaya**,

On behalf of the Editorial Board, I would like to thank you for your contribution in reviewing the following paper submitted to our journal.

CURRENT HARMONICS QUALITY MITIGATION TECHNIQUE FOR THREE-PHASE POWER SYSTEM BASED ON EXTENDED FRYZE ADAPTIVE NOTCH FILTER

I am confident that with your continuous support and commitment, we will be able to maintain the quality and value of the *Journal of Engineering Science & Technology (JESTEC)*.

Yours Sincerely,



Associate Professor Dr. Abdulkareem Sh. Mahdi Al-Obaidi, CEng. MIMechE

Editor-in-Chief, Journal of Engineering Science & Technology (JESTEC)

<http://jestec.taylors.edu.my>

Journal of Engineering Science and Technology (JESTEC)

[Home](#)

[Editorial Board](#)

[Submit a paper](#)

[Indexing and Awards](#)

[Reviewers](#)

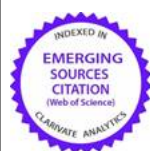
[Articles in Press](#)

[Publication Ethics](#)

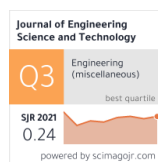
[Archives](#)

Reviewers

JESTEC
Journal of Engineering
Science and Technology



WEB OF SCIENCE



Besides our contributors, we owe our success and sustainability to our reviewers. If you are interested in joining the list of our reviewers, please

- download [JESTEC Reviewers Form](#) for reviewers,
- fill it in completely,
- attach your latest CV and
- send both to the [Executive Editor](#).

- **Abdulkareem Sh. Mahdi Al-Obaidi**, Ph.D., CEng MIMechE (Mechanical Engineering)
Associate Professor, School of Engineering
Taylor's University
Taylor's Lakeside Campus
No. 1 Jalan Taylor's, 47500 Subang Jaya
Selangor DE
Malaysia
- **David WL Hukins**, Ph.D. B.Sc., Ph.D. (London), D.Sc. (Manchester), C.Phys., F.Inst.P., F.I.P.E.M., F.R.S.E.
Professor of Bio-medical Engineering
Head of Mechanical and Manufacturing Engineering
School of Engineering
Mechanical Engineering
The University of Birmingham
Edgbaston
Birmingham, B15 2TT
United Kingdom
E-mail: D.W.Hukins@bham.ac.uk
- **Takayuki Saito**, Ph.D. (Physics and Astronomy)
Professor
Shizuoka University
Graduate School of Science and Engineering
3-5-1 Johoku
Hamamatsu
Shizuoka 432-8561
Japan
E-mail: tsaito@ipc.shizuoka.ac.jp
- **Stephen B M Beck**, Ph.D. (Mechanical Engineering)
Professor in Mechanical Engineering
Faculty Director of Learning and Teaching - Engineering
Department of Mechanical Engineering
The University of Sheffield
Mappin Street
Sheffield
S1 3JD
United Kingdom
E-mail: s.beck@sheffield.ac.uk
- **Sulaiman Al-Zuhair**, Ph.D. (Chemical Engineering)
Associate Professor
Chemical and Petroleum Engineering Department
Faculty of Engineering
UAE University
P.O. Box 17555
AlAin, U.A.E.
E-mail: alzuhair72@yahoo.com
- **Manoj Kulshreshtha**, Ph.D. (Food Engineering)
Professor and Dean, Faculty of Science Engineering & Technology
Director, Amity Institute of Food Technology
Amity University Uttar Pradesh, Noida (UP)
India
E-mail: manojkul@gmail.com
- **Yousif Abdall Abakr**, Ph.D. (Mechanical Engineering)
School of Mechanical Engineering
The University of Nottingham, Malaysia Campus
Jalan Broga, 43500 Semenyih, Selangor
Malaysia
E-mail: yousif.abakr@nottingham.edu.my
- **Marwan Alrubaye**, Ph.D. CEng MICHEI (Chemical Engineering)

San Matias, Dingle, Iloilo
Philippines

E-mail: joelaine91513@isconf.edu.ph

- **Elaine H. Anzures**, Ph. D (Mathematics)
Instructor, College of Education
Iloilo State College of Fisheries-Dingle Campus
San Matias, Dingle, Iloilo
Philippines
E-mail: joelaine91513@isconf.edu.ph
- **Davoud Habibzadeh**, Ph.D (Sciences and Food Industries Engineering -Food Technology)
Department of Food Science and Technology of Agriculture
Faculty of Nutrition Sciences and Food Industries
Islamic Azad University of Tabriz, Tabriz
Iran
E-mail: stu.davoudhabibzadeh@iaut.ac.ir
- **M. Kedar Mallik**, AMIE, M. Tech., Ph. D. (Mechanical Engineering)
Professor,
Department of Mechanical Engineering,
Vasireddy Venkatadri Institute of Technology,
Nambur, Gudur Dist., A.P.
India 522508
E-mail: mallikkedar@vvt.net
- **Amirullah**, Dr., ST., MT. (Electrical Engineering)
Study Program of Electrical Engineering
Faculty of Engineering
Universitas Bhayangkara Surabaya
Jl. Ahmad Yani Frontage Road Ahmad Yani No.114, Surabaya
East-Java, Indonesia 60231
Email: amirullah@ubhara.ac.id
- **Fayas Saffiudeen**, B.E., M.E., MBA (Welding)
Lecturer - Department of Mechanical Skills,
Jubail Technical Institute,
P.O. Box: 10335
Jubail Industrial City 31961
Kingdom of Saudi Arabia
E-mail: Saffiudeen_m@rcjy.edu.sa

[Home](#)

[Editorial
Board](#)

[Submit a
paper](#)

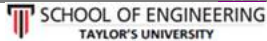
[Indexing and
Awards](#)

[Reviewers](#)

[Articles
in Press](#)

[Publication
Ethics](#)

[Archives](#)



Copyright ©2006-2023 by: School of Engineering. Taylor's University



Source details

Journal of Engineering Science and Technology

Scopus coverage years: from 2009 to 2022

Publisher: Taylor's University

ISSN: 1823-4690

Subject area: Engineering: General Engineering

Source type: Journal

[View all documents >](#)

[Set document alert](#)

[Save to source list](#) [Source Homepage](#)

CiteScore 2021

1.6

SJR 2021

0.243

SNIP 2021

0.525

[CiteScore](#) [CiteScore rank & trend](#) [Scopus content coverage](#)

i Improved CiteScore methodology

CiteScore 2021 counts the citations received in 2018-2021 to articles, reviews, conference papers, book chapters and data papers published in 2018-2021, and divides this by the number of publications published in 2018-2021. [Learn more >](#)

CiteScore 2021

$$1.6 = \frac{2,274 \text{ Citations 2018 - 2021}}{1,391 \text{ Documents 2018 - 2021}}$$

Calculated on 05 May, 2022

CiteScoreTracker 2022

$$1.6 = \frac{2,028 \text{ Citations to date}}{1,296 \text{ Documents to date}}$$

Last updated on 05 January, 2023 • Updated monthly

CiteScore rank 2021

Category	Rank	Percentile
Engineering		
General Engineering	#158/300	47th

[View CiteScore methodology >](#) [CiteScore FAQ >](#) [Add CiteScore to your site](#)

About Scopus

- What is Scopus
- Content coverage
- Scopus blog
- Scopus API
- Privacy matters

Language

- 日本語版を表示する
- 查看简体中文版本
- 查看繁體中文版本
- Просмотр версии на русском языке

Customer Service

- Help
- Tutorials
- Contact us

ELSEVIER

[Terms and conditions ↗](#) [Privacy policy ↗](#)

Copyright © Elsevier B.V. ↗. All rights reserved. Scopus® is a registered trademark of Elsevier B.V.

We use cookies to help provide and enhance our service and tailor content. By continuing, you agree to the use of cookies ↗.





From The Industry Leader

Get peace of mind with protection against sophisticated attacks.

CrowdStrike®

Journal of Engineering Science and Technology

COUNTRY

Malaysia



Universities and research
institutions in Malaysia

SUBJECT AREA AND CATEGORY

Engineering

└ Engineering (miscellaneous)

PUBLISHER

Taylor's
University



Taylor's
University
Scimago
Institutions
Rankings

PUBLICATION TYPE

Journals

ISSN

18234690

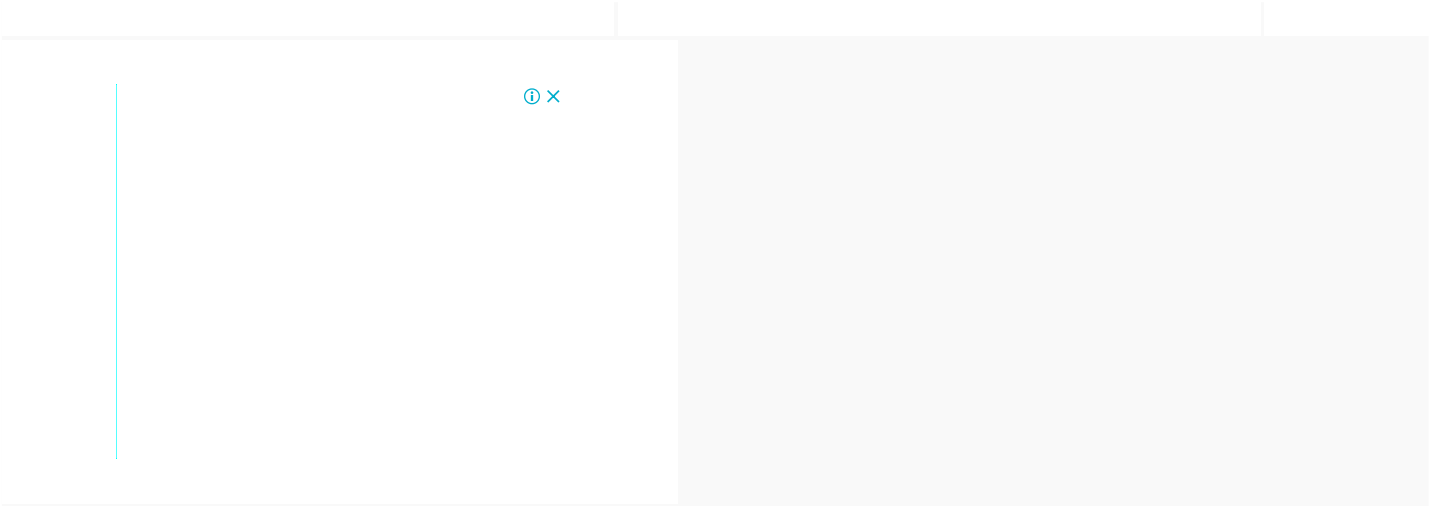
COVERAGE

2009-
2021




From The Industry Leader

Get peace of mind with protection against sophisticated attacks. CrowdStrike®



SCOPE

JESTEC (Journal of Engineering Science and Technology) is a peer-reviewed journal that aims at the publication and dissemination of research articles on the latest developments in all fields of engineering science and technology. The journal publishes original papers in which contribute to the understanding of engineering science and improvement of the engineering technology and education. Papers are theoretical (including computational), experimental or both. The contribution should be unpublished before and not under consideration for publication elsewhere.



 Join the conversation about this journal

From The Industry Leader

Get peace of mind with protection against sophisticated attacks.

CrowdStrike®



 Quartiles




Published with Hindawi

Math, Eng., & Comp. Sci. Articles Are Peer Reviewed, Open Access

Hindawi

1
**Arabian Journal for Science
and Engineering**
DEU

47%
similarity

2
Cogent Engineering
GBR

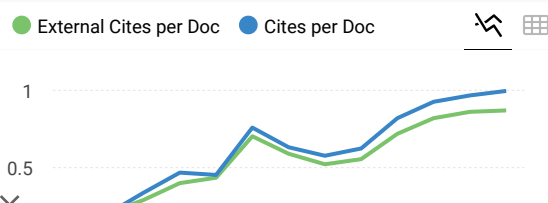
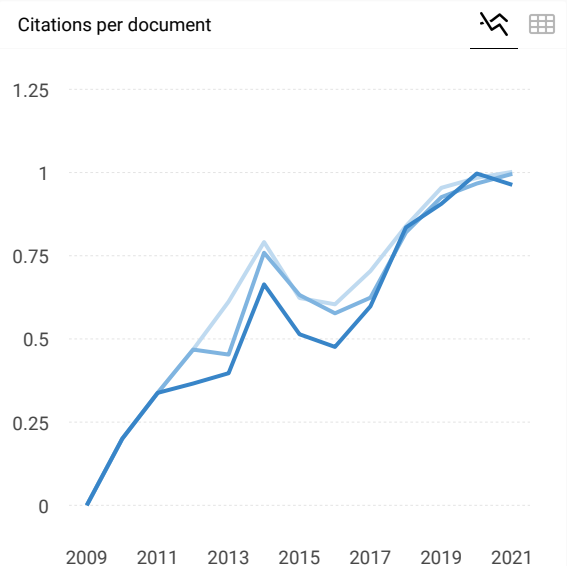
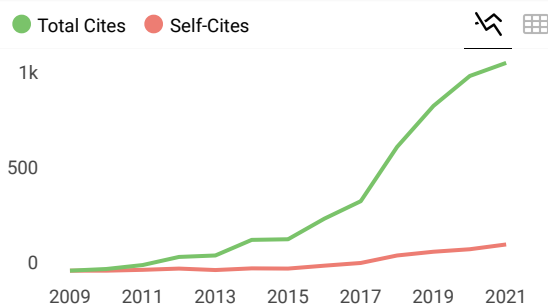
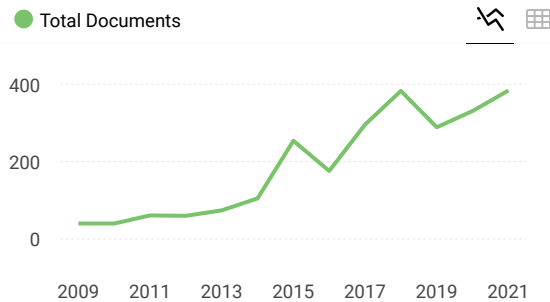
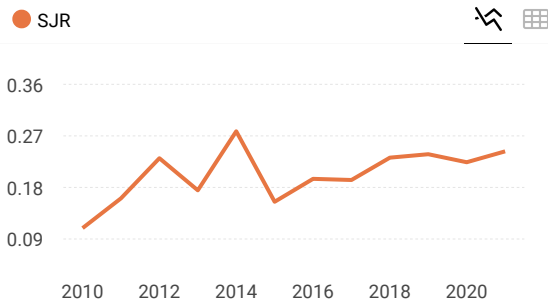
42%
similarity

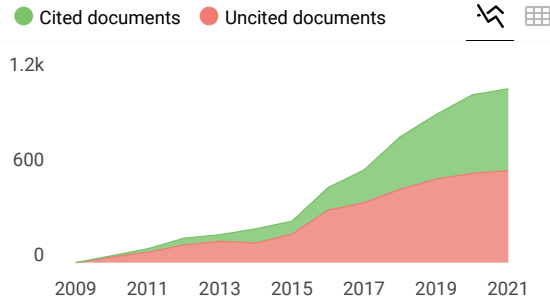
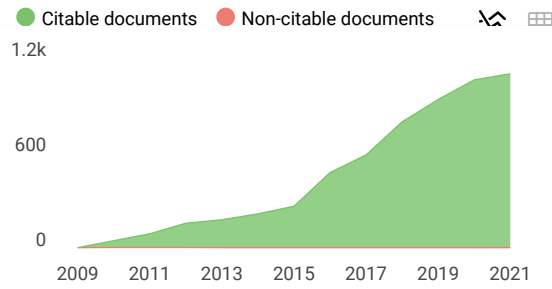
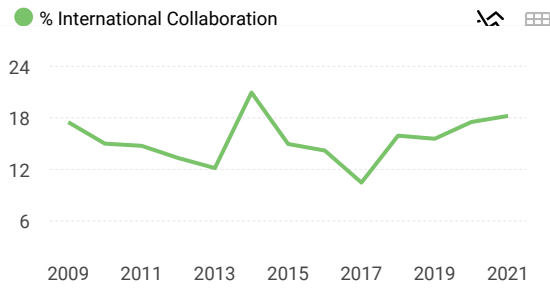
3
**International Journal of
Engineering Research and**
IND

41%
similarity

4
**Journal of Engin
Applied Science**
PAK

39%
similarity





← Show this widget in your own website

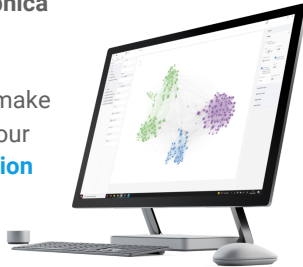
Just copy the code below and paste within your html code:

``



SCImago Graphica

Explore, visually communicate and make sense of data with our [new data visualization tool](#).



From The Industry Leader

Get peace of mind with protection against sophisticated attacks.

CrowdStrike®



Metrics based on Scopus® data as of April 2022



asmaa 4 months ago

if you can help , contact the journal through you

best regards

asmaa

← reply



Melanie Ortiz 4 months ago

SCImago Team

Dear Asmaa,
Thank you for contacting us. Unfortunately, SCImago cannot help you with your request.
SJR is committed to help decision-making through scientometric indicators.
Best Regards, SCImago Team



M.Sivasankara Rao 2 years ago

present how much time it will take to get acceptance and publication in this journal.

← reply



Melanie Ortiz 2 years ago

SCImago Team

Dear M.Sivasankara,
Thank you for contacting us.
Unfortunately, we cannot help you with your request.
Best Regards, SCImago Team



Ponum Almas 2 years ago

hello ,
is this impact factor journal ? what is the publication fee for an aticle ? is there any discout for
developing countries ?

← reply



Melanie Ortiz 2 years ago

SCImago Team



journal's website or contact directly with the editorial staff.
Best Regards, SCImago Team



daus 2 years ago

this is ecsi journal, not scie

← reply



Melanie Ortiz 2 years ago

SCImago Team

Dear Daus, thanks for your participation! Best Regards, SCImago Team



kartik 2 years ago

Hi,

Can i know what is the current Quartile ranking for this journal for the year 2020? tq

← reply



Melanie Ortiz 2 years ago

SCImago Team

Dear Kartik,

Thank you for contacting us. You can consult that information just above. The SJR for 2019 was released on 11 June 2020.

Best Regards, SCImago Team



Raghad Hameed Ahmed 2 years ago

good greeting

What is the time required to obtain a research acceptance letter.

← reply



Melanie Ortiz 2 years ago

SCImago Team

Dear Raghad,

thank you for contacting us





D

deepthi 2 years ago

Hi,

Is it okey to cite an unpublished work can in the manuscript?

← reply



Melanie Ortiz 2 years ago

SCImago Team

Dear Deepthi, thank you very much for your comment. Unfortunately, we cannot help you with your request, we suggest you contact the journal's editorial staff so they could inform you more deeply. Best Regards, SCImago Team

M

M.K. 3 years ago

Dear Melanie

I have submitted a paper for this journal about 6 months ago, and I did not receive the decision yet. The problem is the website of this journal does show any contact details except the email of the Executive Editor, who did not respond to my emails since May 2020. Do you know any other contact details for this journal please?

Best regards

M.K.

← reply



Melanie Ortiz 2 years ago

SCImago Team

Dear M.K.,

Thank you for contacting us. Unfortunately, it seems that there is no other email contact shown in their website.

Best Regards, SCImago Team

D

Dr. Vijaya Shetty S 3 years ago



K. Bhatti 3 years ago

It's 300USD per article.



Melanie Ortiz 3 years ago

SCImago Team

Dear Dr. Vijaya,
thank you for contacting us.
Unfortunately, we cannot help you with your request, we suggest you visit the journal's homepage or contact the journal's editorial staff , so they could inform you more deeply.
Best Regards, SCImago Team



Waleed 3 years ago

Why there is no response to our emails? Someone should tell them that other OA journals respond very fast. It is really a negative point about their performance. Pay attention to your costumers.

← reply



Nibras Khalid 3 years ago

Hello,
I submitted a manuscript for publication more than a week ago, but I haven't received a confirmation email of delivery. Is there a way to know if all the required documents have been received??

← reply



Melanie Ortiz 3 years ago

SCImago Team

Dear Nibras,
thank you for contacting us.
Unfortunately, we cannot help you with your request, we suggest you contact the journal's editorial staff , so they could inform you more deeply.
Best Regards, SCImago Team



Phyu Phyu Thin 3 years ago

Dear Sir,



← reply

S

sukanto wiryono 3 years ago

Dear Melanie Ortiz

Please inform me, is this JESTEC indexed by Q2 Scopus?

Thanks you



Melanie Ortiz 3 years ago

SCImago Team

Dear Sukanto, thank you very much for your comment, unfortunately we cannot help you with your request. We suggest you to consult the Scopus database directly.

Keep in mind that the SJR is a static image (the update is made one time per year) of a database (Scopus) which is changing every day. The SJR's Quartile for 2018 is available just above.

Best Regards, SCImago Team



Melanie Ortiz 3 years ago

SCImago Team

Dear Phyu,

thank you for contacting us.

We are sorry to tell you that SCImago Journal & Country Rank is not a journal. SJR is a portal with scientometric indicators of journals indexed in Elsevier/Scopus.

Unfortunately, we cannot help you with your request, we suggest you to visit the journal's homepage (See submission/author guidelines) or contact the journal's editorial staff , so they could inform you more deeply.

Best Regards, SCImago Team

B

B G Shivaleelavathi 3 years ago

Sir/Madam,

i want to submit review paper. what is procedure.

← reply



Melanie Ortiz 3 years ago

SCImago Team



F

Frans 3 years ago

I want to know, what is journal not a notification after submitting?
Thank you

 reply

K

kareem 3 years ago

Dear Scopus people
I want to if this journal consdiered as an ISI journal and what is its impact factor.
Thanks

 reply**Melanie Ortiz** 3 years ago

SCImago Team

Dear Kareem, SCImago Journal and Country Rank uses Scopus data, our impact indicator is the SJR. Check our web to locate the journal. We suggest you to consult the Journal Citation Report for other indicators (like Impact Factor) with a Web of Science data source. Best Regards, SCImago Team

N

Nacer 3 years ago

Dear Abdulkareem

Please informe me if the publication is free or not?

Best regards

 reply

A

abdulkareem 3 years ago

no, it is not free, USD300/aper

N

Nacer 3 years ago



Melanie Ortiz 3 years ago

SCImago Team

Dear Nacer, SCImago Journal and Country Rank uses Scopus data, our impact indicator is the SJR. Check our web to locate the journal. We suggest you to consult the Journal Citation Report for other indicators (like Impact Factor) with a Web of Science data source. Best Regards, SCImago Team

S

supreetha B.S 3 years ago

I have published my research work in JESTEC. It is a quality journal with systematic review process. I received review comments from 5 reviewers and I answered all the comments and finally after 2 round review process my paper was accepted. Thanks to Dr. Abdulkareem Sh Mahdi Al-obaidi

← reply

V

VIJAY B G 2 years ago

Hello madam, could you please tell me is there any processing charges that you have paid? also suggest some good Scopus indexed journal to publish my paper. Thank you



Sudhakiran Gunda 2 years ago

Could you please tell me the duration for this entire process. I would like to know the time taken for publication.

Thankyou



Melanie Ortiz 3 years ago

SCImago Team

Dear Supreetha, thanks for your participation! Best Regards, SCImago Team

K

Khaled 3 years ago

Hello there!

I have a little question about the publication process timeline, Can I know please how long will take between sending an article and (journal answer by acceptance/rejection) and finally the paper's online availability ????





Khaled 3 years ago

Thanks alot for your valuable response
Are there any publication fees or not ???????



Ali 3 years ago

Dear khaled
The timeline for publishing in this journal about 2-3 months for final acceptance and may be 9 months for online publication
with my regards



Melanie Ortiz 3 years ago

SCImago Team

Dear Ali, thanks for your participation! Best Regards, SCImago Team



Melanie Ortiz 3 years ago

SCImago Team

Dear Khaled,
thank you for contacting us.
Sorry to tell you that SCImago Journal & Country Rank is not a journal. SJR is a portal with scientometric indicators of journals indexed in Elsevier/Scopus.
Unfortunately, we cannot help you with your request, we suggest you to visit the journal's homepage or contact the journal's editorial staff , so they could inform you more deeply.
You can see the updated journal's information just above .
Best Regards, SCImago Team



ASWANT KUMAR SHARMA 3 years ago

I have published a paper with JESTEC in a proper time line. It is good if JESTEC provide DOI for article published with them

← reply



Malathi Kunnudaiyan 2 years ago

Have paid any fees for the publication sir?



R**rati saluja** 3 years ago

The journal that provides best services, never a single follow up query left unanswered. I had written several research papers in numerous journals, but I feel pride the way "Journal of Engineering Science and Technology" works, they reviewed every mm of my manuscript. Their editing team is soul of the body. Mr. Obaidi shares every detail regarding the review process as well as time duration, that made the process easy. Publishing in a reputed journal takes time, So eagerly waiting for the same.

Thanks a million to Dr. Abdulkareem Sh. Mahdi Al-Obaidi for sharing a wonderful platform to enhance one's knowledge and research.

Hats off

A happy author

← reply

M**Melva Silitonga** 4 years ago

This journal template has been used for the 2019 Kyoto APLSBE template that I have participated in, I am interested in the content of this journal and wish for publication in this journal

← reply

W**Wajde Alyhya** 4 years ago

Hi

I sent a manuscript for publication in this journal and I received two months later seven reviewers' comments. I answered all their comments, however, I have not received an acceptance or rejection letter till now. I sent more than one emails regarding the status of my manuscript without an answer. I do not know what to do after nearly more than 6 months of waiting.

← reply

A**Abdulkareem Sh. Mahdi Al-Obaidi** 3 years ago

Dear Wajde

We thank you for the comment.

As you mentioned your experience with JESTEC, I wonder why you did not mention that your paper is accepted and will be published soon.

It is good to give negative feedback for improvement, we thank you but it is also fair to tell positive feedback, right?



E**Emmanuel** 4 years ago

@ Elena:I humbly suggest that the web link of all journals should be published alongside their name.This will eliminate the faking of journals in your data base.

 replyW**Wajde Alyhya** 4 years ago

Dear All

Could you please tell me how long it takes to be accepted and published online.

Thanks

 replyD**Dr. mohammed alwazzan** 4 years ago

3 to 4 month

**Elena Corera** 4 years ago**SCImago Team**

Dear Wadje, in the link below you will find the information corresponding to the author's instructions of this journal. Best regards, SCImago Team

<http://jestec.taylors.edu.my/instructions.html>

Leave a comment

Name

Email

(will not be published)



Submit

The users of Scimago Journal & Country Rank have the possibility to dialogue through comments linked to a specific journal. The purpose is to have a forum in which general doubts about the processes of publication in the journal, experiences and other issues derived from the publication of papers are resolved. For topics on particular articles, maintain the dialogue through the usual channels with your editor.

Developed by:



Powered by:

Scopus

Follow us on @ScimagoJR

Scimago Lab, Copyright 2007-2022. Data Source: Scopus®

EST MODUS IN REBUS

Horatio (Satire 1,1,106)

[Edit Cookie Consent](#)

